THE QUARTERLY JOURNAL OF MECHANICS AND APPLIED MATHEMATICS

Editorial Board

S. GOLDSTEIN R. V. SOUTHWELL
G. I. TAYLOR G. TEMPLE

together with

A. C. AITKEN; S. CHAPMAN; A. R. COLLAR; T. G. COWLING;
C. G. DARWIN; W. J. DUNCAN; A. E. GREEN; A. A. HALL;
D. R. HARTREE; L. HOWARTH; WILLIS JACKSON; H. JEFFREYS;
J. E. LENNARD-JONES; M. J. LIGHTHILL; G. C. McVITTIE;
N. F. MOTT; W. G. PENNEY; A. G. PUGSLEY; L. ROSENHEAD;
O. G. SUTTON; ALEXANDER THOM; A. H. WILSON;
J. R. WOMERSLEY

Executive Editors

V. C. A. FERRARO D. M. A. LEGGETT

VOLUME VII
1954

OXFORD
AT THE CLARENDON PRESS

Oxford University Press, Amen House, London E.C.4

GLASGOW NEW YORK TORONTO MELBOURNE WELLINGTON
BOMBAY CALCUTTA MADRAS KARACHI CAPE TOWN IBADAN

Geoffrey Cumberlege, Publisher to the University

PRINTED IN GREAT BRITAIN
AT THE UNIVERSITY PRESS, OXFORD
BY CHARLES BATEY, PRINTER TO THE UNIVERSITY

RR

THE QUARTERLY JOURNAL OF MECHANICS AND APPLIED MATHEMATICS

VOLUME VII PART 1

MARCH 1954

UNIVERSITY
OF MICHIGAN

APR - 8 1954

ENGINEERING
LIBRARY

OXFORD
AT THE CLARENDON PRESS
1954

Price 15*s. net*

PRINTED IN GREAT BRITAIN BY CHARLES BATEY AT THE UNIVERSITY PRESS, OXFORD

THE QUARTERLY JOURNAL OF MECHANICS AND APPLIED MATHEMATICS

Editorial Board

S. GOLDSTEIN — R. V. SOUTHWELL
G. I. TAYLOR — G. TEMPLE

together with

A. C. AITKEN — H. JEFFREYS
S. CHAPMAN — J. E. LENNARD-JONES
A. R. COLLAR — M. J. LIGHTHILL
T. G. COWLING — G. C. McVITTIE
C. G. DARWIN — N. F. MOTT
W. J. DUNCAN — W. G. PENNEY
A. E. GREEN — A. G. PUGSLEY
A. A. HALL — L. ROSENHEAD
D. R. HARTREE — O. G. SUTTON
L. HOWARTH — ALEXANDER THOM
WILLIS JACKSON — A. H. WILSON

J. R. WOMERSLEY

Executive Editors

V. C. A. FERRARO — D. M. A. LEGGETT

THE QUARTERLY JOURNAL OF MECHANICS AND APPLIED MATHEMATICS is published at 15*s.* net for a single number with an annual subscription (for four numbers) of 50*s.* post free.

NOTICE TO CONTRIBUTORS

1. *Communication.* Papers should be communicated to one or other of the Executive Editors, by name, at King's College, Strand, London, W.C. 2.

2. *Presentation.* Manuscripts should preferably be typewritten, and each paper should be preceded by a summary not exceeding 300 words in length. References to literature should be given in standard order, *author, title of journal, volume number, date, page.* These should be placed at the end of the paper and arranged according to the order of reference in the paper.

3. *Diagrams.* The number of diagrams should be kept to the minimum consistent with clarity. The lines of the figures should be drawn in ink either on draughtsman's paper or on good quality white paper. Each individual line in the figure should bear reducing to one-half of the size of the original, and great care should be exercised to see that the lines are regular in thickness, especially where they meet. Lettering of the figure should be in pencil and should be sufficient to define clearly the lines and curves in it. The writing of formulae or of explanations on the diagram itself should be avoided. All explanations of symbols, etc., should be given in underline. Contributors should indicate on their manuscripts where figures should be inserted.

4. *Tables.* Tables should preferably be arranged so that they can be printed with the columns parallel to the longer edge of the page.

5. *Notation.* All single letters used to denote vectors in the manuscript should be marked by underlining with a wavy line. Scalar and vector products should be denoted by $\underset{\sim}{a} . \underset{\sim}{b}$ and $\underset{\sim}{a} \wedge \underset{\sim}{b}$ respectively. Real and imaginary parts of complex quantities should be denoted by re and im respectively.

6. *Offprints.* Authors of papers will be entitled to 25 free offprints. This number is available for sharing between authors of joint papers.

7. All correspondence other than that dealing with contributions should be addressed to the Publisher:

GEOFFREY CUMBERLEGE
OXFORD UNIVERSITY PRESS
AMEN HOUSE, LONDON, E.C. 4

TH

Th
right
Th
and
∫ Bi(
Tal
being

1. In
THE
incli
door
of bo
oppo
Th
be at
infini
a suit
Ot
and b

2. In
We
be fre
Also
plane

where
bendi
If

[Qua
5092.

THE PROBLEM OF AN INFINITE PLATE UNDER AN INCLINED LOADING, WITH TABLES OF THE INTEGRALS OF $\mathrm{Ai}(\pm x)$ AND $\mathrm{Bi}(\pm x)$

By M. ROTHMAN (*The Northern Polytechnic, Holloway, N.7*)

[Received 4 September 1951; revised 8 May 1952]

SUMMARY

The present paper deals with the problem of an infinite plate uniformly loaded at right angles to the infinite edges which are freely pivoted, the other two being free.

The solution is found to depend ultimately on tables of the functions $\int \mathrm{Ai}(\pm x)\,dx$ and $\int \mathrm{Bi}(\pm x)\,dx$, all of which have been tabulated over the range $|x| \leqslant 10$ except $\int \mathrm{Bi}(+x)\,dx$ which is given for the range $x \leqslant 2$.

Tables of the functions $\int \mathrm{Gi}(x)\,dx$ and $\int \mathrm{Hi}(-x)\,dx$ are also given to $x = 2$, these being necessary for the complete solution of the problem.

1. Introduction

THE action of wind or rain on a large door introduces the problem of an inclined loading; this may be assumed constant over the surface of the door, taken to be a rectangular plate, which may be subject to a variety of boundary conditions but which is commonly freely pivoted along two opposite edges and free along the other two as in a sliding door.

This paper considers the simplest case in which the load is assumed to be at right angles to the freely pivoted edges, which are in turn assumed infinitely long, and at a constant angle to the plane of the plate. This is a suitable approximation for a long door.

Other possible cases are those of a finite plate subject to the same loading, and both cases subject to a skew loading.

2. Infinite plate under constant inclined loading

We assume the plate to be freely pivoted along the infinite edges and to be free along the other two, so that the problem becomes two-dimensional. Also if the loading be p per unit width and be inclined at an angle θ to the plane of the plate, then, taking axes as in Fig. 1, we are led to the equation

$$\frac{dM}{dx} = -Y + X\frac{dy}{dx},$$

where X, Y are the horizontal and vertical components of force and M the bending moment at the point (x, y).

If D is the plate modulus, this equation becomes

$$-D\frac{d^3y}{dx^3} - X\frac{dy}{dx} = -Y,$$

and as $X = px\cos\theta + S$ and $Y = px\sin\theta - \frac{1}{2}pl\sin\theta$, it can be written as

$$\frac{d^3y}{d\xi^3} + A\xi\frac{dy}{d\xi} = B\xi + C, \tag{2.1}$$

where $\xi \equiv X$, and A, B, C are constants given by the relations

$$A = (Dp^2\cos^2\theta)^{-1}, \qquad B = \tan\theta(Dp^3\cos^3\theta)^{-1},$$

$$C = (C_2 - C_1\tan\theta)(Dp^3\cos^3\theta)^{-1}, \quad C_1 = S, \quad \text{and} \quad C_2 = -\tfrac{1}{2}pl\sin\theta,$$

S being the horizontal reaction at the hinge O.

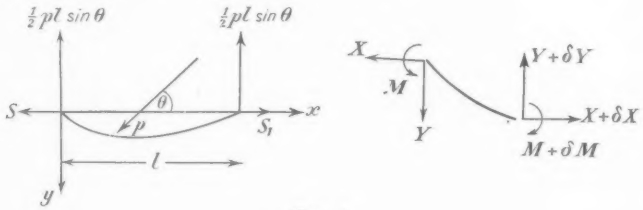

FIG. 1.

The complementary function of (2.1) is given by

$$W = \xi^{\frac{1}{2}}[\alpha J_{\frac{1}{3}}(\tfrac{2}{3}A^{\frac{1}{2}}\xi^{\frac{3}{2}}) + \beta J_{-\frac{1}{3}}(\tfrac{2}{3}A^{\frac{1}{2}}\xi^{\frac{3}{2}})], \qquad W = dy/d\xi,$$

or $W = a\mathrm{Ai}(-\xi) + b\mathrm{Bi}(-\xi)$, α, β, a, b being constants, and the particular integrals corresponding to $B\xi$ and C by

$$B\xi/A \quad \text{and} \quad C\sum_0^{\infty}[(-3A)^r r!\,\xi^{3r+3}/(3r+3)!]$$

respectively, so that the complete solution of equation (2.1) is

$$y = \alpha\int \xi^{\frac{1}{2}}J_{\frac{1}{3}}(\tfrac{2}{3}A^{\frac{1}{2}}\xi^{\frac{3}{2}})\,d\xi + \beta\int \xi^{\frac{1}{2}}J_{-\frac{1}{3}}(\tfrac{2}{3}A^{\frac{1}{2}}\xi^{\frac{3}{2}})\,d\xi +$$

$$+ B\xi/A + C\sum_0^{\infty}[(-3A)^r r!\,\xi^{3r+3}/(3r+3)!] + F. \tag{2.2}$$

The last but one term on the right-hand side of (2.2) can also be written

$$-\frac{C}{\pi}\int_0^{-\xi}\mathrm{Gi}(t)\,dt,$$

$\mathrm{Gi}(t)$ being the function defined by Scorer (**1**), which can be shown to satisfy the equations

$$\mathrm{Gi}(t) = \tfrac{1}{3}\mathrm{Bi}(t) + \mathrm{Ai}(t)\int_0^t \mathrm{Bi}(u)\,du - \mathrm{Bi}(t)\int_0^t \mathrm{Ai}(u)\,du,$$

$$\mathrm{Gi}'(t) = \tfrac{1}{3}\mathrm{Bi}'(t) + \mathrm{Ai}'(t)\int_0^t \mathrm{Bi}(u)\,du - \mathrm{Bi}'(t)\int_0^t \mathrm{Ai}(u)\,du,$$

$$\mathrm{Gi}''(t) - t\,\mathrm{Gi}(t) = -1/\pi.$$

Thus (2.2) can be written

$$y = -a\int_0^{\xi} \mathrm{Ai}(t)\,dt - b\int_0^{\xi} \mathrm{Bi}(t)\,dt - \frac{C}{\pi}\int_0^{\xi} \mathrm{Gi}(t)\,dt + \frac{B\xi}{A} + F. \quad (2.3)$$

Substituting the boundary conditions

$$y = 0, \quad \frac{d^2y}{dx^2} = 0 \quad \text{when } x = 0 \text{ and } l,$$

i.e. $$y = 0, \quad \frac{d^2y}{dx^2} = 0 \quad \text{when } \xi = C_1 \text{ and } pl\cos\theta + C_1$$

we then have four equations for the four constants a, b, F, and C (which depends on the unknown S).

3. Tables of the integrals of $\mathrm{Ai}(\pm x)$ and $\mathrm{Bi}(\pm x)$

It is seen from (2.3) that the complete solution of the problem is dependent on tables of $\int \mathrm{Ai}(x)\,dx$ and $\int \mathrm{Bi}(x)\,dx$.

These integrals were computed at intervals of 0·1 using the method of reduced derivatives described in (**2**), and the author is grateful to Dr. J. C. P. Miller for lending him the manuscript of his tables of reduced derivatives of $\mathrm{Bi}(x)$, his unpublished table of same for $\mathrm{Ai}(x)$, and for some very helpful advice and criticism.

This integral of $\mathrm{Ai}(x)$ was taken to $|x| \leqslant 10$, but is given here only as far as $x = 7{\cdot}5$ in the positive sense, having reached its asymptotic value of $\frac{1}{3}$ to 7 decimal places. The integral of $\mathrm{Bi}(x)$ was also taken to $x = -10$ but only to $x = +2$ as it tends to infinity in the positive sense and it is the integral of $\mathrm{Bi}(-x)$ which is of primary importance.

Both integrals were also computed from their ascending power series

$$\int \mathrm{Ai}(\pm x)\,dx = \frac{2}{3^{\frac{2}{3}}\Gamma(\frac{5}{3})}\left[x \pm \frac{x^4}{2.3.4} + \frac{x^7}{2.3.5.6.7} \pm \frac{x^{10}}{2.3.5.6.8.9.10} + \cdots\right] -$$

$$- \frac{1}{3^{\frac{1}{3}}\Gamma(\frac{4}{3})}\left[\pm\frac{x^2}{2} + \frac{x^5}{3.4.5} \pm \frac{x^8}{3.4.6.7.8} + \cdots\right],$$

$$\frac{1}{\sqrt{3}}\int \mathrm{Bi}(\pm x)\,dx = \frac{2}{3^{\frac{2}{3}}\Gamma(\frac{5}{3})}\left[x \pm \frac{x^4}{2.3.4} + \cdots\right] + \frac{1}{3^{\frac{1}{3}}\Gamma(\frac{4}{3})}\left[\pm\frac{x^2}{2} + \frac{x^5}{3.4.5} \pm \cdots\right]$$

for $|x| \leqslant 2$, at intervals of 0·1.

The results here given are to 7 decimals, though the tables have been computed to 8 decimals throughout and for intervals of 0·01 to $x = 2$.

It might be noted that

$$\int_0^x \mathrm{Ai}(t)\,dt = \pi\{\mathrm{Ai}'(x)\mathrm{Gi}(x) - \mathrm{Ai}(x)\mathrm{Gi}'(x)\} + \tfrac{1}{3}$$
$$= \pi\{\mathrm{Ai}(x)\mathrm{Hi}'(x) - \mathrm{Ai}'(x)\mathrm{Hi}(x)\} - \tfrac{2}{3},$$
$$\int_0^x \mathrm{Bi}(t)\,dt = \pi\{\mathrm{Bi}'(x)\mathrm{Gi}(x) - \mathrm{Bi}(x)\mathrm{Gi}'(x)\} = \pi\{\mathrm{Bi}(x)\mathrm{Hi}'(x) - \mathrm{Bi}'(x)\mathrm{Hi}(x)\} \tag{3.1}$$

so that the tables of $\mathrm{Gi}(x)$, $\mathrm{Gi}'(x)$, or $\mathrm{Hi}(x)$, $\mathrm{Hi}'(x)$ could have been computed as alternatives. In general this would be preferable and, in fact, tables of $\mathrm{Gi}(x)$ and $\mathrm{Hi}(x)$, but not their derivatives, are available in (**1**), as these are better behaved functions than the ones computed; but the solution of the problem under consideration would necessitate the application of formulae (3.1) so frequently that it was thought advisable to keep to the integrals of $\mathrm{Ai}(\pm x)$ and $\mathrm{Bi}(\pm x)$.

It is hoped to publish tables of integrals of $\mathrm{Gi}(x)$ and $\mathrm{Hi}(-x)$ later.

I also wish to express my thanks to my former colleague Mr. R. D. Lord for his helpful criticism and suggestions.

REFERENCES

1. R. S. Scorer, *Quart. J. Mech. and Applied Math.* **3** (1950), 107.

2. J. C. P. Miller, *B.A. Mathematical Tables*, Part-volume B, 'The Airy Integral' (1946), B7.

REFERENCE TABLES

TABLE 1

x	$\int_0^x \mathrm{Ai}(+x)\,dx$	δ_m^2	x	$\int_0^x \mathrm{Ai}(+x)\,dx$	δ_m^2
0·0	+0·00000 00	−259 19	5·0	+0·33328 76	−25
·1	·03421 01	257 42	·1	·33329 73	20
·2	·06585 15	252 67	·2	·33330 50	16
·3	·09497 09	245 35	·3	·33331 11	13
·4	·12164 06	236 00	·4	·33331 59	10
0·5	+0·14595 33	−225 03	5·5	+0·33331 97	− 8
·6	·16801 79	212 89	·6	·33332 27	7
·7	·18795 52	199 89	·7	·33332 50	4
·8	·20589 45	186 46	·8	·33332 69	5
·9	·22196 97	172 75	·9	·33332 83	2
1·0	+0·23631 73	−169 10	6·0	+0·33332 95	− 1
·1	·24907 33	135 76	·1	·33333 03	1
·2	·26037 12	132 71	·2	·33333 10	1
·3	·27034 09	120 29	·3	·33333 16	1
·4	·27910 66	108 43	·4	·33333 20	1
1·5	+0·28678 67	− 97 30	6·5	+0·33333 23	− 1
·6	·29349 24	86 92	·6	·33333 25	0
·7	·29932 75	77 30	·7	·33333 27	0
·8	·30438 82	68 47	·8	·33333 29	0
·9	·30876 29	60 33	·9	·33333 30	0
2·0	+0·31253 28	− 53 04	7·0	+0·33333 31	0
·1	·31577 11	46 38	·1	·33333 31	0
·2	·31854 43	40 45	·2	·33333 32	0
·3	·32091 19	35 09	·3	·33333 32	0
·4	·32292 74	30 39	·4	·33333 33	0
2·5	+0·32463 80	− 26 20	7·5	+0·33333 33	0
·6	·32608 57	22 52			
·7	·32730 74	19 28			
·8	·32833 55	16 46			
·9	·32919 83	14 01			
3·0	+0·32992 04	− 11 89			
·1	·33052 31	10 04			
·2	·33102 49	8 48			
·3	·33144 15	7 12			
·4	·33178 65	5 97			
3·5	+0·33207 15	− 4 99			
·6	·33230 63	4 16			
·7	·33249 93	3 45			
·8	·33265 76	2 88			
·9	·33278 70	2 35			
4·0	+0·33289 27	− 1 98			
·1	·33297 86	1 60			
·2	·33304 84	1 31			
·3	·33310 50	1 09			
·4	·33315 07	87			
4·5	+0·33318 76	− 71			
·6	·33321 73	59			
·7	·33324 11	46			
·8	·33326 02	39			
·9	·33327 54	29			
5·0	+0·33328 76	− 25			

x	$\int_0^x \mathrm{Bi}(+x)\,dx$	δ_m^2	γ^4
0·0	+0·00000 00	+ 447 67	+ 1
·1	·06373 67	450 82	1
·2	·13199 45	460 98	1
·3	·20487 68	479 13	1
·4	·28256 70	506 29	1
0·5	+0·36533 85	+ 543 41	+ 1
·6	·45356 50	591 89	1
·7	·54773 36	652 97	1
·8	·64845 82	728 37	2
·9	·75649 64	820 03	2
1·0	+0·87276 91	+ 930 31	+ 2
·1	·99838 41	1061 90	2
·2	1·13466 38	1218 36	3
·3	1·28318 00	1403 58	3
·4	1·44579 42	1622 70	4
1·5	+1·62470 81	+1881 46	+ 5
·6	1·82252 33	2187 41	6
·7	2·04231 52	2549 16	7
·8	2·28772 12	2977 52	8
·9	2·56304 90	3485 58	10
2·0	+2·87340 83	+4089 12	+12

TABLE 2

x	$\int_0^x \mathrm{Ai}(-x)\,dx$	δ_m^2	γ^4	x	$\int_0^x \mathrm{Ai}(-x)\,dx$	δ_m^2	γ^4
0·0	−0·00000 00	−259 19	+[illegible]	5·0	−0·71788 22	+ 328 48	− 1
·1	·03679 54	257 37	0	·1	·75103 62	496 83	[illegible]
·2	·07615 70	251 49	[illegible]	·2	·77926 27	643 00	3
·3	·11802 51	241 04	1	·3	·80111 58	758 43	4
·4	·16229 44	225 58	1	·4	·81545 49	835 67	4
0·5	−0·20880 95	−204 67	+1	5·5	−0·82151 82	+ 868 97	− 5
·6	·25736 07	177 96	1	·6	·81897 90	854 93	5
·7	·30768 05	145 24	1	·7	·80797 96	792 52	5
·8	·35944 15	106 43	1	·8	·78914 06	783 65	4
·9	·41225 56	60 51	1	·9	·76354 19	533 08	3
1·0	−0·46567 40	− 10 69	+ 1	6·0	−0·73267 53	+ 348 38	− [illegible]
·1	·51918 94	+ 45 53	0	·1	·69836 93	+ 139 58	− 1
·2	·57224 05	106 65	[illegible]	·2	·66268 96	− 81 20	[illegible]
·3	·62421 79	171 68	0	·3	·62781 93	300 59	+ 2
·4	·67447 31	239 67	0	·4	·59592 62	504 39	3
1·5	−0·72232 88	+309 20	[illegible]	6·5	−0·56902 35	− 679 17	+ 4
·6	·76709 26	378 73	[illegible]	·6	·54883 59	812 33	5
·7	·80807 24	446 49	0	·7	·53667 65	893 86	6
·8	·84459 41	510 59	− 1	·8	·53334 74	916 55	6
·9	·87602 06	568 89	1	·9	·53906 98	877 22	6
2·0	−0·90177 28	+619 26	− 1	7·0	−0·55345 17	− 776 66	+ 6
·1	·92135 09	659 60	1	·1	·57549 72	620 23	5
·2	·93435 56	687 65	1	·2	·60365 96	417 47	3
·3	·94050 97	701 62	2	·3	·63593 60	− 181 07	2
·4	·93967 67	699 76	2	·4	·66999 96	+ 70 46	0
2·5	−0·93187 78	+680 68	− 2	7·5	−0·70336 19	+ 320 89	− 2
·6	·91730 54	643 50	2	·6	·73355 34	550 66	4
·7	·89633 20	587 85	2	·7	·75830 99	741 56	5
·8	·86951 37	513 95	2	·8	·77575 13	877 92	7
·9	·83758 77	422 76	2	·9	·78453 65	947 54	7
3·0	−0·80146 29	+315 93	− 1	8·0	−0·78398 26	+ 943 21	− 7
·1	·76220 32	195 84	1	·1	·77413 57	863 39	7
·2	·72100 37	+ 65 67	1	·2	·75578 55	712 71	6
·3	·67915 91	− 70 76	[illegible]	·3	·73041 93	501 75	4
·4	·63802 56	209 08	[illegible]	·4	·70011 70	+ 246 65	2
3·5	−0·59897 71	−344 27	+ 1	8·5	−0·66739 21	− 32 36	0
·6	·56335 61	471 24	1	·6	·63499 08	311 50	+ 2
·7	·53242 25	584 61	[illegible]	·7	·60566 32	567 69	5
·8	·50730 05	679 25	2	·8	·58192 70	777 28	6
·9	·48892 77	750 36	3	·9	·56584 22	921 00	8
4·0	−[illegible]·47800 75	−793 76	+ 3	9·0	−[illegible]·55881 97	− 976 58	+ 9
·1	·47496 79	806 20	3	·1	·56148 12	960 36	9
·2	·47992 95	785 61	3	·2	·57358 51	848 68	8
·3	·49268 51	731 30	3	·3	·59403 00	657 92	6
·4	·51269 28	643 92	3	·4	·62093 76	403 96	4
4·5	−0·53908 35	−526 06	+ 3	9·5	−0·65181 01	− 109 40	+ 1
·6	·57068 59	381 64	2	·6	·68375 25	+ 198 55	− 2
·7	·60606 63	216 38	1	·7	·71373 85	490 81	4
·8	·64358 51	− 37 35	1	·8	·73889 84	738 58	7
·9	·68146 70	+147 31	[illegible]	·9	·75680 07	916 79	9
5·0	−0·71788 22	+328 48	− 1	10·0	−0·76569 84	+1006 41	−10

TABLE 3

x	$\int_0^x \mathrm{Bi}(-x)\,dx$	δ_m^2	γ^4	x	$\int_0^x \mathrm{Bi}(-x)\,dx$	δ_m^2	γ^4
0·0	−0·00000 00	+447 67	+1	5·0	−0·15873 09	+782 47	−4
·1	·05924 87	450 67	0	·1	·14113 39	693 27	4
·2	·11398 10	458 98	0	·2	·11667 30	566 72	3
·3	·16411 57	471 53	0	·3	·08660 41	408 04	2
·4	·20952 89	487 50	0	·4	·05250 03	224 69	2
0·5	−0·25006 28	+505 82	0	5·5	−0·01617 86	+ 25 60	0
·6	·28553 62	525 37	0	·6	+0·02038 99	−178 46	+1
·7	·31575 56	545 12	0	·7	·05518 54	376 23	2
·8	·34052 58	563 75	0	·8	·08625 18	555 96	3
·9	·35966 27	580 03	0	·9	·11181 25	706 43	4
1·0	−0·37300 50	+592 35	0	6·0	+0·13038 11	−817 70	+5
·1	·38042 77	600 74	−1	·1	·14086 00	881 59	5
·2	·38185 43	602 46	1	·2	·14262 05	892 55	5
·3	·37726 99	596 76	1	·3	·13555 73	848 35	5
·4	·36673 34	582 63	1	·4	·12011 15	749 64	5
1·5	−0·35038 81	+558 92	−1	6·5	+0·09726 08	−601 36	+4
·6	·32847 24	525 01	1	·6	·06847 29	411 65	3
·7	·30132 67	480 17	1	·7	·03562 42	−191 73	2
·8	·26939 97	424 26	1	·8	+0·00088 80	+ 44 33	0
·9	·23325 04	357 33	1	·9	−0·03340 40	280 86	−2
2·0	−0·19354 74	+279 76	−1	7·0	−0·06491 67	+501 46	−3
·1	·15106 46	192 56	1	·1	·09147 36	690 14	5
·2	·10667 18	+ 96 88	1	·2	·11121 47	832 35	6
·3	·06132 23	− 5 34	0	·3	·12273 90	917 00	6
·4	−0·01603 45	112 39	0	·4	·12521 80	934 75	7
2·5	+0·02812 94	−220 54	0	7·5	−0·11847 31	+884 62	−7
·6	·07009 01	327 85	0	·6	·10300 57	767 00	6
·7	·10878 06	430 69	+1	·7	·07997 85	589 58	5
·8	·14317 88	525 62	1	·8	·05114 35	364 40	3
·9	·17234 20	609 02	1	·9	−0·01872 22	+107 91	−1
3·0	+0·19544 25	−677 46	+2	8·0	+0·01475 64	−160 40	+1
·1	·21180 21	727 58	2	·1	·04664 84	419 27	3
·2	·22092 49	756 41	2	·2	·07440 43	647 41	5
·3	·22252 61	761 82	3	·3	·09577 87	825 29	7
·4	·21655 57	741 84	3	·4	·10902 22	936 97	8
3·5	+0·20321 50	−695 75	+3	8·5	+0·11303 86	−971 26	+8
·6	·18296 47	623 66	2	·6	·10749 35	923 59	8
·7	·15652 33	526 88	2	·7	·09285 98	795 99	7
·8	·12485 43	407 78	2	·8	·07039 64	597 77	5
·9	·08914 28	269 74	1	·9	·04205 63	344 75	3
4·0	+0·05076 01	−117 55	+1	9·0	+0·01033 04	− 58 27	+1
·1	+0·01121 78	+ 43 25	0	·1	−0·02196 26	+236 67	−2
·2	−0·02788 79	206 26	0	·2	·05192 24	513 42	4
·3	·06494 00	364 40	−1	·3	·07682 93	746 04	7
·4	·09837 02	510 56	2	·4	·09439 87	911 97	8
4·5	−0·12673 04	+637 36	−3	9·5	−0·10300 27	+994 17	−9
·6	·14876 50	738 18	3	·6	·10183 70	983 06	9
·7	·16347 66	806 98	4	·7	·09101 44	877 69	8
·8	·17018 59	839 33	4	·8	·07157 33	686 38	7
·9	·16857 74	831 38	4	·9	·04539 57	426 03	4
5·0	−0·15873 09	+782 47	−4	10·0	−0·01504 04	+120 95	−1

THE EFFECT OF HEAT TRANSFER ON THE SEPARATION OF A COMPRESSIBLE LAMINAR BOUNDARY LAYER

By C. R. ILLINGWORTH

(*Department of Mathematics, The University, Manchester*)

[Received 13 March 1952; revised 19 September 1952]

SUMMARY

The paper treats problems of laminar boundary layers with non-uniform density, due either to large temperature differences or to large Mach numbers. An approximate method is developed for cases when the stream velocity and the wall temperature are non-uniform. In the examples to which the method is applied, only uniform wall temperatures are considered. Attention is concentrated on the effect of a given pressure gradient in producing thinning, thickening, or separation of the boundary layer at a wall at various uniform temperatures.

For zero Mach number and a small temperature difference, and various given main-stream velocity distributions, the calculations show fairly satisfactory agreement with known exact results. Under other conditions the effect of the pressure gradient is found to be enhanced or reduced according as the ratio of stream temperature to wall temperature is less or greater than 1. Thus, in uniformly retarded flow the relative fall in velocity before separation varies as the square root of this ratio, showing little independent variation with Mach number. This result is checked against previous calculations at high Mach numbers for zero heat transfer. The general conclusion mentioned above is explained by the fact that pressure gradient produces thinning, thickening, or separation principally by its action on the fluid very near the wall, and so the effects are enhanced if and only if this fluid is hotter (and so lighter) than that in the main stream.

1. Introduction

THE study of the laminar boundary layer of a gas in steady two-dimensional flow past a rigid wall is now well developed in the case when the main stream is uniform. The work of Crocco (**1**) deals with the boundary-layer flow when the temperature of the wall is uniform, both with and without heat transfer between the wall and the gas, and the work of Chapman and Rubesin (**2**) is concerned with the flow when the wall temperature is non-uniform, in which case there is heat transfer.

However, when the main-stream velocity is non-uniform, the calculation of the boundary-layer flow is in general a formidable task, which may require the employment of an electronic calculating machine along the lines initiated by Cope and Hartree (**3**). This task is very much simplified under three conditions, viz. (i) that the Prandtl number of the gas is 1, (ii) that its viscosity is proportional to the absolute temperature, and (iii) that there

is no heat interchange between the wall and the gas. The first and third of these conditions together imply that the wall temperature is uniform. The simplicity effected under these conditions lies in the fact that the compressible boundary-layer flow can be easily expressed in terms of a related incompressible flow.

The object of the present paper is to examine compressible boundary layers with non-uniform main streams and non-uniform wall temperatures. The condition of zero heat transfer at the wall is of course discarded, but only at the cost of introducing approximations in the boundary-layer equations: the other two conditions concerning the Prandtl number and the viscosity are retained. These approximations are made by means of an artifice used by Lighthill (**4**) in his discussion of heat transfer in boundary layers. After solutions of the approximate equations have been given in section 2 for cases when the main-stream velocity and the wall-temperature distributions can be expressed as power series, some particular cases are discussed. These all concern uniform wall temperature for which the computation is relatively simple. In section 4 the boundary layer of a blunt-nosed symmetrical cylinder is considered, and in section 5 the boundary layer corresponding to a linearly decreasing main-stream velocity is discussed in some detail. This is a suitable test case as regards separation of the boundary layer. For in this case the point of separation for incompressible flow has been calculated with 1 per cent. accuracy by Howarth (**5**), and Stewartson (**6**) has solved the same problem in compressible flow, under the three simplifying conditions already referred to. It has been found convenient, therefore, to use this particular flow in looking for alterations in the position of separation when the wall temperature is changed from the uniform value corresponding to no heat transfer.

2. The approximate equations

The exact equations of steady two-dimensional boundary-layer flow when the Prandtl number is 1 are

$$\partial(\rho u)/\partial x+\partial(\rho v)/\partial y = 0, \tag{1}$$

$$\rho(u\,\partial u/\partial x+v\,\partial u/\partial y) = \rho_1 u_1 du_1/dx+\partial(\mu\,\partial u/\partial y)/\partial y, \tag{2}$$

$$\rho(u\,\partial i/\partial x+v\,\partial i/\partial y)+u\,\rho_1 u_1\,du_1/dx = \partial(\mu\,\partial i/\partial y)/\partial y+\mu(\partial u/\partial y)^2, \tag{3}$$

where x, y are orthogonal curvilinear coordinates measured along and perpendicular to the wall, u, v are the corresponding velocity components, ρ, i are the density and specific enthalpy, μ is the viscosity, and the suffix 1 refers to the main stream, where conditions depend only on x. From (2) and (3) it follows that

$$\rho(u\,\partial h/\partial x+v\,\partial h/\partial y) = \partial(\mu\,\partial h/\partial y)/\partial y, \tag{4}$$

where h is the specific total energy $i+\frac{1}{2}u^2$. In the main stream h_1 is a constant (equal to the stagnation enthalpy) by Bernoulli's equation, and h = constant = h_1 is the particular integral of (4) appropriate for the case of no heat transfer at the wall.

In terms of von Mises's coordinates x, ψ, where ψ is the stream function defined by $\rho u = \partial\psi/\partial y$, $\rho v = -\partial\psi/\partial x$, (2) and (4) become

$$\rho u\,\partial u/\partial x = \rho_1 u_1\,du_1/dx + \rho u\,\partial(\mu\rho u\,\partial u/\partial\psi)/\partial\psi, \tag{5}$$

$$\partial h/\partial x = \partial(\mu\rho u\,\partial h/\partial\psi)/\partial\psi. \tag{6}$$

It is now convenient to introduce non-dimensional dependent variables f, g instead of u, h by means of the equation

$$u^2 = i_1(b-f), \tag{7}$$

where $b = u_1^2/i_1 = (\gamma-1)M_1^2$, M_1 being the Mach number of the main stream, and the equation

$$h = h_1(1-g). \tag{8}$$

With the help of Bernoulli's equation in the form $di_1/dx + u_1\,du_1/dx = 0$, (5) becomes

$$u\,\partial(\mu\rho\,\partial f/\partial\psi)/\partial\psi - \partial f/\partial x + db/dx + (di_1/i_1\,dx)[2(\rho_1/\rho)+b-f] = 0. \tag{9}$$

Now the pressure p in the boundary layer at the station x is the same as the main-stream pressure $p_1(x)$, and therefore, with attention restricted to a perfect gas with constant specific heats for which $p = (\gamma-1)\rho i/\gamma$, it follows that

$$\rho_1/\rho = i/i_1. \tag{10}$$

From (7) and (8), $$i/i_1 = (1+\tfrac{1}{2}b)(1-g) - \tfrac{1}{2}(b-f), \tag{11}$$

and, since $i_1(1+\frac{1}{2}b) = h_1 = \text{constant}$,

$$di_1/i_1\,dx = -(db/dx)/(2+b). \tag{12}$$

Equations (9)–(12) give

$$u\,\partial(\mu\rho\,\partial f/\partial\psi)/\partial\psi - \partial f/\partial x + (db/dx)g = 0, \tag{13}$$

and (6) and (8) give

$$\partial(\mu\rho u\,\partial g/\partial\psi)/\partial\psi - \partial g/\partial x = 0. \tag{14}$$

Equations (13) and (14) are our final forms for the exact boundary-layer equations when the Prandtl number is 1, and they are completed by the addition of boundary conditions. The latter are derived from the facts that u and h must be equal to u_1 and h_1 at the edge of the boundary layer, and that at the wall (quantities relating to which will be characterized by the suffix 0) $u = 0$ and either the enthalpy distribution $i_0(x)$ or the rate $q_0(x)$ of heat transfer per unit area from the wall to the gas is prescribed. Hence the boundary conditions are:

$f = g = 0$ at $x = 0$, for all values of ψ, and at $\psi = \infty$ for all positive values of x;

$f = b$, and either $g = 1 - i_0/h_1$ or $-\mu\,\partial i/\partial y = \mu\rho u h_1\,\partial g/\partial\psi = q_0$ at $\psi = 0$ for all positive values of x.

Following Lighthill (4), approximations are made in (13) and (14) by replacing the factor u which occurs in each equation by an expression obtained as follows. By identifying the shearing stress at the point (x, ψ) with the stress $\tau_0(x)$ at the wall at the same station, the equation

$$\mu\,\partial u/\partial y = \mu\rho u\,\partial u/\partial\psi = \tau_0(x) \tag{15}$$

is obtained. Now the remaining condition to be imposed, that viscosity is proportional to absolute temperature, implies that

$$\mu\rho/\mu_1\rho_1 = \rho i/\rho_1 i_1 = 1. \tag{16}$$

Hence (15) can be integrated to give

$$u = \left[\frac{2\tau_0(x)\psi}{\mu_1(x)\rho_1(x)}\right]^{\frac{1}{2}}. \tag{17}$$

This approximate expression for u is substituted in (13) and (14). It is most accurate near the wall (according to (15) it gives the slope of the velocity profile correctly at $\psi = 0$), but it overestimates u in the outer parts of the boundary layer. However, the inaccuracy of u becomes less serious the greater the distance from the wall, because the cofactors of u in (13) and (14) tend to zero as $\psi \to \infty$. In making this substitution it is timely to recall Lighthill's quantitative statement concerning the errors which the substitution involves at low speeds. For main streams of the form $u_1 = cx^m$, Lighthill shows that the shearing stress at the wall is underestimated by 6 per cent. when the index $m = 0$ and by nearly 8 per cent. for all values of m greater than $\frac{1}{3}$, and that the heat transfer to the wall, when it is at a uniform temperature, is overestimated by 3 per cent. when $m = 0$, by $18\frac{1}{2}$ per cent. when $m = 1$, and by 24 per cent. as $m \to \infty$.

When the substitution is made, (13) and (14) become, with the help of (16),

$$\psi^{\frac{1}{2}}\,\partial^2 f/\partial\psi^2 - \partial f/\partial t + (db/dt)g = 0, \tag{18}$$

$$\partial(\psi^{\frac{1}{2}}\,\partial g/\partial\psi)/\partial\psi - \partial g/\partial t = 0, \tag{19}$$

where $t = \int_0^x [2\mu_1(\xi)\rho_1(\xi)\tau_0(\xi)]^{\frac{1}{2}}\,d\xi$ is the new independent variable. The Heaviside transforms of these equations are

$$\psi^{\frac{1}{2}}\frac{d^2\bar{f}}{d\psi^2} - p\bar{f} + \overline{\frac{db}{dt}}\,g = 0, \tag{20}$$

$$\frac{d}{d\psi}\left(\psi^{\frac{1}{2}}\frac{d\bar{g}}{d\psi}\right) - p\bar{g} = 0, \tag{21}$$

since $f = g = 0$ at $t = 0$, where bars denote transforms and p denotes

the operator $\partial/\partial t$.† These equations are formally the same as equations (66) and (21) of Lighthill's paper, save for the extra term $\overline{(db/dt)g}$ in (20) arising from the Mach-number gradient in the main stream. The solution of (21) satisfying the conditions $g = 0$ at $\psi = \infty$ and $g = 1-i_0(t)/h_1$ at $\psi = 0$ is

$$\bar{g} = \frac{\pi}{(-\frac{2}{3})!}(\tfrac{2}{3}p^{\frac{1}{2}}\psi^{\frac{3}{2}})^{\frac{1}{3}}\mathrm{Kh}_{\frac{1}{3}}(\tfrac{4}{3}p^{\frac{1}{2}}\psi^{\frac{3}{2}})\left(1-\frac{i_0(t)}{h_1}\right), \tag{22}$$

where $\mathrm{Kh}_n(z)$ is the Bessel function $[I_{-n}(z)-I_n(z)]/\sin n\pi$. If q_0, and not i_0, is specified, (22) will still stand as the operational form of $\bar{g}$ with $i_0(t)$ to be determined from the relation

$$q_0 = [\mu\rho u h_1\,\partial g/\partial\psi]_{\psi=0} = [(2\mu_1\rho_1\tau_0\psi)^{\frac{1}{2}}h_1\,\partial g/\partial\psi]_{\psi=0},$$

which gives

$$\left(\frac{2}{\mu_1\rho_1\tau_0}\right)^{\frac{1}{2}}\frac{q_0}{h_1} = \left(\frac{\partial g}{\partial\psi^{\frac{1}{2}}}\right)_{\psi=0} = -\frac{(\frac{2}{3})^{\frac{2}{3}}}{(\frac{1}{3})!}\left[\frac{1-i_0(+0)/h_1}{t^{\frac{1}{3}}}-\frac{1}{h_1}\int_0^t\frac{di_0(\xi)/d\xi}{(t-\xi)^{\frac{1}{3}}}\,d\xi\right], \tag{23}$$

corresponding to Lighthill's equation (26). The problem is clearly more straightforward if the wall temperature is specified, and in what follows only this alternative will be considered.

At this stage it is also convenient to introduce restrictions on the forms of the main-stream velocity and wall-temperature distributions, namely that

$$b(t) = \sum_{n=0}^{\infty}\beta_n t^{mn}, \qquad 1-i_0(t)/h_1 = \sum_{n=0}^{\infty}\alpha_n t^{mn}, \tag{24}$$

where m is a positive number and where the α's and β's are constants to be determined later. Then (22) becomes

$$\bar{g} = \frac{\pi}{(-\frac{2}{3})!}(\tfrac{2}{3}\psi^{\frac{3}{2}})^{\frac{1}{3}}\sum_{n=0}^{\infty}(mn)!\,\alpha_n\,p^{-mn+\frac{1}{3}}\mathrm{Kh}_{\frac{1}{3}}(\tfrac{4}{3}p^{\frac{1}{2}}\psi^{\frac{3}{2}}),$$

and so, according to Jeffreys and Jeffreys (*Methods of Mathematical Physics*, 2nd edition, p. 613),

$$g = \sum_{n=0}^{\infty}\alpha_n g_n(\eta)t^{mn}, \tag{25}$$

where $\eta = 4\psi^{\frac{3}{2}}/9t$ and

$$g_n(\eta) = \frac{(mn)!}{(-\frac{2}{3})!}e^{-\eta}U(mn+\tfrac{2}{3},\tfrac{2}{3},\eta) = \frac{1}{(-\frac{2}{3})!}\int_{\eta}^{\infty}e^{-\xi}(\xi-\eta)^{mn}\xi^{-mn-\frac{4}{3}}\,d\xi, \tag{26}$$

in which

$$U(\alpha,\gamma,\eta) = \frac{(-\gamma)!}{(\alpha-\gamma)!}{}_1F_1(\alpha,\gamma,\eta)+\frac{(\gamma-2)!}{(\alpha-1)!}\eta^{1-\gamma}{}_1F_1(1+\alpha-\gamma,2-\gamma,\eta),$$

† Since the pressure will not be required again, there should be no confusion in this new use of the letter p.

in the usual notation for confluent hypergeometric functions. The function f is given by

$$f = \sum_{n=0}^{\infty} h_n(\eta) t^{mn}, \tag{27}$$

where $h_n(0) = \beta_n$, $h_n(\infty) = 0$, and

$$\eta h_n'' + (\eta + \tfrac{1}{3}) h_n' - mnh_n + m \sum_{r=0}^{n-1} (n-r) \alpha_r \beta_{n-r} g_r = 0 \tag{28}$$

(where dashes denote differentiation with respect to η), as can easily be verified by substitution in (18). The solution of (28) for the given boundary conditions is

$$h_n(\eta) = \beta_n f_n(\eta) + \tfrac{3}{2} m \sum_{r=0}^{n-1} (n-r) \alpha_r \beta_{n-r} \Big[f_n(\eta) \int_0^{\eta} {}_1F_1(mn+1, \tfrac{5}{3}, \xi) g_r(\xi)\, d\xi + \\ + e^{-\eta} \eta^{\frac{2}{3}} {}_1F_1(mn+1, \tfrac{5}{3}, \eta) \int_{\eta}^{\infty} \xi^{-\frac{2}{3}} e^{\xi} f_n(\xi) g_r(\xi)\, d\xi \Big], \tag{29}$$

where

$$f_n(\eta) = \frac{(mn)!}{(-\frac{1}{3})!} e^{-\eta} U(mn+\tfrac{1}{3}, \tfrac{1}{3}, \eta) = \frac{1}{(-\frac{1}{3})!} \int_{\eta}^{\infty} e^{-\xi} (\xi - \eta)^{mn} \xi^{-mn-\frac{1}{3}}\, d\xi.$$

The solution is completed by expressing x in terms of t, because it is then a straightforward matter to find the α's and β's from the data, which give b and i_0 as functions of x. To do this, τ_0 must be expressed in terms of t by means of the equation

$$\tau_0 = (\mu \rho u\, \partial u / \partial \psi)_{\psi=0} = -\tfrac{1}{2} \mu_1 \rho_1 i_1 (\partial f / \partial \psi)_{\psi=0} \\ = -2^{-\frac{2}{3}} 3^{-\frac{1}{3}} \mu_1 \rho_1 i_1 t^{-\frac{2}{3}} \sum_{n=0}^{\infty} \Big(\lim_{\eta \to 0} \eta^{\frac{1}{3}} h_n' \Big) t^{mn}.$$

Now, for small η,

$$f_n(\eta) = 1 + \frac{(mn)!}{(-\frac{1}{3})!} \frac{(-\frac{5}{3})!}{(mn-\frac{2}{3})!} \eta^{\frac{2}{3}} + O(\eta),$$

so that

$$\lim_{\eta \to 0} (\eta^{\frac{1}{3}} h_n') = -k_n \beta_n + \sum_{r=0}^{n-1} k_{nr} \alpha_r \beta_{n-r},$$

where

$$k_n = \frac{(mn)!\,(-\frac{2}{3})!}{(mn-\frac{2}{3})!\,(-\frac{1}{3})!}$$

and

$$k_{nr} = m(n-r) \int_0^{\infty} \xi^{-\frac{2}{3}} e^{\xi} f_n(\xi) g_r(\xi)\, d\xi.$$

Since $f_n(\eta)$ is a solution of $\eta f_n'' + (\eta + \frac{1}{3}) f_n' - mnf_n = 0$,

$$k_{nr} = \frac{m(n-r)}{mn} \int_0^{\infty} \frac{d}{d\xi} [\xi^{\frac{1}{3}} e^{\xi} f_n'(\xi)] g_r(\xi)\, d\xi \\ = \frac{n-r}{n} \Big[k_n - \int_0^{\infty} \xi^{\frac{1}{3}} e^{\xi} f_n'(\xi) g_r'(\xi)\, d\xi \Big]. \tag{30}$$

It is convenient at this juncture to evaluate k_{n0}, which will be required later. Since

$$f_n'(\xi) = -\frac{mn}{(-\frac{1}{3})!}\int_\xi^\infty e^{-u}(u-\xi)^{mn-1}u^{-mn-\frac{1}{3}}\,du,$$

$$\int_0^\infty \xi^{\frac{1}{3}}e^{\xi}f_n(\xi)g_0'(\xi)\,d\xi = -\frac{1}{(-\frac{2}{3})!}\int_0^\infty \xi^{-\frac{1}{3}}f_n'(\xi)\,d\xi$$

$$= \frac{mn}{(-\frac{1}{3})!\,(-\frac{2}{3})!}\int_0^\infty \xi^{-\frac{1}{3}}\left[\int_\xi^\infty e^{-u}\sum_{r=0}^\infty \binom{mn-1}{r}(-\xi)^r u^{-\frac{1}{3}-r}\,du\right]d\xi$$

$$= \frac{mn}{(-\frac{1}{3})!\,(-\frac{2}{3})!}\sum_{r=0}^\infty \binom{mn-1}{r}(-1)^r\frac{1}{r+\frac{2}{3}}\int_0^\infty e^{-u}u^{-\frac{2}{3}}\,du$$

after integration by parts, and this is equal to

$$\frac{mn}{(-\frac{1}{3})!}\int_0^1 \xi^{-\frac{1}{3}}(1-\xi)^{mn-1}\,d\xi = \frac{(mn)!}{(mn-\frac{1}{3})!}.$$

Hence
$$k_{n0} = k_n\left[1-\frac{(mn-\frac{2}{3})!\,(-\frac{1}{3})!}{(mn-\frac{1}{3})!\,(-\frac{2}{3})!}\right]$$
where
$$k_n = \frac{(mn)!\,(-\frac{2}{3})!}{(mn-\frac{2}{3})!\,(-\frac{1}{3})!} \qquad (31)$$

The skin friction may now be expressed as

$$\tau_0(t) = 2^{-\frac{1}{3}}3^{-\frac{1}{3}}\mu_s\rho_s i_s t^{-\frac{1}{3}}\Big(1+\tfrac{1}{2}\sum_{n=0}^\infty \beta_n t^{mn}\Big)^{-(2\gamma-1)/(\gamma-1)}\sum_{n=0}^\infty\Big(k_n\beta_n-\sum_{r=0}^{n-1}k_{nr}\alpha_r\beta_{n-r}\Big)t^{mn}, \qquad (32)$$

where the suffix s refers to stagnation conditions in the main stream, so that

$$\frac{\mu_1\rho_1 i_1}{\mu_s\rho_s i_s} = \frac{\rho_1 i_1^2}{\rho_s i_s^2} = \left(\frac{i_1}{i_s}\right)^{(2\gamma-1)/(\gamma-1)} = (1+\tfrac{1}{2}b)^{-(2\gamma-1)/(\gamma-1)}.$$

It follows that

$$x = \int_0^t [2\mu_1(\xi)\rho_1(\xi)\tau_0(\xi)]^{-\frac{1}{2}}\,d\xi$$

$$= 3^{\frac{1}{2}}(2^{\frac{1}{2}}\mu_s\rho_s i_s^{\frac{1}{2}})^{-1}\int_0^t \xi^{\frac{1}{2}}\Big(1+\tfrac{1}{2}\sum_{n=0}^\infty\beta_n\xi^{mn}\Big)^{(3\gamma-1)/2(\gamma-1)}\times$$
$$\times\Big[\sum_{n=0}^\infty\Big(k_n\beta_n-\sum_{r=0}^{n-1}k_{nr}\alpha_r\beta_{n-r}\Big)\xi^{mn}\Big]^{-\frac{1}{2}}\,d\xi. \qquad (33)$$

Finally, from (23), the rate of heat transfer per unit area from the wall is

$$q_0 = -[2^{\frac{1}{3}}3^{\frac{2}{3}}(\tfrac{1}{3})!]^{-1}\mu_s\rho_s i_s^{\frac{3}{2}}t^{-\frac{1}{2}}\Big(1+\tfrac{1}{2}\sum_{n=0}^{\infty}\beta_n t^{mn}\Big)^{-(3\gamma-1)/2(\gamma-1)}\times$$

$$\times\Big[\sum_{n=0}^{\infty}\Big(k_n\beta_n-\sum_{r=0}^{n-1}k_{nr}\alpha_r\beta_{n-r}\Big)t^{mn}\Big]^{\frac{1}{2}}\sum_{n=0}^{\infty}\frac{(mn)!\,(-\frac{1}{3})!}{(mn-\frac{1}{3})!}\alpha_n t^{mn}. \quad (34)$$

The boundary-layer flow has now been expressed in terms of the parameter t. The velocity is given by

$$u^2 = \frac{i_s(b-f)}{1+\frac{1}{2}b},$$

the enthalpy by

$$i = i_s\Big(\frac{1+\frac{1}{2}f}{1+\frac{1}{2}b}-g\Big),$$

and the value of x by (33). The y-coordinate is recovered from

$$y = \int_0^{\psi}\frac{d\psi}{\rho u} = \frac{3^{\frac{1}{2}}}{2^{\frac{1}{2}}\rho_s i_s^{\frac{1}{2}}}(1+\tfrac{1}{2}b)^{(\gamma+1)/2(\gamma-1)}\eta^{\frac{1}{3}}\int_0^{\eta}\frac{1+\frac{1}{2}f-(1+\frac{1}{2}b)g}{\eta^{\frac{1}{3}}(b-f)^{\frac{1}{2}}}\,d\eta.$$

Finally, the shearing stress and heat transfer at the wall are given by (32) and (34).

So far the number m has not been specified. It is clear, from (33), that if β_r is the first non-vanishing β, then $x \propto t^{\frac{1}{3}-\frac{1}{2}mr}$ near $t = 0$, so that the series for $b(x)$ begins with the term constant $\times x^{mr/(\frac{4}{3}-\frac{1}{2}mr)}$ and the powers of successive terms in the series differ by $m/(\frac{4}{3}-\frac{1}{2}mr)$. Hence, if $u_1(x)$ begins with the term x^N and continues with the terms x^{N+P}, x^{N+2P},..., $b(x)$ will contain the terms x^{2N}, x^{2N+P}, x^{2N+2P},... and so $m = \frac{4}{3}P/(N+1)$, $r = 2N/P$ with the restriction that r is an integer. It should be noticed here that the power series for $i_0(x)$ must be of the same kind as that for $b(x)$, because of (24). Therefore the choice of N and P automatically determines the form of the power series for $i_0(x)$. In particular, for the case when

$$u_1(x) = B_1 x + B_3 x^3 + B_5 x^5 + \ldots,$$

which corresponds to low-speed flow past a symmetrical blunt-nosed cylinder, $m = \frac{4}{3}$, $r = 1$. Also, for $u_1(x) = B_0 - B_1 x$, $m = \frac{4}{3}$, $r = 0$. Both these examples are considered further in following sections. The case $m = 1$, which is particularly simple mathematically but not very important in applications, is discussed in the Appendix.

Before proceeding to the examples themselves, it is desirable to make some general remarks about the application of the foregoing method. There is no doubt that it is best suited to the construction of solutions, and their associated main streams and wall-temperature distributions, starting from chosen forms for $i_0(t)$ and $b(t)$, i.e. from chosen values of the

α's and β's. If, on the other hand, the series $i_0(x)$, $b(x)$ are given, it is necessary to invert them in order to obtain the series $i_0(t)$, $b(t)$, whose coefficients are the α's and β's. As the examples will verify, this inversion is a drawback to the method from the point of view of the computer.

Furthermore, in order to describe the distributions of velocity and temperature *through* the layer, it is necessary to use confluent hypergeometric functions of the types ${}_1F_1(\alpha, \frac{1}{3}, \eta)$, ${}_1F_1(\alpha, \frac{2}{3}, \eta)$, etc., and these do not appear to have been tabulated. If, however, only the skin friction and the heat transfer at the wall are required, the main computational task is the calculation of the k_{nr}'s (equation (30)). Now, k_{n0} is easily found (equation (31)), and for uniform wall temperatures, $\alpha_r = 0$ $(r > 0)$ so that no other k_{nr} is needed. For this reason, only uniform wall temperatures are considered in the subsequent examples. Otherwise, to determine an adequate number of k_{nr}'s would involve the determination of, say, f_n $(n = 1, 2, ..., 5)$ and g_r $(r = 1, 2, ..., 5)$ by integrating the differential equations which they satisfy. Once these functions were determined, it would be relatively simple to calculate the k_{nr}'s and so extend the application of the method to non-uniform wall temperatures. Incidentally, this procedure would also provide the velocity and temperature distribution functions.

3. The solution for low-speed flow

If $M_1 \approx 0$, but $1-i_0/i_1$ is not small, it is necessary to take account of compressibility, not because high speeds are involved but because of temperature variations. The boundary-layer equations (1) and (2) remain unaltered, but the term $u\rho_1 u_1 du_1/dx$ and the dissipation term $\mu(\partial u/\partial y)^2$ disappear from (3) because they are $O(M_1^2)$ compared with the surviving terms. The resulting equations are not so easy to solve as the better-known equations for incompressible flow ($M_1 \approx 0$, $1-i_0/i_1 \approx 0$), because the momentum and energy equations are still linked through the density and the viscosity. However, at least for problems of forced convection in which the wall temperature is uniform, the low-speed compressible flow can be found, even without the restrictions that the Prandtl number is 1 and the viscosity is proportional to the temperature, for those main-stream distributions for which the incompressible flow solutions have been obtained (**7**). The problem is the same and involves the solution of two ordinary differential equations. The extra difficulty in the compressible case is that these differential equations are simultaneous, whereas they are separate in the incompressible case.

In the present work it will be seen that $i = h$, since $u^2/i = O(M_1^2)$ is being neglected. Also, for the same reason, $i_1 =$ constant $= i_s$ in the main stream.

The quantity b is therefore the square of the main-stream velocity divided by the constant i_s.

The solution developed in section 2 applies to the case $M_1 \approx 0$ with one or two small modifications, which lead to considerable simplification as regards computation. The velocity is given by

$$u^2 = i_s(b-f),$$

and the enthalpy by $$i = i_s(1-g),$$

where f, g are given by (27) and (25) respectively. The expressions (32), (33), and (34) for τ_0, x, and q_0 still apply, provided the factors involving

$$1+\tfrac{1}{2}\sum_{n=0}^{\infty}\beta_n t^{mn}$$

are removed in each case.

As an example, consider the problem in which

$$u_1(x) = Bx^N,$$

$$1-i_0(x)/i_s = A\ (=\alpha_0).$$

Then all the β's vanish except β_1, and $m = \frac{8}{3}N/(N+1)$, so that

$$x = 3^{\frac{2}{3}}\left[2^{\frac{10}{3}}\mu_s\rho_s i_s^{\frac{1}{2}}\beta_1^{\frac{1}{2}}(N+1)(k_1-k_{10}A)^{\frac{1}{2}}\right]^{-1}t^{4/3(N+1)},$$

and

$$\tau_0\left(\frac{x}{\mu_s\rho_s u_1^3}\right)^{\frac{1}{2}} = 2^{-\frac{2}{3}}3^{\frac{1}{3}}(N+1)^{\frac{1}{3}}(k_1-k_{10}A)^{\frac{2}{3}},$$

$$q_0 = -\left[2^{\frac{2}{3}}3^{\frac{1}{3}}(\tfrac{1}{3})!\right]^{-1}(\mu_s\rho_s)^{\frac{1}{3}}i_s A B^{\frac{1}{3}}(N+1)^{\frac{1}{3}}(k_1-k_{10}A)^{\frac{1}{3}}x^{\frac{1}{3}(N-1)}.$$

The heat transfer can also be expressed in terms of the Nusselt number defined by

$$\mathrm{Nu} = \int_0^x q_0(\xi)\,d\xi/\mu_s(i_0-i_s).$$

With the Reynolds number defined by $R = u_1(x)x\rho_s/\mu_s$,

$$\mathrm{Nu}\,R^{-\frac{1}{2}} = \left[2^{\frac{1}{3}}3^{\frac{1}{3}}(\tfrac{1}{3})!\right]^{-1}(N+1)^{-\frac{1}{3}}(k_1-k_{10}A)^{\frac{1}{3}}.$$

In these expressions,

$$k_1 = \left\{\left(\frac{8N}{3N+3}\right)!\left(-\frac{2}{3}\right)!\right\}\Big/\left\{\left(\frac{6N-2}{3N+3}\right)!\left(-\frac{1}{3}\right)!\right\},$$

$$k_{10} = k_1\left[1-\left\{\left(\frac{6N-2}{3N+3}\right)!\left(-\frac{1}{3}\right)!\right\}\Big/\left\{\left(\frac{7N-1}{3N+3}\right)!\left(-\frac{2}{3}\right)!\right\}\right],$$

which follow from (31).

The effect of wall temperature on skin friction and heat transfer is illustrated in Tables 1 and 2. The numerical values shown there are based on $i_s/c_p = 288°$ K. (60° F.), and $i_0/c_p =$ (i) 273° K. (f.p.), (ii) 373° K. (b.p.). When the wall temperature is at freezing-point $A = 0{\cdot}0521$, and when it

is at boiling-point $A = -0{\cdot}2951$. When $A = 0$ the results apply to both the incompressible case and the compressible case without heat transfer.

TABLE 1 (*for low-speed flow*)

Values of $\tau_0 \left(\dfrac{x}{\mu_s \rho_s u_1^3}\right)^{\frac{1}{2}}$, *where* $u_1 = Bx^N$

N	$-0{\cdot}0904$	$-0{\cdot}0654$	0	$\frac{1}{9}$	$\frac{1}{3}$	1	4	*large*
$A = 0{\cdot}0521$ . . .	0·109	0·180	0·312	0·468	0·686	1·112	2·165	$1{\cdot}073N^{\frac{1}{2}}$
$A = 0$	0·101	0·175	0·312	0·473	0·698	1·136	2·218	$1{\cdot}100N^{\frac{1}{2}}$
$A = -0{\cdot}2951$ . . .	0·045	0·145	0·312	0·502	0·764	1·270	2·511	$1{\cdot}252N^{\frac{1}{2}}$
Exact values for $A = 0$ . .	0	0·157	0·332	0·512	0·757	1·233	2·405	$1{\cdot}193N^{\frac{1}{2}}$

The second and fourth lines, referring to $A = 0$, are quoted from Lighthill's paper (**4**, p. 376).

TABLE 2 (*for low-speed flow*)

Values of $\mathrm{Nu}\, R^{-\frac{1}{2}}$, *with* $u_1 = Bx^N$

N	$-0{\cdot}0904$	$-0{\cdot}0654$	0	$\frac{1}{9}$	$\frac{1}{3}$	1	4	*large*
$A = 0{\cdot}0521$ . . .	0·498	0·578	0·663	0·708	0·712	0·638	0·433	$1{\cdot}001N^{-\frac{1}{2}}$
$A = 0$	0·485	0·572	0·663	0·710	0·716	0·643	0·436	$1{\cdot}010N^{-\frac{1}{2}}$
$A = -0{\cdot}2951$ . . .	0·371	0·538	0·663	0·725	0·738	0·667	0·455	$1{\cdot}054N^{-\frac{1}{2}}$
Values for $A = 0$ deduced from exact values for Prandtl number = 0·7 .	0·493	0·609	0·659	0·671	0·649	0·557	0·366	$0{\cdot}835N^{-\frac{1}{2}}$

The values in the fourth line are deduced from the exact values for Prandtl number = 0·7 given in Lighthill's paper (**4**, p. 367). The deduction is made by using the rule that $\mathrm{Nu}\, R^{-\frac{1}{2}}$ varies as the cube root of the Prandtl number. The resulting figures in the fourth line should be close to the exact values for $A = 0$ and Prandtl number = 1; for instance, for $N = 0$ the exact value is 0·664, and for $N = 1$ it is 0·570 (see *Modern Developments in Fluid Dynamics*, pp. 624, 632).

The tables show that the non-dimensional coefficients for the skin friction and the heat transfer are not affected by changes in the uniform wall temperature for flow past a flat plate ($N = 0$). This result is not peculiar to the present approximate method of solution, but is valid for the exact solution of the low-speed flow. In both tables the trends, for varying A, which appear for the non-zero values of N, are doubtless more reliable than the absolute values. They show that when the wall is heated the skin friction and heat transfer are increased for accelerated flow and decreased for retarded flow. In other words, the effect of pressure gradient, in respectively thinning or thickening the boundary layer in these two cases, is *enhanced* when the wall is heated. Now it has been realized for some time that pressure

gradient produces such thinning or thickening mainly by speeding up or slowing down the slowly moving fluid very near the wall (and so contracting or dilating the stream tubes), and this makes the results easily understandable. For when the wall is heated the fluid near it is lighter and is therefore more readily accelerated or retarded by a pressure gradient.†

4. The boundary layer of a symmetrical blunt-nosed cylinder

The main stream round a cylinder whose section is symmetrical with respect to the direction of the undisturbed stream is given by

$$u_1(x) = B_1 x + B_3 x^3 + B_5 x^5 + \dots .$$

For simplicity, we again assume uniform wall temperature, i.e. that $1-i_0(x)/h_1 = A\ (= \alpha_0)$.

Then, according to section 2, $m = \frac{4}{3}$ and $r = 1$, so that

$$x = 3^{\frac{1}{3}}(2^{\frac{1}{3}}\mu_s\rho_s i_s^{\frac{1}{3}})^{-1}\int_0^t \xi^{\frac{1}{3}}(1+\tfrac{1}{2}\beta_1\xi^{\frac{4}{3}}+\tfrac{1}{2}\beta_2\xi^{\frac{8}{3}}+\dots)^4\times$$

$$\times[(k_1-k_{10}A)\beta_1\xi^{\frac{4}{3}}+(k_2-k_{20}A)\beta_2\xi^{\frac{8}{3}}+(k_3-k_{30}A)\beta_3\xi^4+\dots]^{-\frac{1}{3}}\,d\xi.$$

It follows that

$$\beta_1 = 3^{\frac{2}{3}}(2^{\frac{1}{3}}\mu_s\rho_s i_s)^{-1}(k_1-k_{10}A)^{-\frac{1}{3}}B_1,$$

$$\beta_2/\beta_1^2 = \left(\tfrac{11}{6}+2\frac{B_3 i_s}{B_1^3}\right)\Big/(1+r_1),$$

where $r_1 = \frac{1}{3}(k_2-k_{20}A)/(k_1-k_{10}A)$, and

$$\beta_3/\beta_1^3 = \frac{1}{(1+r_1)^2}\left[\tfrac{73}{36}+r_1-\tfrac{3}{10}r_1^2+(\tfrac{10}{3}+\tfrac{3}{2}r_1)\frac{B_3 i_s}{B_1^3}+\left(\frac{B_3 i_s}{B_1^3}\right)^2\right]+$$

$$+\frac{2}{(1+r_1)^2(1+r_2)}\left[\tfrac{31}{30}+\tfrac{7}{30}r_1+\tfrac{47}{32}r_1^2-r_2(\tfrac{73}{72}+\tfrac{1}{2}r_1-\tfrac{3}{32}r_1^2)+\right.$$

$$+\frac{B_3 i_s}{B_1^3}\{\tfrac{14}{5}+\tfrac{17}{20}r_1+3r_1^2-r_2(\tfrac{5}{3}+\tfrac{3}{4}r_1)\}-\left(\frac{B_3 i_s}{B_1^3}\right)^2(3r_1+\tfrac{3}{10}r_1^2+\tfrac{1}{2}r_2)+$$

$$\left.+\frac{B_5 i_s}{B_1^5}(1+r_1)^2\right],$$

where $r_2 = \frac{1}{5}(k_3-k_{30}A)/(k_1-k_{10}A)$.

In these expressions,

$$k_n = \frac{(\frac{4}{3}n)!\,(-\frac{2}{3})!}{(\frac{4}{3}n-\frac{2}{3})!\,(-\frac{1}{3})!}, \qquad k_{n0} = k_n\left[1-\frac{(\frac{4}{3}n-\frac{2}{3})!\,(-\frac{1}{3})!}{(\frac{4}{3}n-\frac{1}{3})!\,(-\frac{2}{3})!}\right],$$

which are obtained from (31).

If the non-dimensional coordinate $\theta = x/a$, where a is a representative length, is introduced, the shearing force on the cylinder is

$$\tau_0 = 2^{-\frac{2}{3}}3^{\frac{1}{3}}(\mu_s\rho_s)^{\frac{1}{3}}(k_1-k_{10}A)^{\frac{1}{3}}B_1^{\frac{2}{3}}a\theta(1+T_1\theta^2+T_2\theta^4+\dots), \qquad (35)$$

† Note that the magnitude of the said pressure gradient is determined by the acceleration of the fluid in the main stream, whose density is not reduced.

where $$T_1 = \frac{7r_1}{1+r_1}\frac{B_3a^2}{B_1} + \frac{\frac{7}{2}r_1 - \frac{35}{12}}{1+r_1}\frac{B_1^2a^2}{i_s}$$

and

$$T_2 = \frac{11r_2}{1+r_2}\frac{B_5a^4}{B_1} + \left[\frac{\frac{183}{10}r_1^2 + r_2(\frac{11}{2} - 33r_1 + 15r_1^2)}{(1+r_1)^2(1+r_2)}\right]\left(\frac{B_3a^2}{B_1}\right)^2 +$$
$$+ \left[\frac{-(\frac{53}{10} + \frac{807}{20}r_1 + \frac{3}{2}r_1^2) + r_2(\frac{263}{6} - \frac{91}{4}r_1 + \frac{63}{2}r_1^2)}{(1+r_1)^2(1+r_2)}\right]\frac{B_1^2a^2}{i_s}\frac{B_3a^2}{B_1} +$$
$$+ \left[\frac{\frac{603}{160} - \frac{296}{15}r_1 - \frac{65}{8}r_1^2 + r_2(\frac{7571}{288} - \frac{35}{3}r_1 + 7r_1^2)}{(1+r_1)^2(1+r_2)}\right]\left(\frac{B_1^2a^2}{i_s}\right)^2.$$

Similarly, the local rate of heat transfer from the cylinder is

$$q_0 = -[2^{\frac{4}{3}}3^{\frac{1}{2}}(\tfrac{1}{3})!]^{-1}(\mu_s\rho_s)^{\frac{1}{2}}i_s(k_1 - k_{10}A)^{\frac{1}{3}}AB_1^{\frac{1}{3}}(1 + Q_1\theta^2 + Q_2\theta^4 + \ldots),$$

where $$Q_1 = \frac{3r_1}{1+r_1}\frac{B_3a^2}{B_1} + \frac{\frac{3}{4}r_1 - 2}{1+r_1}\frac{B_1^2a^2}{i_s}$$

and

$$Q_2 = \frac{5r_2}{1+r_2}\frac{B_5a^4}{B_1} + \left[\frac{\frac{3}{2}r_1^2 + r_2(\frac{5}{2} - 15r_1)}{(1+r_1)^2(1+r_2)}\right]\left(\frac{B_3a^2}{B_1}\right)^2 +$$
$$+ \left[\frac{-(4 + 18r_1 + \frac{45}{4}r_1^2) + r_2(\frac{55}{3} - 10r_1 + \frac{15}{4}r_1^2)}{(1+r_1)^2(1+r_2)}\right]\frac{B_1^2a^2}{i_s}\frac{B_3a^2}{B_1} +$$
$$+ \left[\frac{\frac{1}{2} - \frac{49}{6}r_1 - \frac{237}{32}r_1^2 + r_2(\frac{773}{72} - \frac{9}{2}r_1 - \frac{17}{32}r_1^2)}{(1+r_1)^2(1+r_2)}\right]\left(\frac{B_1^2a^2}{i_s}\right)^2.$$

The case when the cylinder is circular is particularly interesting, because it has been studied for incompressible flow by various authors beginning with Hiemenz (see *Modern Developments in Fluid Dynamics*, pp. 148–50). In this case, a being the radius of the cylinder, θ is the angle at the axis measured from the forward stagnation point, and Hiemenz's calculations, based on the exact boundary-layer equations, give

$$\tau_0 = 1{\cdot}2326(\mu_s\rho_s)^{\frac{1}{2}}B_1^{\frac{3}{2}}a\theta \times$$
$$\times \left[1 + 2{\cdot}351\frac{B_3a^2}{B_1}\theta^2 + \left\{3{\cdot}10\frac{B_5a^4}{B_1} + 0{\cdot}58\left(\frac{B_3a^2}{B_1}\right)^2\right\}\theta^4 + \ldots\right].$$

The present method in the incompressible case ($B_1^2a^2/i_s = 0$, $A = 0$) gives, from (35),

$$\tau_0 = 1{\cdot}1360(\mu_s\rho_s)^{\frac{1}{2}}B_1^{\frac{3}{2}}a\theta \times$$
$$\times \left[1 + 2{\cdot}355\frac{B_3a^2}{B_1}\theta^2 + \left\{3{\cdot}10\frac{B_5a^4}{B_1} + 0{\cdot}57\left(\frac{B_3a^2}{B_1}\right)^2\right\}\theta^4 + \ldots\right]$$

to the same order of accuracy. Hence, although the present approximate method underestimates the skin friction for incompressible flow everywhere by about 8 per cent., it predicts very satisfactorily the shape of the function $\tau_0(x)$, and in particular the point of separation ($\tau_0 = 0$).

With this in mind, it is tempting to examine the effect of wall temperature and Mach number on the position of separation. For this purpose it is assumed that the non-dimensional parameters of the main-stream velocity distribution, $B_3 a^2/B_1$ and $B_5 a^4/B_1$, remain fixed while $B_1^2 a^2/i_s$ and A are varied. In the low-speed experimental results used by Hiemenz, $a = 4{\cdot}87$ cm.,

$$B_1 = 7{\cdot}151, \qquad B_3 = -0{\cdot}04497, \qquad B_5 = -0{\cdot}0003300,$$

so that $\qquad B_3 a^2/B_1 = -0{\cdot}1491(5), \qquad B_5 a^4/B_1 = -0{\cdot}02596.$

It is easy to derive, from Bernoulli's equation, that

$$B_1^2 a^2/i_s = \frac{(\gamma-1)M^2}{\left(\frac{\pi}{2}\right)^2\left[1+\frac{B_3 a^2}{B_1}\left(\frac{\pi}{2}\right)^2+\frac{B_5 a^4}{B_1}\left(\frac{\pi}{2}\right)^4\right]\left(1+\frac{\gamma-1}{2}M^2\right)},$$

where M is the Mach number of the flow at the shoulder ($\theta = \frac{1}{2}\pi$), and i_s is the enthalpy at the forward stagnation point ($\theta = 0$).

TABLE 3

Values of θ at the point of separation

A \ M	0	0·1	0·5
−1	1·402	1·404	1·459
0	1·429	1·431	1·511
1	1·550	1·556	—

From Table 3 it is clear that there would be no appreciable difference in the position of separation between the cases when the cylinder has temperature 0° C. ($A = 0{\cdot}0521$) and 100° C. ($A = -0{\cdot}2951$).

It is interesting to examine these results in the light of the remarks at the end of section 3. From those one would expect that a retarded flow

TABLE 4

θ	$u_1/B_1 a$	$\frac{(\tau_0)_{A=-1}-(\tau_0)_{A=0}}{(\tau_0)_{A=0}}$ %	
0	0	38·5	
0·2	0·198	38·4	
0·4	0·390	38·2	
0·6	0·566	37·6	
0·8	0·715	36·5	
1·0	0·825	34·0	
1·1	0·860	31·5	
1·2	0·878	26·6	
1·3	0·876	13·8	
1·4	0·851	−88·9	
1·402	0·850	−100	(separation for $A = -1$)

would be not negligibly influenced by wall heating and would separate earlier (owing to its general reduction of skin friction), and this supposition will be confirmed in section 5. In the present problem the effect is only small because the flow over the first 90 per cent. of the unseparated boundary layer is accelerated. Hence, as Table 4 shows, the skin friction has time to reach a considerably larger value at the pressure minimum than for the unheated cylinder; and though thickening subsequently takes place more rapidly than for the unheated cylinder it is insufficient to cause much change in the point of separation.

5. The retarded main stream $u_1 = B_0 - B_1 x$

The boundary layer for an incompressible flow with the main stream given by $u_1(x) = B_0 - B_1 x$ has been studied by Howarth (**5**), who found that there would be separation at $X = B_1 x/B_0 = 0{\cdot}120$. In order to obtain this result, accurate to 1 per cent., Howarth found it necessary to employ nine terms in the series for $\tau_0(x)$.

In the compressible case, with

$$u_1 = B_0 - B_1 x = \beta_0 + \beta_1 t^{-\frac{1}{3}} + \beta_2 t^{-\frac{2}{3}} + \ldots,$$

$$1 - i_0/h_1 = A_0 + A_1 x + A_2 x^2 + \ldots = \alpha_0 + \alpha_1 t^{\frac{1}{3}} + \alpha_2 t^{\frac{2}{3}} + \ldots,$$

$$x = 3^{\frac{1}{3}}(2^{\frac{1}{3}}\mu_s \rho_s i_s^{\frac{1}{3}})^{-1} \int_0^t \xi^{\frac{1}{3}}(1 + \tfrac{1}{2}\beta_0 + \tfrac{1}{2}\beta_1 \xi^{\frac{1}{3}} + \tfrac{1}{2}\beta_2 \xi^{\frac{2}{3}} + \ldots)^{\frac{4}{3}} \times$$

$$\times [k_0\beta_0 + (k_1 - k_{10}\alpha_0)\beta_1 \xi^{\frac{1}{3}} + \{(k_2 - k_{20}\alpha_0)\beta_2 - k_{21}\alpha_1\beta_1\}\xi^{\frac{2}{3}} + \ldots]^{-\frac{1}{3}}\, d\xi.$$

The first term in the expansion in series on the right-hand side is $Et^{\frac{4}{3}}$, where

$$E = 3^{\frac{2}{3}}(2^{\frac{1}{3}}\mu_s \rho_s i_s^{\frac{1}{3}})^{-1}(1 + \tfrac{1}{2}\beta_0)^{\frac{4}{3}}(k_0\beta_0)^{-\frac{1}{3}}$$

$$= 3^{\frac{2}{3}}[(-\tfrac{1}{3})!]^{\frac{1}{3}}[2^{\frac{1}{3}}\mu_1(0)\rho_1(0)\{i_1(0)\}^{\frac{1}{3}}\beta_0^{\frac{1}{3}}]^{-1}.$$

With the substitution $z = B_1 Et^{\frac{4}{3}}/B_0$ it follows that X may be expressed as a power series in z, starting with the term z. Therefore, let

$$u_1 = B_0(1 - X) = B_0(1 - z + a_2 z^2 + a_3 z^3 + \ldots), \tag{36}$$

where the a's are to be determined. The expression for x may be rewritten as

$$x = \tfrac{3}{4}E \int_0^t t^{\frac{1}{3}}\Big(1 + \sum_{n=1}^{\infty} \gamma_n z^n\Big)^{\frac{4}{3}}\Big(1 + \sum_{n=1}^{\infty} \delta_n z^n\Big)^{-\frac{1}{3}}\, dt, \tag{37}$$

where

$$\gamma_n = \frac{\beta_n}{2 + \beta_0}\left(\frac{B_0}{B_1 E}\right)^n, \qquad \delta_n = \frac{k_n\beta_n - \sum_{r=0}^{n-1} k_{nr}\alpha_r\beta_{n-r}}{k_0\beta_0}\left(\frac{B_0}{B_1 E}\right)^n. \tag{38}$$

Equation (37) as well as (36) gives x as a power series in z, and by comparing the two series it follows that

$$\left.\begin{gathered} a_2 = -\tfrac{1}{2}(C_1+D_1), \qquad a_3 = -\tfrac{1}{3}(C_2+C_1D_1+D_2) \\ a_4 = -\tfrac{1}{4}(C_3+C_2D_1+C_1D_2+D_3) \\ a_5 = -\tfrac{1}{5}(C_4+C_3D_1+C_2D_2+C_1D_3+D_4) \\ a_6 = -\tfrac{1}{6}(C_5+C_4D_1+C_3D_2+C_2D_3+C_1D_4+D_5) \end{gathered}\right\}$$

where

$$\left.\begin{gathered} C_1 = 4\gamma_1, \qquad C_2 = 4\gamma_2+6\gamma_1^2, \qquad C_3 = 4\gamma_3+12\gamma_1\gamma_2+4\gamma_1^3 \\ C_4 = 4\gamma_4+12\gamma_1\gamma_3+6\gamma_2^2+12\gamma_1^2\gamma_2+\gamma_1^4 \\ C_5 = 4\gamma_5+12\gamma_1\gamma_4+12\gamma_2\gamma_3+12\gamma_1^2\gamma_3+12\gamma_1\gamma_2^2+4\gamma_1^3\gamma_2 \end{gathered}\right\} \tag{39}$$

and

$$\left.\begin{gathered} D_1 = -\tfrac{1}{2}\delta_1, \qquad D_2 = -\tfrac{1}{2}\delta_2+\tfrac{3}{8}\delta_1^2, \qquad D_3 = -\tfrac{1}{2}\delta_3+\tfrac{3}{4}\delta_1\delta_2-\tfrac{5}{16}\delta_1^3 \\ D_4 = -\tfrac{1}{2}\delta_4+\tfrac{3}{4}\delta_1\delta_3+\tfrac{3}{8}\delta_2^2-\tfrac{15}{16}\delta_1^2\delta_2+\tfrac{35}{128}\delta_1^4 \\ D_5 = -\tfrac{1}{2}\delta_5+\tfrac{3}{4}\delta_1\delta_4+\tfrac{3}{4}\delta_2\delta_3-\tfrac{15}{16}\delta_1^2\delta_3-\tfrac{15}{16}\delta_1\delta_1^2+\tfrac{35}{32}\delta_1^3\delta_2-\tfrac{63}{256}\delta_1^5 \end{gathered}\right\}$$

Moreover,

$$1+\tfrac{1}{2}b = \frac{i_s}{i_s-\frac{1}{2}u_1^2} = \frac{i_s}{i_s-\frac{1}{2}B_0^2(1-z+a_2z^2+\ldots)^2}.$$

With $z = 0$, this becomes

$$1+\tfrac{1}{2}\beta_0 = \frac{i_s}{i_s-\frac{1}{2}B_0^2},$$

so that

$$1+\tfrac{1}{2}b = \left[1-\frac{\beta_0}{2+\beta_0}(1-z+a_2z^2+a_3z^3+\ldots)^2\right]^{-1}. \tag{40}$$

But

$$1+\tfrac{1}{2}b = (1+\tfrac{1}{2}\beta_0)\Big(1+\sum_{n=1}^{\infty}\gamma_n z^n\Big). \tag{41}$$

Comparison of (40) and (41) gives

$$\left.\begin{gathered} \gamma_1 = -\beta_0, \qquad \gamma_2 = E_2\beta_0+\beta_0^2, \qquad \gamma_3 = E_3\beta_0-2E_2\beta_0^2-\beta_0^3 \\ \gamma_4 = E_4\beta_0-(-E_2^2+2E_3)\beta_0^2+3E_2\beta_0^3+\beta_0^4 \\ \gamma_5 = E_5\beta_0-(-2E_2E_3+2E_4)\beta_0^2+(3E_3-3E_2^2)\beta_0^3-4E_2\beta_0^4-\beta_0^5 \end{gathered}\right\} \tag{42}$$

where

$$\left.\begin{gathered} E_2 = a_2+\tfrac{1}{2}, \qquad E_3 = a_3-a_2 \\ E_4 = a_4-a_3+\tfrac{1}{2}a_2^2, \qquad E_5 = a_5-a_4+a_2a_3 \end{gathered}\right\}$$

Similarly, by substituting for x in terms of z from (37) into the identity

$$\sum_{n=0}^{\infty}A_n x^n = \sum_{n=0}^{\infty}\alpha_n\left(\frac{B_0}{B_1E}\right)^n z^n,$$

the values of $\alpha_n(B_0/B_1E)^n$ $(n = 1, 2, 3,\ldots)$ are found in terms of the γ's, δ's, and A's. Using this last procedure together with the relations (39) and

(42) we can determine a_n, γ_n, δ_n, $\alpha_n(B_0/B_1 E)^n$ for all n when the values of $\beta_0 = B_0$ and the A's are known.

Next, if $$\tau_0 = FX^{-\frac{1}{2}}\Big(1+\sum_{r=1}^{\infty} T_r X^r\Big),$$

the substitution $X = z-a_2 z^2-a_3 z^3-\ldots$ provides a power series for τ_0 in terms of z which must be the same as the expansion

$$\tau_0 = 2^{-\frac{1}{2}}3^{-\frac{1}{2}}\mu_s \rho_s i_s t^{-\frac{1}{2}}\Big(1+\tfrac{1}{2}\sum_{n=0}^{\infty}\beta_n t^{\frac{1}{2}n}\Big)^{-\frac{3}{2}}\sum_{n=0}^{\infty}\Big(k_n\beta_n-\sum_{r=0}^{n-1}k_{nr}\alpha_r\beta_{n-r}\Big)t^{\frac{1}{2}n}$$

$$= 2^{-\frac{1}{2}}3^{-\frac{1}{2}}\mu_1(0)\rho_1(0)k_0 B_0^2\Big(\frac{B_0}{B_1 E}\Big)^{-\frac{1}{2}} z^{-\frac{1}{2}}\Big(1+\sum_{n=1}^{\infty}\gamma_n z^n\Big)^{-\frac{3}{2}}\Big(1+\sum_{n=1}^{\infty}\delta_n z^n\Big).$$

Hence, $F = 2^{-\frac{1}{2}}3^{\frac{1}{2}}[(-\frac{1}{3})!]^{-\frac{3}{2}}[\mu_1(0)\rho_1(0)]^{\frac{1}{2}}B_1^{\frac{1}{2}}B_0$.

$$T_1 = F_1+\delta_1-G_1,$$

$$T_2 = F_2+F_1\delta_1+\delta_2+T_1 a_2-T_1 G_1-G_2.$$

$$T_3 = F_3+F_2\delta_1+F_1\delta_2+\delta_3+T_1 a_3+2T_2 a_2-(T_2-T_1 a_2)G_1-T_1 G_2-G_3,$$

$$T_4 = F_4+F_3\delta_1+F_2\delta_2+F_1\delta_3+\delta_4+T_1 a_4+T_2(2a_3-a_2^2)+3T_3 a_2-$$
$$-(T_3-2T_2 a_2-T_1 a_3)G_1-(T_2-T_1 a_2)G_2-T_1 G_3-G_4,$$

$$T_5 = F_5+F_4\delta_1+F_3\delta_2+F_2\delta_3+F_1\delta_4+\delta_5+T_1 a_5+2T_2(a_4-a_2 a_3)+$$
$$+3T_3(a_3-a_2^2)+4T_4 a_2-[T_4-3T_3 a_2-T_2(2a_3-a_2^2)-T_1 a_4]G_1-$$
$$-(T_3-2T_2 a_2-T_1 a_3)G_2-(T_2-T_1 a_2)G_3-T_1 G_4-G_5,$$

where

$$F_1 = -\tfrac{9}{2}\gamma_1, \qquad F_2 = -\tfrac{9}{2}\gamma_2+\tfrac{99}{8}\gamma_1^2, \qquad F_3 = -\tfrac{9}{2}\gamma_3+\tfrac{99}{4}\gamma_1\gamma_2-\tfrac{429}{16}\gamma_1^3,$$

$$F_4 = -\tfrac{9}{2}\gamma_4+\tfrac{99}{4}\gamma_1\gamma_3+\tfrac{99}{8}\gamma_2^2-\tfrac{1287}{16}\gamma_1^2\gamma_2-\tfrac{6435}{128}\gamma_1^4,$$

$$F_5 = -\tfrac{9}{2}\gamma_5+\tfrac{99}{4}\gamma_1\gamma_4+\tfrac{99}{4}\gamma_2\gamma_3-\tfrac{1287}{16}\gamma_1^2\gamma_3-\tfrac{1287}{16}\gamma_1\gamma_2^2+\tfrac{6435}{32}\gamma_1^3\gamma_2-\tfrac{21879}{256}\gamma_1^5,$$

and

$$G_1 = \tfrac{1}{2}a_2, \qquad G_2 = \tfrac{1}{2}a_3+\tfrac{3}{8}a_2, \qquad G_3 = \tfrac{1}{2}a_4+\tfrac{3}{4}a_2 a_3+\tfrac{5}{16}a_2^3,$$

$$G_4 = \tfrac{1}{2}a_5+\tfrac{3}{4}a_2 a_4+\tfrac{3}{8}a_3^2+\tfrac{15}{16}a_2^2 a_3+\tfrac{35}{128}a_2^4,$$

$$G_5 = \tfrac{1}{2}a_6+\tfrac{3}{4}a_2 a_5+\tfrac{3}{4}a_3 a_4+\tfrac{15}{16}a_2^2 a_4+\tfrac{15}{16}a_2 a_3^2+\tfrac{35}{32}a_2^3 a_3+\tfrac{63}{256}a_2^5.$$

The computation of results is simplest when the wall temperature is uniform, in which case the α's are all zero except α_0 $(= A)$. Then

$$\delta_n = \frac{k_n-k_{n0}A}{k_0}\frac{\beta_n}{\beta_0}\Big(\frac{B_0}{B_1 E}\Big)^n = \frac{k_n-k_{n0}A}{k_0}\frac{2+\beta_0}{\beta_0}\gamma_n,$$

where

$$k_n = \frac{(\frac{4}{3}n)!\,(-\frac{2}{3})!}{(\frac{4}{3}n-\frac{2}{3})!\,(-\frac{1}{3})!} \quad \text{and} \quad k_{n0} = \frac{(\frac{4}{3}n)!\,(-\frac{2}{3})!}{(\frac{4}{3}n-\frac{2}{3})!\,(-\frac{1}{3})!}-\frac{(\frac{4}{3}n)!}{(\frac{4}{3}n-\frac{1}{3})!}.$$

This is the case for which numerical results have been obtained.

Before proceeding to these results it is appropriate to mention the choice of the constant A. The stagnation enthalpy of the main stream is

$$h_1 = i_1(1+\tfrac{1}{2}b) = i_1(0)(1+\tfrac{1}{2}\beta_0),$$

where $i_1(0)$ is the enthalpy of the main stream at the beginning of the boundary layer, and $A = 1-i_0/h_1$, where i_0 is the enthalpy at the boundary.

Hence
$$A = 1-\frac{i_0}{i_1(0)(1+\tfrac{1}{2}\beta_0)}.$$

Suppose now that the boundary wall is initially at rest at the temperature $i_1(0)/c_p$ of the surrounding air. If the wall is accelerated so as to attain a steady speed B_0 relative to the air at the station $x = 0$, there will be a period of unsteady flow, longer than the period of acceleration, during which the temperature of the wall increases from $i_1(0)/c_p$ to $i_1(0)(1+\frac{1}{2}\beta_0)/c_p$. The latter is the final temperature of the wall, at which heat transfer between the wall and the air ceases. If the wall is the surface of a body with a large heat capacity, the unsteady régime may last much longer than the period of acceleration. In fact, as an extreme example of this kind of behaviour, one may envisage a quasi-steady state in which the wall temperature is still at its initial value $i_1(0)/c_p$ when the final speed has been reached. Under these extreme conditions,

$$A = 1-\frac{1}{1+\tfrac{1}{2}\beta_0} = \frac{\beta_0}{2+\beta_0}$$

and particular values of A are:

$M_1(0)$	0	1	$\sqrt{10}$	10
β_0	0	0·4	4	40
A	0	$\frac{1}{6}$	$\frac{2}{3}$	$\frac{20}{21}$

These are examples of a cold wall. As an example of a hot wall, one may take low-speed flow ($M_1(0) = 0$) with $i_1(0)/c_p = 288°$ K., and the wall maintained at the temperature of steam. Then $A = -0{\cdot}2951$, as in section 3.

The case $A = 0$, with no heat transfer, will be used to introduce the numerical results, because exact results are available in this case for purposes of comparison. The first five T_r's have been calculated, and they are given in the following table.

TABLE 5

Coefficients in the series for τ_0, when $A = 0$

$M_1(0)$	0	1	$\sqrt{10}$	10
T_1	−6·183	−6·020	−4·550	+10·152
T_2	−5·067	−10·762	−74·23	−1918
T_3	−37·22	−53·71	−445·5	$-5{\cdot}010\times10^4$
T_4	−250·9	−408·6	−5389	$-3{\cdot}106\times10^6$
T_5	−1851	−3311	$-7{\cdot}539\times10^4$	$-2{\cdot}021\times10^8$

The results given in the first column of Table 5 may be expressed by means of the series

$$\tau_0 = 0{\cdot}312[\mu_1(0)\rho_1(0)B_0^3/x]^{\frac{1}{2}} \times$$
$$\times[1-0{\cdot}7728Y-0{\cdot}0792Y^2-0{\cdot}0727Y^3-0{\cdot}0612Y^4-0{\cdot}0565Y^5-\ldots], \quad (43)$$

where $Y = 8X$, whereas Howarth (**5**) gives

$$\tau_0 = 0{\cdot}332[\mu_1(0)\rho_1(0)B_0^3/x]^{\frac{1}{2}} \times$$
$$\times[1-0{\cdot}7683Y-0{\cdot}0521Y^2-0{\cdot}0422Y^3-0{\cdot}280Y^4-0{\cdot}205Y^5-\ldots] \quad (44)$$

followed by further terms, in the same low-speed case. With either series, the position of separation, viz. the smallest positive root of $\tau_0(Y) = 0$, may be circumscribed, at the stage where n terms have been retained in the series, by finding the roots of $\tau_0 = 0$ first under the assumption that

$$T_r = 0 \quad (r > n) \quad (45)$$

and then under the assumption that

$$T_r^* = T_n^* \quad (r > n), \quad \text{where } T_r^* = 8^{-r}T_r. \quad (46)$$

With $n = 3, 6$ the roots are

	Assumption (45)	*Assumption* (46)
Equation (43)	$X = 0{\cdot}145, 0{\cdot}122$	$0{\cdot}105, 0{\cdot}109$
Equation (44)	$0{\cdot}150, 0{\cdot}134$	$0{\cdot}110, 0{\cdot}116$

respectively. Now, Howarth (**5**) finds $X = 0{\cdot}120$ for the exact root of (44), which, it will be noticed, is about one-quarter of the way from the lower bound to the upper bound of the root whether $n = 3$ or 6. On the rather crude assumption that there is similar behaviour in connexion with (43), the present method estimates that separation will occur at $X = 0{\cdot}112$ for low-speed flow with no heat transfer (incompressible case). This gives an error of $-7{\cdot}5$ per cent., which may be compared with -15 per cent. for the Kármán–Millikan method and $+30$ per cent. for Pohlhausen's method (see *Modern Developments in Fluid Dynamics*, p. 171).

In turning to high-speed flow, the procedure just outlined has to be modified slightly. The merit of the figure 8 occurring in the definition $Y = 8X$, is that it leads to values for the T_r^*'s which slowly decrease in magnitude beyond a certain stage ($r = 4$ in Howarth's series), and it thereby justifies assumption (46) as a means of setting a lower limit to the position of separation. The figure 8 is not, however, appropriate for all the cases considered here. Therefore the following has been adopted as a standard procedure:

(1) calculate X_0, the lowest positive root of $\tau_0(X) = 0$, under the assumption that $T_r = 0$, $r > 5$;

(2) with $Y = X/X_0$, $T_r^* = X_0^r T_r$, calculate the lowest positive root Y_0 of $1 + \sum_{r=1}^{\infty} T_r^* Y^r = 0$, where $T_r^* = T_5^*$ $(r > 5)$;

(3) let $X_{\text{sep}} = \frac{X_0}{4}(1+3Y_0)$ be the estimated point of separation.

This leads to the results given in Table 6.

TABLE 6 ($A = 0$)

$M_1(0)$	0	1	$\sqrt{10}$	10
X_0	0·122	0·112	0·0675	0·0162
T_1^*	−0·7543	−0·6742	−0·3071	+0·1644
T_2^*	−0·07542	−0·1350	−0·3382	−0·5034
T_3^*	−0·06759	−0·07546	−0·1370	−0·2130
T_4^*	−0·05558	−0·06429	−0·1119	−0·2139
T_5^*	−0·05003	−0·05835	−0·1056	−0·2255
$X_0 Y_0$	0·107	0·097	0·0578	0·0135
X_{sep}	0·111	0·101	0·0602	0·0142
X_{sep} (Stewartson)	0·120	0·110	0·074	0·024

The last line in Table 6 is quoted from Stewartson's paper (**6**). He obtained these results by correlating the compressible flow $u_1 = B_0 - B_1 x$ with an incompressible flow, and solving the boundary layer of the latter flow by Howarth's approximate method (**5**). The only approximation involved is that of Howarth's method, and, as Stewartson says (**6**, p. 98), the true values of X_{sep} should be lower than those quoted, except at $M_1(0) = 0$. The case $M_1(0) = 0$ suggests that the values in the penultimate line of Table 6, obtained by the present approximate method, are too low, so perhaps the true values of X_{sep} are between the values given in the last two lines of Table 6, except for $M_1(0) = 0$. Although the proportional deviation of X_{sep} from X_{sep} (Stewartson) increases fairly consistently with increasing Mach number, the reliability of the values of X_{sep} decreases at the same time. For a glance at the T_r^*'s in the last column of Table 6 shows that more terms would have to be calculated in order to achieve the required decrease of T_r^* with increase in r.

In this case of no heat transfer, the distribution of velocity and enthalpy through the boundary layer can be found when the functions $f_n(\eta)$ are known. For both the linearly decreasing main stream and certain other main streams, the required functions are

$$f_n(\eta) = \frac{(\frac{4}{3}n)!}{(-\frac{1}{3})!} e^{-\eta} U\left(\frac{4n+1}{3}, \frac{1}{3}, \eta\right)$$

and values of f_1, f_2, f_3, f_4, and f_5 are given in Table 7.

TABLE 7

η	f_1	f_2	f_3	f_4	f_5
0	1	1	1	1	1
0·005	0·9053	0·8650	0·8332	0·8064	0·7828
0·01	0·8577	0·8009	0·7572	0·7211	0·6901
0·02	0·7895	0·7126	0·6559	0·6102	0·5718
0·03	0·7380	0·6489	0·5846	0·5340	0·4923
0·04	0·6957	0·5981	0·5291	0·4758	0·4327
0·05	0·6594	0·5556	0·4838	0·4291	0·3854
0·06	0·6276	0·5193	0·4455	0·3903	0·3467
0·07	0·5991	0·4875	0·4127	0·3574	0·3142
0·08	0·5734	0·4593	0·3839	0·3289	0·2864
0·09	0·5498	0·4340	0·3585	0·3041	0·2624
0·10	0·5282	0·4111	0·3359	0·2821	0·2414
0·15	0·4405	0·3224	0·2508	0·2020	0·1665
0·20	0·3753	0·2609	0·1947	0·1513	0·1209
0·25	0·3243	0·2154	0·1550	0·1168	0·0907
0·30	0·2831	0·1804	0·1256	0·0920	0·0697
0·35	0·2490	0·1528	0·1032	0·0737	0·0545
0·40	0·2204	0·1306	0·0858	0·0597	0·0433
0·45	0·1961	0·1124	0·0719	0·0490	0·0348
0·50	0·1752	0·0974	0·0608	0·0405	0·0282
0·55	0·1571	0·0848	0·0517	0·0337	0·0231
0·60	0·1413	0·0742	0·0442	0·0283	0·0190
0·65	0·1274	0·0651	0·0380	0·0239	0·0158
0·70	0·1152	0·0574	0·0328	0·0202	0·0132
0·75	0·1044	0·0507	0·0284	0·0172	0·0110
0·80	0·0948	0·0450	0·0247	0·0147	0·0093
0·85	0·0862	0·0400	0·0215	0·0126	0·0079
0·90	0·0786	0·0356	0·0188	0·0109	0·0067
0·95	0·0717	0·0317	0·0165	0·0094	0·0057
1·00	0·0655	0·0285	0·0145	0·0082	0·0049
1·1	0·0549	0·0229	0·0113	0·0062	0·0036
1·2	0·0462	0·0186	0·0089	0·0047	0·0027
1·3	0·0390	0·0151	0·0070	0·0036	0·0020
1·4	0·0331	0·0124	0·0056	0·0028	0·0015
1·5	0·0282	0·0102	0·0045	0·0022	0·0012
1·6	0·0240	0·0084	0·0036	0·0017	0·0009
1·7	0·0205	0·0070	0·0029	0·0014	0·0007
1·8	0·0176	0·0058	0·0024	0·0011	0·0005
1·9	0·0151	0·0048	0·0019	0·0009	0·0004
2·0	0·0130	0·0040	0·0016	0·0007	0·0003
2·2	0·0097	0·0028	0·0010	0·0004	0·0002
2·4	0·0072	0·0020	0·0007	0·0003	0·0001
2·6	0·0054	0·0014	0·0005	0·0002	
2·8	0·0041	0·0010	0·0003	0·0001	
3·0	0·0031	0·0008	0·0002		
3·2	0·0024	0·0006	0·0002		
3·4	0·0018	0·0004	0·0001		
3·6	0·0014	0·0003			
3·8	0·0011	0·0002			
4·0	0·0008	0·0002			
4·2	0·0006	0·0001			
4·4	0·0005				
4·6	0·0004				
4·8	0·0003				
5·0	0·0002				
5·2	0·0002				
5·4	0·0001				

Two examples of flow at low speed past a hot wall are given in Table 8.

TABLE 8

$M_1(0) = 0$

A	-1	$-0{\cdot}2951$	A	-1	$-0{\cdot}2951$
T_1	$-9{\cdot}545$	$-7{\cdot}175$	T_1^*	$-0{\cdot}7073$	$-0{\cdot}7355$
T_2	$-18{\cdot}24$	$-8{\cdot}158$	T_2^*	$-0{\cdot}10014$	$-0{\cdot}08571$
T_3	$-187{\cdot}7$	$-66{\cdot}20$	T_3^*	$-0{\cdot}07636$	$-0{\cdot}07129$
T_4	-2092	$-532{\cdot}3$	T_4^*	$-0{\cdot}06308$	$-0{\cdot}05875$
T_5	$-2{\cdot}333\times10^4$	-4246	T_5^*	$-0{\cdot}05211$	$-0{\cdot}04804$
X_0	$0{\cdot}0741$	$0{\cdot}1025$	$X_0\,Y_0$	$0{\cdot}0649$	$0{\cdot}0900$
X_{sep}	$0{\cdot}067$	$0{\cdot}093$			

Table 8 shows that separation is estimated to occur at $X = 0{\cdot}067$ for a wall maintained at the uniform temperature of 303° C., whereas the same method of estimation gives $X = 0{\cdot}111$ for the wall at 15° C., the temperature of the main stream. The table also shows that raising the temperature of the wall from room temperature to boiling-point ($A = -0{\cdot}2951$) would cause the separation distance to decrease by about 16 per cent. Table 9

TABLE 9

	$A = 0{\cdot}2$			$A = \frac{2}{3}$
$M_1(0)$	0	1	$\sqrt{10}$	$\sqrt{10}$
T_1	$-5{\cdot}511$	$-5{\cdot}233$	$-2{\cdot}533$	$+2{\cdot}174$
T_2	$-3{\cdot}352$	$-8{\cdot}197$	$-55{\cdot}78$	$-23{\cdot}46$
T_3	$-23{\cdot}34$	$-32{\cdot}59$	$-255{\cdot}2$	$-65{\cdot}20$
T_4	$-136{\cdot}8$	$-216{\cdot}8$	-2370	$-128{\cdot}3$
T_5	$-790{\cdot}2$	-1393	$-4{\cdot}006\times10^4$	$-1{\cdot}167\times10^4$
X_0	$0{\cdot}140$	$0{\cdot}130$	$0{\cdot}0827$	$0{\cdot}140$
T_1^*	$-0{\cdot}7737$	$-0{\cdot}6787$	$-0{\cdot}2094$	$+0{\cdot}3037$
T_2^*	$-0{\cdot}06608$	$-0{\cdot}13788$	$-0{\cdot}3815$	$-0{\cdot}4578$
T_3^*	$-0{\cdot}06459$	$-0{\cdot}07111$	$-0{\cdot}1444$	$-0{\cdot}1778$
T_4^*	$-0{\cdot}05317$	$-0{\cdot}06136$	$-0{\cdot}1109$	$-0{\cdot}04888$
T_5^*	$-0{\cdot}04311$	$-0{\cdot}05111$	$-0{\cdot}1549$	$-0{\cdot}6211$
$X_0\,Y_0$	$0{\cdot}124$	$0{\cdot}114$	$0{\cdot}0696$	$0{\cdot}110$
X_{sep}	$0{\cdot}128$	$0{\cdot}118$	$0{\cdot}0729$	$0{\cdot}117$
X_{sep} ($A = 0$)	$0{\cdot}111$	$0{\cdot}101$	$0{\cdot}0602$	$0{\cdot}0602$

shows an effect of similar degree concerning the greater separation distance for a wall colder than the main stream. The effect of wall temperature on separation is much more marked in this case of a linearly decreasing mainstream velocity than in the previous case of flow round a cylinder, and it is perhaps sufficiently strong to be observed in experiments.

As regards relatively cold boundaries, attention has been restricted to one or two values of A, and different Mach numbers. Table 9 refers mainly

to $A = 0{\cdot}2$, chosen as representative of the flow at $M_1(0) = 1$ when the wall is kept at the temperature of the incident stream.

The results for $M_1(0) = 10$ have been omitted because it is clear that already at $M_1(0) = \sqrt{10}$ the coefficients T_r^* are no longer decreasing in magnitude as r increases, and therefore that more terms are required in the series for τ_0 in order to obtain a reliable estimate of X_{sep}. The last column

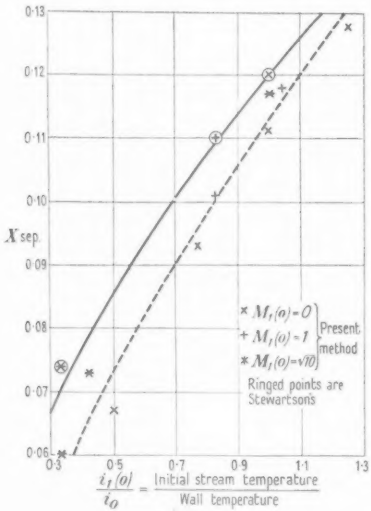

FIG. 1.

illustrates the trend of the results when A is still larger. The value $A = \frac{2}{3}$ is appropriate for a flow at $M_1(0) = \sqrt{10}$ with the wall at the temperature of the incident stream. Again it is obvious from the values of T_r^* that more terms would be required in reaching a reliable answer for X_{sep}. Even so, there does not seem to be any noticeable inconsistency in the various values of X_{sep}.

Acceptance of the figure 0·117 for X_{sep} in the last column leads to the following result. If the temperature of the wall is always kept at that of the incident stream, the position of separation will not change very much as the Mach number increases, for at $M_1(0) = 0, 1, \sqrt{10}$ the corresponding values of A are then $0, \frac{1}{6}, \frac{2}{3}$, and $X_{\text{sep}} = 0{\cdot}111, 0{\cdot}115, 0{\cdot}117$.

This, if accepted, strongly confirms the theory of section 3 that the degree of influence of a given pressure gradient on a boundary layer depends considerably upon the wall temperature, because this fixes the density of the fluid very near the wall, and through it the effectiveness of pressure gradient in slowing down or speeding up the fluid, and hence the thickening

or thinning of the boundary layer. It is now seen that this conclusion is almost independent of the Mach number.

Still greater confirmation is obtained by plotting all the values of X_{sep} in Tables 6, 8, and 9 (excluding cases with $M_1(0) = 10$) against the ratio

$$\frac{i_1(0)}{i_0} = \frac{1}{(1-A)(1+\frac{1}{2}\beta_0)}$$

of the initial stream temperature to the wall temperature.

It is seen in Fig. 1 that the relationship may be represented by a curve nearly independent of Mach number (the broken line), especially since the point $X_{sep} = 0{\cdot}0729$ is less trustworthy than neighbouring points (see Table 9). The figure also shows Stewartson's points. By means of these, the relationship between X_{sep} and $i_1(0)/i_0$ which has just been obtained can be corrected for the tendency of the present method to underestimate X_{sep}. Taking into account that Stewartson's lower values are probably slight overestimates we can suppose that the full line (which has been drawn roughly parallel to the broken line) gives a reasonably good description of the effect of wall temperature on separation in uniformly retarded flow. This full line has the equation

$$X_{sep} = 0{\cdot}120[i_1(0)/i_0]^{\frac{1}{2}},$$

or, in other words,

$$\text{relative fall in velocity before separation (per cent.)} = 12\left(\frac{\text{incident stream temperature}}{\text{wall temperature}}\right)^{\frac{1}{2}}.$$

One may reasonably expect this rule to be equally good for Prandtl numbers other than 1.†

At the same time, Table 9 shows that this result has not been verified for large Mach number. To test it at high speeds would require the introduction of further terms in the series.

The general conclusion that the separation distance increases as the temperature of the wall is lowered has previously been obtained by Dr. N. Hoskin at Manchester University in unpublished work. Of the present quantitative information, perhaps the result to be stressed, as being the most trustworthy, is the result in low-speed flow that the separation

† Brown and Donoughe (7) find, when calculating flows with large temperature difference, small Mach number, Prandtl number 0·7, and $u_1 \propto x^{-N}$, that the separation values of N are 0·0600, 0·0904, 0·1178, 0·1351 for $i_1/i_0 = \frac{1}{2}$, 1, 2, 4 respectively. Now

$$N = -(x/u_1)(du_1/dx)$$

bears a resemblance to X_{sep}, and so it is interesting that it increases with i_1/i_0 in a way similar to X_{sep}; also its slower rate of increase for values of i_1/i_0 greater than those in Fig. 1 may be significant.

distance should decrease by about 20 per cent. as the temperature of the wall is changed from 0° C. to 100° C.

Acknowledgement

I am indebted to Professor M. J. Lighthill, F.R.S., for interpreting the results in sections 3, 4, and 5 in terms of the thickening or thinning of the boundary layer, and thereby explaining how the results reflect the influence of wall temperature. I am also grateful to Mr. D. F. Ferguson, M.A., for carrying out the computational work connected with this paper.

REFERENCES

1. L. Crocco, Monogr. Sci. Aeronaut. No. 3 (Rome, 1946).
2. D. R. Chapman and M. W. Rubesin, *J. Aero. Sci.* **16** (1949), 547.
3. W. F. Cope and D. R. Hartree, *Phil. Trans.* A, **241** (1948), 1.
4. M. J. Lighthill, *Proc. Roy. Soc.* A, **202** (1950), 359.
5. L. Howarth, ibid. **164** (1938), 547.
6. K. Stewartson, ibid. **200** (1949), 84.
7. W. B. Brown and P. L. Donoughe, N.A.C.A., T.N. No. 2479 (1951).

APPENDIX

The solution when $m = 1$

When $m = 1$, we have $N = r/(\frac{8}{3}-r)$ and $P = 2/(\frac{8}{3}-r)$, where r is an integer, so that the solution applies to main streams such as

$$u_1(x) = B_0 + B_1 x^{\frac{3}{2}} + B_2 x^{\frac{6}{2}} + \ldots,$$
$$u_1(x) = B_1 x^{\frac{3}{2}} + B_3 x^{\frac{5}{2}} + B_5 x^{3} + \ldots,$$
$$u_1(x) = B_1 x^{3} + B_2 x^{6} + B_3 x^{9} + \ldots,$$

with wall-temperature distributions expressed in the forms of series of integral powers of $x^{\frac{3}{2}}$, $x^{\frac{5}{2}}$, x^3, respectively.

The reason for singling out this case for special mention is that the solution for h_n is, at least formally, simpler than the more general solution given by (29), for (28) is satisfied by $h_{1,n} = c_n f_{1,n} + \sum_{r=0}^{n} d_{nr} g_{1,r}$ provided that

$$\sum_{r=0}^{n} d_{nr}[\tfrac{1}{3}g'_{1,r} + (n-r)g_{1,r}] = \sum_{r=0}^{n-1} (n-r)\alpha_r \beta_{n-r} g_{1,r}, \tag{47}$$

where the extra suffix 1 has been attached to f, g, h to emphasize that $m = 1$. In obtaining (47), it is necessary to use the equation $\eta g''_{1,r} + (\eta + \frac{2}{3})g'_{1,r} - r g_{1,r} = 0$. Now, starting from the formula

$$g_{1,r} = \frac{1}{(-\frac{2}{3})!} \int_{\eta}^{\infty} e^{-\xi}(\xi - \eta)^r \xi^{-\frac{8}{3}-r}\, d\xi,$$

it is easy to verify the recurrence relation

$$(3r-1)g'_{1,r} = 3r(g'_{1,r-1} + g_{1,r-1}),$$

from which it follows that

$$g'_{1,n} = \frac{n!}{(n-\frac{1}{3})!}\sum_{r=1}^{n}\frac{(n-r-\frac{1}{3})!}{(n-r)!}g_{1,n-r} + \frac{n!\,(-\frac{1}{3})!}{(n-\frac{1}{3})!}g'_{1,0} \quad (n \geqslant 1).$$

Hence (47) is satisfied if, for $n \geqslant 1$,

$$(n-r)d_{nr} + \frac{1}{3}\frac{(r-\frac{1}{3})!}{r!}\sum_{s=r+1}^{n}\frac{s!}{(s-\frac{1}{3})!}d_{ns} = (n-r)\alpha_r\beta_{n-r} \quad (r = 0, 1, \ldots, n-1), \quad (48)$$

and

$$d_{n0} + (-\tfrac{1}{3})!\sum_{r=1}^{n}\frac{r!}{(r-\frac{1}{3})!}d_{nr} = 0, \quad (49)$$

which suffice to determine d_{nr} $(r = 0, 1, \ldots, n)$. The boundary condition $f = 0$ at $\psi = \infty$ is satisfied because $f_{1,n}(\infty) = g_{1,n}(\infty) = 0$ so that $h_{1,n}(\infty) = 0$ for all n. The boundary condition $f = \sum_{n=0}^{\infty}\beta_n t^n$ at $\psi = 0$ is satisfied if

$$c_n = \beta_n - \sum_{r=0}^{\infty}d_{nr}, \quad (50)$$

for all n.

The first few values of the c's and d's obtained from (47)–(49) are

$d_{00} = 0, \quad c_0 = \beta_0;$

$d_{10} = \frac{3}{2}\alpha_0\beta_1, \quad d_{11} = -\alpha_0\beta_1, \quad c_1 = (1-\frac{1}{2}\alpha_0)\beta_1;$

$d_{20} = \frac{6}{5}\alpha_0\beta_2, \quad d_{21} = \frac{2}{5}\alpha_0\beta_2 + \frac{3}{2}\alpha_1\beta_1, \quad d_{22} = -\alpha_0\beta_2 - \frac{5}{4}\alpha_1\beta_1, \quad c_2 = (1-\frac{3}{5}\alpha_0)\beta_2 - \frac{1}{4}\alpha_1\beta_1;$

$d_{30} = \frac{9}{8}\alpha_0\beta_3, \quad d_{31} = \frac{3}{20}\alpha_0\beta_3 + \frac{6}{5}\alpha_1\beta_2, \quad d_{32} = \frac{3}{5}\alpha_0\beta_3 + \frac{1}{2}\alpha_1\beta_2 + \frac{3}{2}\alpha_2\beta_1,$

$d_{33} = -\alpha_0\beta_3 - \frac{4}{3}\alpha_1\beta_2 - \frac{4}{3}\alpha_2\beta_1, \quad c_3 = (1-\frac{13}{20}\alpha_0)\beta_3 - \frac{11}{30}\alpha_1\beta_2 - \frac{1}{6}\alpha_2\beta_1.$

It remains to find x in terms of t, a process which involves determining τ_0 and $\lim_{\eta\to 0}\eta^{\frac{1}{3}}h'_{1,n}$ as before. Since

$$h'_{1,n} = c_n f'_{1,n} + \sum_{r=0}^{n}d_{nr}g'_{1,r} \quad \text{and} \quad \lim_{\eta\to 0}\sum_{r=0}^{n}d_{nr}g'_{1,r} = 3\sum_{r=0}^{n-1}(n-r)(\alpha_r\beta_{n-r} - d_{nr})$$

from (47), it follows that

$$\lim_{\eta\to 0}\eta^{\frac{1}{3}}h'_{1,n} = c_n\lim_{\eta\to 0}\eta^{\frac{1}{3}}f'_{1,n} = -\frac{n!\,(-\frac{2}{3})!}{(n-\frac{2}{3})!\,(-\frac{1}{3})!}c_n.$$

Therefore, the equation corresponding to (33) is

$$x = 3^{\frac{1}{3}}[(-\tfrac{1}{3})!]^{\frac{1}{3}}[2^{\frac{1}{3}}\{(-\tfrac{2}{3})!\}^{\frac{1}{3}}\mu_s\rho_s i_s^{\frac{1}{3}}]^{-1}\times$$
$$\times\int_0^t \xi^{\frac{1}{3}}\left(1 + \tfrac{1}{2}\sum_{n=0}^{\infty}\beta_n\xi^n\right)^{(3\gamma-1)/2(\gamma-1)}\left(\sum_{n=0}^{\infty}\frac{n!}{(n-\frac{2}{3})!}c_n\xi^n\right)^{-\frac{1}{3}}d\xi. \quad (51)$$

For an example, consider the case where the data are

$$u_1(x) = Bx^{\frac{1}{3}},$$
$$1 - i_0(x)/h_1 = A \;(= \alpha_0),$$

for which $\beta_0 = 0, \beta_1 \neq 0$. If $X = B^2x^{\frac{2}{3}}i_s^{-1}$ is a non-dimensional measure of position along the boundary layer

$$b = \frac{u_1^2}{i_1} = \frac{u_1^2}{i_s - \frac{1}{2}u_1^2} = \frac{X}{1-\frac{1}{2}X} = X + \tfrac{1}{2}X^2 + \tfrac{1}{4}X^3 + \ldots.$$

Under the assumption that $\gamma = 1{\cdot}4$,

$$x = 3^{\frac{1}{3}}[(-\tfrac{1}{3})!]^{\frac{1}{3}}(2^{\frac{1}{3}}\mu_s\rho_s i_s^{\frac{1}{3}})^{-1}\int_0^t \xi^{\frac{1}{3}}[1+2\beta_1\xi+(2\beta_2+\tfrac{3}{2}\beta_1^2)\xi^2+\ldots]\times$$
$$\times[3c_1\xi+\tfrac{9}{2}c_2\xi^2+\tfrac{81}{14}c_3\xi^3+\ldots]^{-\frac{1}{3}}\,d\xi$$
$$= 2^{\frac{2}{3}}3^{\frac{2}{3}}[(-\tfrac{1}{3})!]^{\frac{1}{3}}(5\mu_s\rho_s i_s^{\frac{1}{3}}c_1^{\frac{1}{3}})^{-1}t^{\frac{2}{3}}\times$$
$$\times\Big[1+\frac{5}{11}\Big(2\beta_1-\frac{3}{4}\frac{c_2}{c_1}\Big)t+\frac{5}{17}\Big(2\beta_2+\tfrac{3}{2}\beta_1^2-\tfrac{3}{2}\beta_1\frac{c_2}{c_1}+\frac{27}{32}\frac{c_2^2}{c_1^2}-\frac{27}{28}\frac{c_3}{c_1}\Big)t^2+\ldots\Big].$$

Comparison of the x- and t-series for b now shows that

$$\beta_1 = C = 2^{\frac{2}{3}}3^{\frac{1}{3}}[(-\tfrac{1}{3})!]^{\frac{2}{3}}(5\mu_s\rho_s)^{-\frac{2}{3}}i_s^{-1}B^{\frac{2}{3}}(1-\tfrac{1}{2}A)^{-\frac{2}{3}},$$

$\beta_2 = S_1C^2$, where $S_1 = 35/(22+9R_1)$, $R_1 = (1-\frac{3}{5}A)/(1-\frac{1}{2}A)$, and $\beta_3 = S_2C^3$, where

$$S_2 = (\tfrac{11343\,5}{242}+168S_1-\tfrac{29169}{121}R_1S_1+\tfrac{718\,20}{968}R_1^2S_1^2)/(238+81R_2),$$
$$R_2 = (1-\tfrac{13}{20}A)/(1-\tfrac{1}{2}A).$$

The shearing stress at the wall is

$$\tau_0 = 3[2^{\frac{1}{3}}5^{\frac{1}{3}}\{(-\tfrac{1}{3})!\}^{\frac{2}{3}}]^{-1}(\mu_s\rho_s)^{\frac{1}{3}}B^{\frac{2}{3}}(1-\tfrac{1}{2}A)^{\frac{2}{3}}x^{\frac{2}{3}}\times$$
$$\times[1+(\tfrac{18}{11}R_1S_1-\tfrac{115}{44})X+(\tfrac{243}{110}R_2S_2+\tfrac{33211}{41114}R_1^2S_1^2-\tfrac{116487}{164556}R_1S_1-$$
$$-\tfrac{169}{68}S_1+\tfrac{448795}{658224})X^2+\ldots],$$

and the heat transfer from the wall is given by

$$q_0 = -2^{\frac{1}{3}}[5^{\frac{1}{3}}(\tfrac{1}{3})!\,\{(-\tfrac{1}{3})!\}^{\frac{1}{3}}]^{-1}(\mu_s\rho_s)^{\frac{1}{3}}i_sA(1-\tfrac{1}{2}A)^{\frac{1}{3}}B^{\frac{1}{3}}x^{-\frac{1}{3}}\times$$
$$\times[1+(\tfrac{15}{22}R_1S_1-\tfrac{9}{11})X+(\tfrac{1089}{1119}R_2S_2-\tfrac{2757}{20057}R_1^2S_1^2-\tfrac{34209}{20057}R_1S_1-\tfrac{15}{17}S_1+\tfrac{122201}{82228})X^2+\ldots].$$

The corresponding expressions for incompressible flow are obtained by putting $X = 0$ and deleting the terms in $1-\frac{1}{2}A$.

CHARACTERISTIC SURFACES IN IDEAL PLASTICITY IN THREE DIMENSIONS

By J. W. CRAGGS (*University College, Dundee*)†

[Received 29 May 1952]

SUMMARY

Conditions are found for the existence of characteristic surfaces for the equations of ideal plasticity in three dimensions. It is observed that the conditions are everywhere satisfied in the problem of plane strain, so that there is then a complete set of characteristics. In more general problems, including those with axial symmetry, there are only isolated characteristic surfaces. An example is given of an axially symmetric solution with an isolated characteristic surface.

Introduction

THE theory of characteristics as applied to the equations of ideal plasticity with plane strain has been extensively studied and is now a standard method (**1**). Hill (**2**) and Symonds (**3**) have discussed the equations in the case of axial symmetry, and shown, by different methods, that these are not hyperbolic, and so have no characteristics at a general point. The purpose of this paper is to show that characteristic surfaces may nevertheless exist, not only in the case of axial symmetry, but also in general three-dimensional problems. Such characteristic surfaces are in general isolated and no general methods for the solution of special problems can be obtained by their use, but their existence does imply that of plastic rigid solutions with discontinuities of stress and velocity components, and such solutions are more easily obtained by relaxation or other methods than the corresponding solutions for plastic-elastic problems.

1. The conditions for the existence of a characteristic surface

Write σ_{ij} for the stress tensor and u_i for the velocity vector ($i, j = 1, 2, 3$). Then the equations of ideal plasticity are the Mises–Hencky yield condition

$$\sigma'_{ij}\sigma'_{ij} = 2k^2, \tag{1}$$

where σ'_{ij} represents the reduced stress tensor formed by subtracting the mean hydrostatic stress from each of the diagonal elements of σ_{ij}, the Lévy–Mises flow equation,

$$\frac{1}{2}\left(\frac{\partial u_i}{\partial x_j}+\frac{\partial u_j}{\partial x_i}\right) = \lambda\sigma'_{ij}, \tag{2}$$

and the equilibrium conditions,

$$\frac{\partial \sigma_{ij}}{\partial x_j} = 0. \tag{3}$$

† Now at King's College, Newcastle on Tyne.

A characteristic surface S may be defined as a surface such that, when the nine variables σ_{ij}, u_i are given at every point of it, the equations (1), (2), and (3) do not suffice to determine the normal derivatives of the variables across the surface.

Choose axes at a point O of S with Oz normal to the surface and Ox, Oy, Oz forming a rectangular Cartesian set. Then, at O, it is required to find the first derivatives with respect to z, assuming the first derivatives with respect to x and y to be known. Let u, v, w now represent the velocity components along the axes, then

$\partial w/\partial z$ is determined by the compressibility condition;

$\partial\sigma_{xz}/\partial z$, $\partial\sigma_{yz}/\partial z$, and $\partial\sigma_{zz}/\partial z$ follow from the equilibrium conditions.

The flow equations (2) reduce to

$$\frac{\partial u}{\partial x} = \lambda\sigma'_{xx}, \quad \frac{\partial v}{\partial y} = \lambda\sigma'_{yy}, \quad \frac{\partial w}{\partial z} = \lambda\sigma'_{zz}, \quad \text{and} \quad \frac{\partial u}{\partial y}+\frac{\partial v}{\partial x} = 2\lambda\sigma_{xy}, \tag{4}$$

and

$$\frac{\partial u}{\partial z}+\frac{\partial w}{\partial x} = 2\lambda\sigma_{xz}, \quad \frac{\partial v}{\partial z}+\frac{\partial w}{\partial y} = 2\lambda\sigma_{yz}. \tag{5}$$

Suppose first that at least one of the stress components on the right-hand sides of equations (4) is non-zero at O. Then the corresponding equation determines λ, and $\partial u/\partial z$, $\partial v/\partial z$ follow from (5). The incompressibility condition may therefore be differentiated with respect to z to give $\partial^2 w/\partial z^2$, and $\partial\lambda/\partial z$ follows from the third of (4). The remaining equations of (4) may then be differentiated with respect to z, determining the stress derivatives $\partial\sigma_{xx}/\partial z$, $\partial\sigma_{xy}/\partial z$, and $\partial\sigma_{yy}/\partial z$ so that all the stress and velocity derivatives are determinate, and S is not a characteristic surface through O.

Next suppose that, at O,

$$\sigma'_{xx} = \sigma'_{yy} = \sigma'_{zz} = \sigma_{xy} = 0. \tag{6}$$

Then (4) do not determine λ, and (5) reduce to a single relation between $\partial u/\partial z$ and $\partial v/\partial z$.

The yield condition, differentiated with respect to z, gives a single relation between the three stress derivatives $\partial\sigma'_{xx}/\partial z$, $\partial\sigma_{xy}/\partial z$, and $\partial\sigma'_{yy}/\partial z$, but one velocity component and two stress components have indeterminate derivatives with respect to z over S at O. The element of S at O is therefore an element of a characteristic surface.

Now (6) will be satisfied for some elementary surface through O whenever the determinant of the reduced stress tensor vanishes at O. Any such point may be called a characteristic point.

Finally, if the characteristic points lie on a finite or infinite surface such that the maximum shear stress over the surface is k, the surface is a characteristic of the equations.

2. Special cases

In problems of plane strain, the determinant of the reduced stress tensor vanishes at every point. Every point is therefore a characteristic point, and two characteristic surfaces pass through every point of the plane.

Two other special types of problem have complete sets of characteristic surfaces:

(i) problems in spherical polar coordinates with zero radial velocity, and the other two velocity components proportional to the radius, and

(ii) problems in cylindrical polars with the radial velocity zero and the circumferential velocity proportional to the radius.

3. Application to a plastic-rigid problem

The importance of the existence of characteristic surfaces lies in the fact that such a surface may divide a rigid region from a plastic one, when the plastic-rigid approximation is made. It follows that the full plastic-elastic problem may be simplified, for large plastic flow, by neglect of elastic strains.

As an example, consider the spherically symmetric form of the equations of motion, with solution independent of the azimuth angle ϕ and the polar radius r. The equilibrium equations are then

$$\frac{\partial \sigma_{\theta\theta}}{\partial \theta} + (\sigma_{\theta\theta} - \sigma_{\phi\phi}) \cot \theta + 3\sigma_{r\theta} = 0 \tag{7}$$

and

$$\frac{\partial \sigma_{r\theta}}{\partial \theta} + (2\sigma_{rr} - \sigma_{\theta\theta} - \sigma_{\phi\phi}) + \sigma_{r\theta} \cot \theta = 0. \tag{8}$$

The flow equations, with u, v for radial and transverse velocity components, and primes for derivatives with respect to the polar angle θ, are

$$\frac{0}{2\sigma_{rr} - \sigma_{\theta\theta} - \sigma_{\phi\phi}} = \frac{v' + u}{2\sigma_{\theta\theta} - \sigma_{\phi\phi} - \sigma_{rr}} = \frac{u + v \cot \theta}{2\sigma_{\phi\phi} - \sigma_{rr} - \sigma_{\theta\theta}} = \frac{u' - v}{6\sigma_{r\theta}}. \tag{9}$$

Two possibilities arise from (9).

(i) Take the numerators all zero, then

$$u = -W \cos \theta, \qquad v = W \sin \theta, \tag{10}$$

and the material flows as a rigid body with axial velocity W.

(ii) Take $2\sigma_{rr} - \sigma_{\theta\theta} - \sigma_{\phi\phi} = 0$.

Substitution in (8) then leads to

$$\frac{\partial \sigma_{r\theta}}{\partial \theta} + \sigma_{r\theta} \cot \theta = 0,$$

whence

$$\sigma_{r\theta} = -k \sin \alpha \operatorname{cosec} \theta, \tag{11}$$

where the constant of integration has been so chosen that $\theta = \alpha$ is a characteristic surface.

The yield condition now is

$$\sigma_{\phi\phi}-\sigma_{\theta\theta} = \pm 2k(1-\sin^2\alpha\,\mathrm{cosec}^2\theta)^{\frac{1}{2}}, \tag{12}$$

and (9) reduce to

$$\frac{v'+u}{\sigma_{\theta\theta}-\sigma_{\phi\phi}} = \frac{u+v\cot\theta}{\sigma_{\phi\phi}-\sigma_{\theta\theta}} = \frac{u'-v}{4\sigma_{r\theta}}. \tag{13}$$

Assume that the radial velocity component is greater than zero, then the rate of plastic work will be positive only if the upper sign is taken in (12).

Substitution of (11) and (12) in (13) leads to a pair of equations for u, v, the solution of which is easily seen to be

$$v = \{A+Bf(\theta)\}\sin\theta \tag{14}$$

and

$$u = -(v'+v\cot\theta), \tag{15}$$

where A, B are constants and

$$\log f'(\theta) = -\int_{\alpha}^{\theta}\left\{3\cot\theta+\frac{2\sin\alpha}{\sin\theta\sqrt{(1-\sin^2\alpha\,\mathrm{cosec}^2\theta)}}\right\}d\theta. \tag{16}$$

(The integral can be expressed in terms of Jacobian elliptic functions, but it was found easier to evaluate it numerically for the particular case required.)

Now choose A, B such that for $\theta = \theta_1 \geqslant \frac{1}{2}\pi$, $v = 0$. Then the equations correspond to a material flowing past the outside of a cone of semi-angle $\pi-\theta_1$. There is a characteristic surface at $\theta = \alpha$, and for $\theta < \alpha$ the material moves as a rigid body, with axial velocity W given by the condition that the normal component of velocity across the characteristic is continuous.

The solution has been computed for the particular case $\alpha = \frac{1}{6}\pi$, $\theta_1 = \frac{1}{2}\pi$. This corresponds to the flow pattern when an infinite block of material is pressed against a rigid wall by a suitably chosen pressure distribution at infinity. The radial and transverse components of velocity are tabulated below, and streamlines ABC, $A'B'C'$ are shown in the diagram which illustrates the flow on one side of the axis OS of symmetry. Notice that, just as in plastic-rigid solutions with plane strain, there is a discontinuity in the tangential component of velocity across the characteristic surface which forms the rigid-plastic boundary.

TABLE

θ	< 30	30+	40	50	60	70	80	90
u	$-0{\cdot}944\cos\theta$	1·183	0·239	0·141	0·105	0·081	0·066	0·058
v	$0{\cdot}944\sin\theta$	0·472	0·230	0·142	0·090	0·051	0·023	0·000

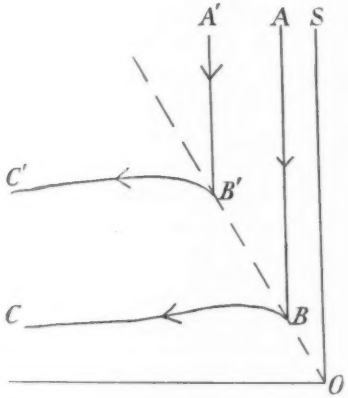

FIG 1.

The stress distribution is given by (11) and (12), $\sigma_{\theta\theta}$ being arbitrary to the extent of an additive constant. This may be chosen such that the relation between the shear stress, $\frac{1}{2}k$, and the normal pressure on the plane boundary fits any desired coefficient of friction.

REFERENCES

1. R. HILL, *The Mathematical Theory of Plasticity*, ch. vi (Oxford, 1951).
2. —— ibid. p. 263.
3. P. S. SYMONDS, 'The general equations of problems of axial symmetry in the theory of plasticity', *Quart. App. Math.* **6** (1949), 448.

THE VARIATION OF COMPRESSIBLE FLOWS

By A. R. MANWELL (*University College, Swansea*)

[Received 18 October 1951; revised 5 June 1952]

SUMMARY

The theory of the perturbation of those compressible flows in which there are only two independent variables is developed, with special reference to steady plane transonic flow. Expressions are found for variations of both the physical flow and of its hodograph and relations obtained between the two sorts of variation. It is then proved that even if the Jacobian of the hodograph of a flow should vanish on the boundary the flow need not be critical. Using the expressions for variations in the physical plane of flow, boundary-value problems for perturbations can be discussed directly in the physical plane. The methods are applied to the case of circulatory flow outside circular or nearly circular cylinders. It is proved that instability can arise by a resonance process near certain critical speeds, measured on the boundary of the flow, and that at these speeds Dirichlet's problem for the perturbation stream function has no unique solution.

1. Introduction

It has been conjectured that transonic flows may be unstable even on the perfect fluid theory of compressible flow. In the attempt to demonstrate mathematically the existence of a singularity in the hodograph equations of transonic flow the behaviour of 'limit lines' has been studied in detail, cf., for example, refs. (**1**)–(**5**), but the 'limit line' singularity cannot appear in flows of the type usually investigated, as has been shown in (**4**), (**5**). On the other hand, Frankl (**6**) has endeavoured to prove instability by a general argument concerning the non-existence of solutions for contours adjacent to a given flow. Again, Guderley (**7**) has put forward arguments to show that singularities of the flow solutions arising at the end of a local supersonic region, due to initially small disturbances, will be accompanied by instability of the actual physical flow. Neither of these papers, however, gives any precise example of the breakdown of potential flow solutions.

In the present investigation, in which variational methods are used extensively, the basic step is to show that the perturbations of potential or stream function satisfy some particularly simple equations in the characteristic plane, or better, if this is available, the hodograph plane. The functions which arise in the perturbation theory are distinct from the ordinary hodograph solutions but can be expressed by means of them in an elementary way. The equation for perturbation of both physical and hodograph flow is derived and it is proved that even if the Jacobian of the

transformation from the physical flow plane to hodograph space should vanish on a (special) boundary, such a flow need not be critical. The perturbation theory is then applied to the case of a transonic vortex, i.e. a circulatory flow outside a circular cylinder. It is found that for most changes of the boundary there exist corresponding small changes of the flow. However, near many speeds of the stream at the boundary there are critical perturbations which give proportionately large changes of the flow. The situation is closely analogous to resonance in linear vibration theory. The critical speeds themselves are characterized by the non-uniqueness of Dirichlet's problem for the perturbation stream function and so for the stream function of the compressible flow in the physical plane. The solution of Dirichlet's problem regular within the flow region and taking the value zero on the boundary appears in a similar role to that of a proper mode in the theory of vibrations.

This investigation is limited to plane transonic flow having a simple one–one hodograph representation. It seems to give a more precise formulation of the general notion of Frankl's paper (**6**) inasmuch as potential flow for adjacent yet *smooth* boundaries is shown to be unstable. Here, however, non-uniqueness is proved, not, as in (**6**), the non-existence of solutions. It may be, however, that the type of breakdown suggested by Guderley (**7**) has also an exact formulation. The present method seems the most natural since only continuous perturbations of the boundary and of the velocity field are required to give instability, whereas Guderley considers small discontinuities in velocity.

2. Basic equations for perturbations

The equations of compressible potential flow with two independent variables can be written in the form

$$A_x + B_y = 0, \tag{2.1}$$

$$C_x + D_y = 0, \tag{2.2}$$

where u, v are functions of the variables (x, y), A, B, C, D are given functions of u, v, and suffixes denote derivatives. For plane flow u, v are components of velocity, and (2.1), (2.2) are equivalent to

$$\left.\begin{aligned} A &= -v = \Phi_y \\ B &= u = -\Phi_x \end{aligned}\right\}, \tag{2.1.1}$$

$$\left.\begin{aligned} C &= \Psi_y = -\rho u \\ D &= -\Psi_x = -\rho v \end{aligned}\right\}, \tag{2.2.1}$$

where Φ, Ψ are the usual potential function and stream function respectively, while $p = p(\rho)$ is pressure and ρ is the density. Pressure and density are determined as functions of the speed by

$$\int \rho^{-1}\, dp + \tfrac{1}{2}(u^2+v^2) = \text{const.}$$

The forms (2.1) and (2.2) reappear in the equations of axially symmetric flow and, with a slight change of notation, the equations for one-dimensional non-linear waves. A linear combination of (2.1), (2.2) such as

$$A_x + B_y + \lambda(C_x + D_y) = 0 \tag{2.3}$$

is said to be in characteristic form if after expansion it appears that both u and v are differentiated in the same direction, say,

$$\left(\frac{dy}{dx}\right)_\Gamma = \mu. \tag{2.4}$$

The condition on λ is clearly that

$$\mu = \frac{B_u + \lambda D_u}{A_u + \lambda C_u} = \frac{B_v + \lambda D_v}{A_v + \lambda C_v}, \tag{2.5}$$

so that λ satisfies the quadratic equation

$$\lambda^2 \begin{bmatrix} C & D \\ u & v \end{bmatrix} + \lambda \left\{ \begin{bmatrix} A & D \\ u & v \end{bmatrix} + \begin{bmatrix} C & B \\ u & v \end{bmatrix} \right\} + \begin{bmatrix} A & B \\ u & v \end{bmatrix} = 0, \tag{2.6}$$

$[\ \ ]$ denoting the Jacobian of the quantities enclosed. For plane flow the term in λ disappears and the roots are given by

$$\lambda_2 = -\lambda_1 = \rho^{-1} \tan \epsilon, \tag{2.7}$$

where ϵ is defined by $\qquad c = q \sin \epsilon,$

c being the speed of sound and q the flow speed. Equation (2.4) therefore defines two families of curves, one of each family passing through every point of the (x, y) plane. To successive members of the system having $dy/dx = \mu_2$ let any monotonic set of numbers α be attached and similarly a set β to the other system. Then α, β are called characteristic coordinates and by the mode of construction are in one–one correspondence with the (x, y) plane.

Let (u^1, v^1) and (u, v) be respectively solutions of equations (2.1), (2.2) and let $\delta u = u^1 - u$, $\delta v = v^1 - v$ be everywhere small; let the corresponding variations of $\Phi(x, y)$, $\Psi(x, y)$ be denoted by χ, η respectively. Then, in the limiting case of infinitesimal velocity changes it follows from equations (2.1.1), (2.2.1) that

$$\left.\begin{aligned} A_u\, \delta u + A_v\, \delta v &= \chi_y, & B_u\, \delta u + B_v\, \delta v &= -\chi_x \\ C_u\, \delta u + C_v\, \delta v &= \eta_y, & D_u\, \delta u + D_v\, \delta v &= -\eta_x \end{aligned}\right\}. \tag{2.8}$$

Therefore, with dx, dy quite general

$$\left.\begin{aligned} d\chi &= -(B_u\delta u+B_v\delta v)\,dx+(A_u\delta u+A_v\delta v)\,dy \\ d\eta &= -(D_u\delta u+D_v\delta v)\,dx+(C_u\delta u+C_v\delta v)\,dy \end{aligned}\right\}. \tag{2.9}$$

However, solving equations (2.5) for λ, we find

$$\lambda = -\frac{(\mu A_u - B_u)}{(\mu C_u - D_u)} = -\frac{(\mu A_v - B_v)}{(\mu C_v - D_v)}, \tag{2.10}$$

so that along a characteristic direction the ratio of the infinitesimal quantities in equation (2.9) satisfies

$$\frac{d\chi}{d\eta} = -\lambda, \tag{2.11}$$

the expressions in δu, δv cancelling. The perturbation functions therefore satisfy the simultaneous partial differential equations

$$\chi_\alpha+\lambda_1\eta_\alpha = 0, \tag{2.12}$$

$$\chi_\beta+\lambda_2\eta_\beta = 0, \tag{2.13}$$

and this result is quite general for all quasi-linear systems which can be written in the form of (2.1), (2.2). In particular, for plane flow it can be shown that

$$\int \cot\epsilon q^{-1}\,dq+\theta = 2g(\beta), \tag{2.14}$$

$$\int \cot\epsilon q^{-1}\,dq-\theta = 2f(\alpha), \tag{2.15}$$

where f and g are arbitrary functions. If both $f(\alpha)$ and $g(\beta)$ are monotonic in their arguments they may be identified with just α, β respectively. Such flows will be described as having a non-degenerate hodograph. The perturbation equations can then be shown to reduce to

$$\rho q\chi_q+\eta_\theta = 0, \tag{2.16}$$

and

$$q\eta_q = (\rho q)_q\chi_\theta. \tag{2.17}$$

The derivations of equations (2.14)–(2.17) are routine and are omitted since equations (2.16) and (2.17) are to be derived by a method which makes use of the variation of the hodograph of the varied flow. It may be remarked here that α, β or q, θ refer to the flow before perturbation so that χ, η retain their identity as perturbations in the physical plane. In particular, the conditions corresponding to a fixed boundary are $\Psi = 0$ and $\Psi^1 = 0$ so that $\eta = 0$ also. This is quite different from the normal hodograph method where the new boundary can only be found after a complicated integration. It is also noteworthy that with the special choice of variables (χ, η) and (q, θ) the single system (2.16), (2.17) suffices for the whole class of flows having non-degenerate hodographs; δu, δv, however, involve the particular hodograph transformation explicitly.

3. Hodograph variations

If Φ^1, Ψ^1 refer to the perturbed flow, regarded as depending on x, y, then

$$\Phi^1 = \Phi+\chi, \qquad \Psi^1 = \Psi+\eta \tag{3.1}$$

and the velocities are given by

$$\left.\begin{aligned} d\Phi &= -(u\,dx+v\,dy)\\ d\Psi &= \rho(v\,dx-u\,dy)\end{aligned}\right\}; \tag{3.2}$$

Φ^1 may therefore be written as $\Phi(q,\theta)+\chi(q,\theta)$ and similarly for Ψ^1, but this is not a hodograph solution since, on account of the perturbation, the velocities are changed according to

$$u^1 = q^1\cos\theta^1 = -\frac{\partial\Phi^1}{\partial x} = u-\chi_x, \tag{3.3}$$

$$v^1 = q^1\cos\theta^1 = -\frac{\partial\Phi^1}{\partial y} = v-\chi_y. \tag{3.4}$$

Hence, with the understanding that χ and η are infinitesimal,

$$q^1\cos\theta^1 = q\cos\theta-(\chi_q q_x+\chi_\theta\theta_x),$$
$$q^1\sin\theta^1 = q\sin\theta-(\chi_q q_y+\chi_\theta\theta_y).$$

Replacing the derivatives with respect to x, y by those with respect to q, θ and solving for δq, $\delta\theta$

$$\mathscr{J}\rho q\,\delta q = -\chi_q\Psi_\theta+\chi_\theta\Psi_q, \tag{3.5}$$

$$\mathscr{J}q^2\delta\theta = \chi_q\Phi_\theta-\chi_\theta\Phi_q, \tag{3.6}$$

where the Jacobian $\mathscr{J}$ is given by

$$\mathscr{J} = \begin{bmatrix} x & y\\ \theta & q\end{bmatrix} = \frac{1}{\rho q^2}(\Phi_\theta\Psi_q-\Phi_q\Psi_\theta), \tag{3.7}$$

and (3.2) has been used to eliminate derivatives of (x, y).

Then

$$\begin{aligned}\Phi^1(q^1,\theta^1) &= \Phi(q,\theta)+\chi(q,\theta)\\ &= \Phi(q^1,\theta^1)+\phi(q^1,\theta^1)\end{aligned}$$

to the first order, where

$$\phi(q^1,\theta^1) \equiv (\chi-\Phi_q\delta q-\Phi_\theta\delta\theta)^1.$$

Using (3.5), (3.6), (3.7) it is found that

$$\phi \equiv \chi-q\chi_q. \tag{3.8}$$

By a similar calculation the perturbation of the hodograph stream function is found to be

$$\psi \equiv \eta-\rho\chi_\theta. \tag{3.9}$$

It is also possible to work in terms of derivatives of η and thus get

$$\phi \equiv \chi + \rho^{-1}\eta_\theta, \tag{3.10}$$

$$\psi \equiv \eta - \frac{(\rho q)}{(\rho q)_q}\eta_q. \tag{3.11}$$

Comparison of (3.8), (3.9) with (3.10), (3.11) gives

$$\eta_\theta + \rho q \chi_q = 0, \tag{3.12}$$

$$q\eta_q = (\rho q)_q \chi_\theta, \tag{3.13}$$

that is, equations (2.16), (2.17) already given above. It will be noted that χ and η are the Legendre transforms associated with the hodograph perturbations ϕ, ψ respectively (cf. (**3**), pp. 248–52). A useful check on these calculations is afforded by the verification that (taking account of these last two equations) ϕ and ψ satisfy the usual hodograph equations, viz.

$$\rho^2 q\phi_q + (\rho q)_q \psi_\theta = 0, \tag{3.14}$$

$$\rho\phi_\theta = q\psi_q. \tag{3.15}$$

Equation (3.11) reduces the calculation of η to the mere integration of standard hodograph solutions according to

$$\eta = -\rho q\Big\{\int \psi\rho^{-2}q^{-2}(\rho q)_q\, dq\Big\}. \tag{3.16}$$

By means of the relations of this section, the variation of the Jacobian

$$\mathscr{J} = \rho^{-2}q\left\{\Psi_q^2 + \frac{(\rho q)_q}{\rho q^2}\Psi_\theta^2\right\} \tag{3.17}$$

on the *fixed boundary* of a flow can be conveniently found. A condition on the perturbation is that $\eta = 0$, for this boundary remains a streamline while the curvature κ also remains constant. It can be easily shown (cf. (**5**)) that

$$\kappa = -\Psi_q/(\rho q \mathscr{J}). \tag{3.18}$$

Hence

$$\begin{aligned}\kappa\delta\mathscr{J} &= -\delta(\Psi_q/\rho q) = -\delta(\Phi_\theta/q^2)\\ &= -\left[\frac{\partial}{\partial\theta^1}(\Phi^1/q^{1^2}) - \frac{\partial}{\partial\theta}(\Phi/q^2)\right].\end{aligned}$$

But $\delta\theta$ vanishes on the boundary so that

$$\frac{\partial}{\partial\theta^1}(\Phi^1) = \frac{\partial}{\partial\theta^1}\{\Phi+\phi\} = \left(\frac{\partial\Phi}{\partial\theta}\right)^1 + \left(\frac{\partial^2\Phi}{\partial q\partial\theta}\right)^1\delta q + \left(\frac{\partial\phi}{\partial\theta}\right)^1,$$

due allowance having been made for both the change of the form of the hodograph of the flow and of the image of the point on the boundary under consideration. Again from (3.5), (3.6)

$$\delta q = q\chi_q/\Phi_q. \tag{3.19}$$

Hence, dropping the accents,

$$\kappa\delta\mathscr{J} = (q^{-3}2\Phi_\theta - q^{-2}\Phi_{q\theta})q\chi_q/\Phi_q - q^{-2}\phi_\theta,$$

which may be conveniently written

$$\delta\mathscr{J}/\mathscr{J} = \frac{\partial(q^{-2}\Phi_\theta)/\partial q}{q^{-2}\Phi_\theta}\left(\frac{q\chi_q}{\Phi_q}\right) + \phi_\theta/\Phi_\theta. \tag{3.20}$$

This result shows that if regular perturbations of the velocities are introduced into a field the change of $\mathscr{J}$ remain small.† Even if $\mathscr{J}$ actually vanishes on the boundary, in the vicinity of the zero the changes of $\mathscr{J}$ in the hodograph of the perturbed flow remain proportionately small, and so flows with isolated zeros of $\mathscr{J}$ are perturbed into similar ones.

This section therefore adds to the existing evidence that the vanishing of the Jacobian does not explain the breakdown of potential flow.

4. Perturbation theory for the vortex

A very simple example of a mixed flow is furnished by the vortex which was studied by Guderley (**7**) by some rather involved calculations in the hodograph plane.

If we suppose that $\Phi = \Phi(\theta)$, $\Psi = \Psi(q)$, then equations (3.14), (3.15) give a solution

$$\Phi = \theta, \tag{4.1}$$

$$\Psi = \int q^{-1}\rho\, dq. \tag{4.2}$$

Using equation (3.2), the streamlines are, with a suitable choice of origin,

$$x = -q^{-1}\sin\theta, \tag{4.3}$$

$$y = q^{-1}\cos\theta. \tag{4.4}$$

The boundary of the flow, which extends to infinity, may be taken to be the image of any supersonic circle, say $q = q_1 > c_*$, with the usual notation for critical speed. Let $\psi = \sum (a_n\cos n\theta + b_n\sin n\theta)\psi_n(q)$, where the ψ_n are the quantities considered in (**8**) and so regular at $q = 0$, which is the image of the point at infinity. Then a general perturbation solution is

$$\eta = \sum (a_n\cos n\theta + b_n\sin n\theta)\eta_n(q), \tag{4.5}$$

where the $\eta_n(q)$ are derived from the $\psi_n(q)$ by means of equation (3.16).

The perturbation of the boundary is then

$$\sum (a_n\cos n\theta + b_n\sin n\theta)\eta_n(q_1) = \sum (A_n\cos n\theta + B_n\sin n\theta). \tag{4.6}$$

The A_n and B_n being specified, the perturbation of the flow is given by

$$\eta = \sum \frac{(A_n\cos n\theta + B_n\sin n\theta)\eta_n(q)}{\eta_n(q_1)}. \tag{4.7}$$

† The difficulty due to the denominator vanishing at the sonic line is only apparent.

Therefore if q_1 is nearly equal to a zero of some $\eta_n(q)$, the term

$$A_n \cos n\theta + B_n \sin n\theta$$

gives a correspondingly large change of the flow for a small perturbation of the boundary of this form. If q_1 is equal to a zero of some $\eta_n(q)$, the solution (4.7) has no meaning but the term $(A_n \cos n\theta + B_n \sin n\theta)\eta_n(q)$ has the property of vanishing on the whole boundary of the flow, being regular within, and yet not vanishing identically. Now it is easily shown by evaluating the $\eta_n(q)$ in terms of the $\Psi_n^*(q)$ of (**8**) that the first few do have roots in the supersonic region (see Appendix). It is also true that for high n the η vanish very near the sonic circle. This may be proved by integrating the asymptotic formulae (**8**) for ψ from the origin up to the first loop of $\psi_n(q)$ in the supersonic region. It is also an immediate consequence of the oscillatory character of the asymptotic expansions of the corresponding functions $\chi_n(q)$. Thus if $\eta_n = g(q)\cos n\theta$, $\chi = f(q)\sin n\theta$ equations (3.12), (3.13) give

$$ng = \rho q f', \tag{4.8}$$

$$n(\rho q)_q f = qg', \tag{4.9}$$

and f satisfies

$$(\rho q f')' = n^2 q^{-1}(\rho q)_q f. \tag{4.10}$$

It is then a well-known result that for large n, f oscillates rapidly in the whole region $q > c_*$, the term $\rho^{-1}(\rho q)_q \equiv 1 - q^2/c^2$ being negative in that region. Therefore, by (4.8), g vanishes frequently in the supersonic region.

It follows that, for many speeds of flow on the boundary of the cylinder, *resonance* can occur between certain perturbations of the boundary and the flow. Such perturbations give rise to proportionately large changes of flow at neighbouring speeds, while at these speeds the functions $\eta(q, \theta)$ may be added as desired. Dirichlet's problem is not unique for a whole sequence of boundary speeds q_1 and, since, for high n, the zeros of $\eta_n(q)$ lie close together, in a practical sense is never unique. Even for low $n \leqslant 7$ there are four roots in the range $0{\cdot}24 < \tau < 0{\cdot}30$ where $\tau = q^2/q_{\max}^2 = \frac{1}{6}$ corresponds to sonic conditions (see Appendix).

The success of the above investigation into instability of the flow around a circular cylinder depends largely on the practicability of constructing general perturbation solutions at all flow speeds. Only a single infinity of speeds furnish examples of resonance, and of the non-uniqueness of Dirichlet's problem for the perturbation stream function. It seems likely, although this fact is not proved, that in other cases the perturbation functions are unique. To prove the existence of unstable flows it is not necessary to construct all the hodograph solutions for a given body as the stream speed, or some equivalent parameter, is varied. This was done for the circular

cylinder, but is clearly a most difficult matter in general. It is *sufficient* to show that there is both a hodograph solution and a regular perturbation function having respectively $\Psi = 0$, $\eta = 0$ on the *same* (hodograph) boundary streamline and that the hodograph corresponds to a true physical flow. This can be readily proved for certain families of boundaries differing slightly from the circle, the behaviour of the flow at infinity still being that of the vortex.

Let $$\eta = \eta_2 \sin 2\theta + \epsilon\eta_4 \sin 4\theta$$

be a perturbation function, where ϵ is small, and let the boundary of the flow be approximately $q = \alpha_2$, where α_2 is the smallest root of $\eta_2(q) = 0$ lying in the supersonic range of q. Then to a first approximation the boundary hodograph is given by

$$q = \alpha_2 + \Delta q(\theta),$$

where $$\Delta q = -2\epsilon\eta_4(\alpha_2)\cos 2\theta/\eta_2'(\alpha_2)$$

and (see Appendix) $\eta_2'(\alpha_2)$ and $\eta_4(\alpha_2)$ do not vanish. Then the hodograph solution having Ψ constant to order ϵ on the same boundary is given by

$$\Psi = \int \rho q^{-1}\, dq + \epsilon' \Psi_2^*(q)\cos 2\theta,$$

provided that $$\epsilon' = 2\epsilon\rho(\alpha_2)\eta_4(\alpha_2)/\{\alpha_2\, \Psi_2^*(\alpha_2)\eta_2'(\alpha_2)\};$$

it being noted (reference (**8**)) that $\Psi(\alpha_2) \neq 0$.

A similar family of hodograph solutions and corresponding perturbation functions is given by

$$\eta = \eta_3(q)\sin 3\theta + \epsilon\eta_6(q)\sin 6\theta,$$

$$\Psi = \int \rho q^{-1}\, dq + \epsilon' \Psi_3(q)\cos 3\theta,$$

the ratio of ϵ' to ϵ being suitably chosen.

To complete the proof of the existence of unstable flows it only remains to be shown that the hodograph solutions Ψ can in such cases be mapped into physical space without limit lines. In reference (**9**) the author has shown that if any analytic hodograph solution is given with the boundary not touching a characteristic in the hodograph plane, then none of the streamlines inside the flow can do so and the whole solution corresponds to a physical flow. With a slight, but obvious change, this result applies in the present case since the boundary streamline is entirely supersonic although the flow is of mixed type. It is also clear that the hodograph of the flow corresponding to the almost circular cylinder differs only slightly from that for the circle and in the latter every streamline cuts the hodograph characteristics at a finite angle. It has therefore been shown that

the resonance effects occur for nearly circular boundaries as well as for the exact solutions for the circle. While the analysis may well be difficult, it seems likely that all families of transonic flows will contain examples of resonance, and of the non-uniqueness of Dirichlet's problem, provided that the parameters on which they depend can be varied sufficiently.

It conclusion, it may be noted that the above discussion of plane transonic compressible flow is carried out entirely within the perfect fluid theory. It has not been necessary to make any allowance for boundary-layer effects; nor have time-dependent disturbances been introduced to prove instability. This phenomenon has been shown to arise as a purely mathematical fact associated with the non-uniqueness of Dirichlet's problem for the perturbation of the stream function in the physical plane at certain critical speeds. It is also noteworthy that, for all supersonic boundary conditions on the cylinder, there are many critical speeds, and that the corresponding proper perturbations of the boundary are rapidly oscillating functions. In physical terms, roughness of the boundary should give rise to instability for supersonic conditions. This is known to be true in practice. There are, it seems, good grounds for expecting the complete explanation of the instability of plane transonic compressible flows to be found in a study of the, admittedly intractable, problem of the uniqueness of Dirichlet's problem for the linear differential equation satisfied by the perturbation stream function.

The author gratefully acknowledges that he was first led to apply variational methods to the problem of the instability of transonic flow by a suggestion of Professor W. R. Sears.

APPENDIX

The perturbation stream function η can, according to equation (3.16), be expressed in terms of the hodograph stream function of ref. (**8**). Thus

$$\eta_n(\tau) = \tfrac{1}{2}(1-\tau)^{2\cdot5}\tau^{0\cdot5} \int_0^\tau \Psi_n^*(\tau)(1-6\tau)(1-\tau)^{-3\cdot5}\tau^{-1\cdot5}\, d\tau$$

for $n > 1$ while for $n = 1$

$$\eta_1(\tau) = \tfrac{1}{2}(1-\tau)^{2\cdot5}\tau^{0\cdot5}$$

and for $n = -1$, $\Psi_n^* = 1/\tau^{0\cdot5}$ and the lower limit is now $\tau = \frac{1}{6}$. The η_n have been tabulated for $n = 1$ to 7 and for $n = -1$ by numerical integration of the tables of $F_n(\tau)$ of ref. (**8**) and for $\tau = q^2/q_{\max}^2$ from 0 to 0·40 at intervals of 0·02. It is hoped to prepare fuller tables at a later date.

For convenience of presentation the functions are given as multiples of $\eta_n(\frac{1}{6})$ and the value of this is given below each column except that $\eta_{-1}(\frac{1}{6})$ can be chosen arbitrarily and is here taken as zero.

Table of Reduced Function $\eta_n(\tau)/\eta_n(\frac{1}{6})$

τ \ n	1	2	3	4	5	6	7	−1
·00	0	0	0	0	0	0	0	—
·02	·519	·253	·119	·040	·024	·014	·008	—
·04	·698	·465	·298	·173	·118	·079	·052	—
·06	·811	·635	·482	·350	·272	·209	·159	—
·08	·887	·767	·651	·538	·460	·389	·329	2·572
·10	·939	·867	·792	·712	·651	·591	·536	1·154
·12	·973	·937	·898	·854	·818	·780	·744	·450
·14	·992	·981	·967	·952	·938	·923	·909	·121
·16	1·000	·999	·998	·997	·996	·995	·994	·006
·18	·998	·995	·992	·988	·983	·978	·972	·018
·20	·989	·973	·951	·924	·897	·866	·832	·108
·22	·974	·933	·879	·809	·741	·662	·574	·245
·24	·953	·879	·778	·649	·523	·378	·218	·410
·26	·928	·812	·654	·451	·255	·033	−·208	·589
·28	·900	·734	·509	·224	−·049	−·349	−·666	·775
·30	·868	·648	·350	−·023	−·371	−·741	−·114	·962
·32	·834	·554	·180	−·281	−·695	−1·114	−1·510	1·145
·34	·798	·456	·003	−·540	−1·004	−1·444	−1·819	1·316
·36	·760	·354	−·175	−·791	−1·281	−1·706	−2·009	1·480
·38	·721	·250	−·352	−1·024	−1·516	−1·884	−2·063	1·639
·40	·682	·145	−·522	−1·233	−1·695	−1·965	−2·018	1·788
$\eta_n(\frac{1}{6})$	·1294	·0750	·01063	·002010	·000461	·0001114	·00002790	0

REFERENCES

1. H. S. Tsien, *The Limiting Line in Mixed Subsonic and Supersonic Flow of Compressible Fluids*, N.A.C.A., T.N. No. 961, 1944.
2. J. W. Craggs, 'The breakdown of the hodograph transformation for irrotational compressible fluid flow in two dimensions', *Proc. Camb. Phil. Soc.* **44** (1948), 360–79.
3. R. Courant and K. O. Friedrichs, *Supersonic Flow and Shock Waves*, Interscience Publishers Inc. (New York, 1948).
4. A. A. Nikolskii and G. I. Taganov, 'Dvizhenia Gaza v Mestnoi Sverkhzvukovoi Zone i Nekotorye Uslovia Razrushenia Potentsialnógo Techenia', *Prikladnaya Matematika i Mekhanika*, **4** (1946), 481–502. ('Gas motion in a local supersonic region and conditions of potential flow breakdown', transl. by S. Reiss, N.A.C.A., Tech. Mem. 1213.)
5. K. O. Friedrichs and D. Flanders, 'On the non-occurrence of a limiting line in transonic flow', *Comm. App. Math.* **1** (1948), 1, 287–301.
6. F. I. Frankl, *On the Formation of Shock Waves in Subsonic Flows with Local Supersonic Velocities.* (Transl. N.A.C.A., Tech. Mem., No. 1251.)
7. G. Guderley, *On the Transition from Transonic Potential Flow to a Flow with Shocks*, Air, Mat. Comm., T–2, F–TR–2160, N.D.
8. D. F. Ferguson and M. J. Lighthill, 'The hodograph transformation in transonic flow, IV. Tables', *Proc. Roy. Soc.* A **192** (1947), 135–42.
9. A. R. Manwell, 'A note on the hodograph transformation', *Quart. App. Math.* **10** (1952), 177–84.

A FOURIER INTEGRAL SOLUTION FOR THE STRESSES IN A SEMI-INFINITE STRIP

By L. H. MITCHELL

(*Dept. of Civil Engineering, The University, Bristol*)†

[Received 5 June 1952]

SUMMARY

A solution is given for a stress diffusion problem in a semi-infinite strip. Fourier integrals are used and the method is applicable to problems where the boundary conditions are given in terms of stresses. Good agreement is found between the theoretical solution and a photoelastic investigation.

Introduction

In this paper Fourier integrals are used to determine the stresses in a semi-infinite strip, the boundary conditions being given in terms of stresses. Both Howland (**1**) and Hopkins (**2**) have used Fourier integrals for the solution of generalized plane stress problems in infinite strips with a variety of boundary conditions. Howland's paper is confined to cases where the stresses along the long edges are prescribed, whereas Hopkins treats the case of mixed boundary conditions.

By adding further terms to the Fourier integral stress function given by Howland, it is shown here that the boundary conditions of a semi-infinite strip can be satisfied if they are expressed in terms of stresses. The particular problem solved is one of stress diffusion and is illustrated in Fig. 1.

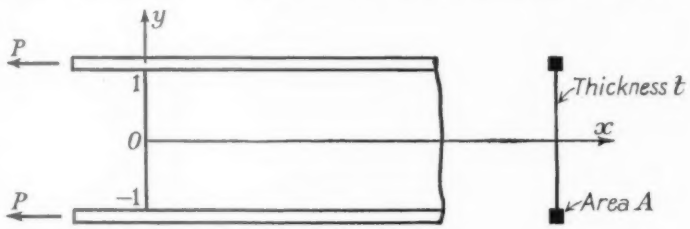

Fig. 1.

Notation

A Area of one stiffener.
b Half-width of strip, taken as the unit of length.
B, C, D Functions of m.
m A parameter.
P Concentrated load applied to stiffener.

† Now at the Aeronautical Research Laboratories, Department of Supply, Melbourne.

t Plate thickness.
(x, y) Rectangular coordinates.
λ Dimensionless parameter $A/bt = A/t$.
σ_x, σ_y Direct stresses in the x, y directions.
σ_0 Direct stress at the end of the stiffeners given by P/A.
τ Shear stress.
$\Phi(x, y)$ Airy stress function.

For convenience the unit of length is taken as the half-width of the strip.

Details of the solution

The stresses are to be found in the plate shown in the above figure, which also shows the position of the rectangular axes. The coordinates (x, y) which have been chosen are dimensionless and are obtained by dividing the true distances by b, the half-width of the strip. In effect b is taken as the unit dimension and consequently all quantities involving length must be modified accordingly; for example the area of the stiffeners must be divided by b^2 and the result is denoted by A. The stiffeners, of the same material as the plate, are assumed to resist longitudinal direct stresses only and it is also assumed that this direct stress is constant over any cross-section of a stiffener. Thus the stiffeners have been idealized since this assumption implies infinite rigidity with respect to shear stresses only. The short side of the strip is required to be stress free.

By means of the Airy stress function

$$\int_0^\infty (B \cosh my + Cy \sinh my) \sin mx \, dm,$$

which can be shown to satisfy the two-dimensional bi-harmonic equation of generalized plane stress, it follows from Howland's paper that the boundary conditions along the two sides of a semi-infinite strip, symmetrically loaded, can be satisfied. However, with this stress function both the direct stresses σ_x and σ_y are automatically zero along the short side of the strip and therefore additional stress functions are required to satisfy the stress-free condition (i.e. $\sigma_x = \tau = 0$) along this edge. The true transverse strain distribution at the end can be represented by a cosine Fourier series, and the suggested additional stress function is†

$$\sum_n D_n F_n(x) \cos \tfrac{1}{2} n\pi y.$$

It is required that $F_n(0) = 0$ to enable the boundary conditions $\sigma_x = 0$ at

† The general form of $F_n(x)$ is $(x + E_n)e^{-\frac{1}{2}n\pi x}$ enabling the two boundary conditions at $x = 0$ to be satisfied.

$x = 0$ to be satisfied and also each term must satisfy the equation of generalized plane stress. Such a series is

$$\tfrac{1}{2}Dx^2 + \sum_n D_n x e^{-\frac{1}{2}n\pi x} \cos \tfrac{1}{2}n\pi y,$$

where $n = 1, 3, 5, \ldots$. The first term permits σ_y, obtained from this series, to assume other than a non-zero value at $y = \pm 1$. Thus the stress function enabling all the boundary conditions to be satisfied is

$$\Phi = \sum_{n=0}^{\infty} \int_0^{\infty} (B_n \cosh my + C_n y \sinh my) \sin mx \, dm + \\ + \tfrac{1}{2}D_0 x^2 + \sum_{n=1}^{\infty} D_n x e^{-\frac{1}{2}n\pi x} \cos \tfrac{1}{2}n\pi y.$$

The boundary conditions to be satisfied are

(1) $\sigma_x = 0, x = 0;$

(2) $\tau = 0, x = 0;$

(3) $\sigma_y = 0, y = \pm 1;$

(4) $\tau t - A \dfrac{\partial \sigma_x}{\partial x} = 0, y = \pm 1.$

The last condition (4), obtained from consideration of the equilibrium of an element of length of the stiffener, does not specify the load applied to the strip. By replacing this condition by the condition that the total load carried by any cross-section of the strip (including the stiffeners) is constant and equal to the applied load, this difficulty is overcome. It can be shown that this latter condition implies the condition (4). With the restriction that the terms with suffix other than zero add nothing to the load carried by the strip, the conditions (3) and (4) lead to the relations†

$$\tfrac{1}{2}\pi B_0 = \frac{(D_0/m^3)(\sinh m + m \cosh m + 2m\lambda \cosh m + \lambda m^2 \sinh m) - (P/tm)\sinh m}{m + \sinh m \cosh m + 2\lambda m \cosh^2 m}$$

$$\tfrac{1}{2}\pi C_0 = \frac{-(D_0/m^3)(m \sinh m + \lambda m^2 \cosh m) + (P/tm)\cosh m}{m + \sinh m \cosh m + 2\lambda m \cosh^2 m}.$$

The shear stress due to these terms involving B_0, C_0, and D_0 is given by

$$\tau = -\frac{\partial^2 \Phi}{\partial x \partial y} = -\int_0^{\infty} m(mB_0 \sinh my + C_0 \sinh my + C_0 my \cosh my) \cos mx \, dm.$$

† Obtained with the use of the identity $\displaystyle\int_0^{\infty} \frac{\sin mx}{m} \, dm = \tfrac{1}{2}\pi.$

For large m and $y \neq 0$ we may neglect me^{-2m} and write

$$\sinh my \doteqdot \cosh my \doteqdot \tfrac{1}{2}e^{my};$$

the integrand of this integral then becomes

$$-\frac{2}{\pi}\frac{[D_0(1+\lambda m)-mP/t](1-y)+\lambda D_0+P/t}{(1+2\lambda m)}e^{-(1-y)m}\cos mx.$$

If the integral is to converge at the point $(0, 1)$ then $D_0 = -P/\lambda t$ and the integrand for large m approaches

$$\frac{2}{\pi}\frac{P}{t\lambda}(1-y)e^{-(1-y)m}\cos mx.$$

Consequently the shear stresses can be written

$$\tau = \int_0^\infty \left[F(m,y)+\frac{2}{\pi}\frac{P}{t\lambda}(1-y)e^{-(1-y)m}\right]\cos mx\, dm,$$

where $F(m, y) \to 0$ exponentially as $m \to \infty$ for $0 < y \leqslant 1$, i.e.

$$\tau = \int_0^\infty F(m,y)\cos mx\, dm+\frac{2}{\pi}\frac{P}{t\lambda}\frac{(1-y)^2}{x^2+(1-y)^2}.$$

Hence, there is a discontinuity at the point $(0, 1)$ such that

$$\lim_{x\to 0}\tau(x,1) = \int_0^\infty F(m,1)\, dm$$

and

$$\lim_{y\to 1}\tau(0,y) = \int_0^\infty F(m,1)\, dm+\frac{2}{\pi}\frac{P}{t\lambda}.$$

Thus, when the end of the strip is free from shear, the peak shear stress along the edge stiffener is $2P/\pi t\lambda$ which is $2/\pi$ times the direct stress in the stiffener. However, this type of discontinuity can be shown to involve a rotation of the corner through 90° and for this reason the analytical solution cannot represent the stresses in small regions near the corners of an actual plate.

There remains the problem of eliminating the finite shear stress left acting over the end. This can be done with the aid of the remaining terms of the stress function. The boundary conditions determining B_n, C_n, and D_n are

(1) $\tau = 0, x = 0$;

(2) $\sigma_y = 0, y = \pm 1$;

(3) The load carried by the plate and stiffeners at any section is zero.

The conditions (2) and (3) lead to the relations

$$B_n = \frac{-\pi n^2 m D_n \sinh m}{(m^2+\frac{1}{4}n^2\pi^2)^2(m+\sinh m\cosh m+2m\lambda\cosh^2 m)},$$

$$C_n = \frac{\pi n^2 D_n m\cosh m}{(m^2+\frac{1}{4}n^2\pi^2)^2(m+\sinh m\cosh m+2m\lambda\cosh^2 m)}.$$

Thus the expression for the shear stress at $x = 0$ can be written in the form

$$\tau = \sum_{n=1}^{\infty} D_n \tfrac{1}{2}n\pi \sin \tfrac{1}{2}n\pi y + \sum_{n=1}^{\infty} D_n \int_0^{\infty} f_n(m,y)\,dm + P\int_0^{\infty} f_0(m,y)\,dm = 0,$$

where the infinite integrals are uniformly convergent for $|y| \leqslant 1$. It is therefore possible to find the coefficients D_n by normal Fourier series methods and thus completely determine the desired stress function.

Convergence of the infinite integrals

If the above stress function is examined it will be found that certain of the integrals do not converge at the lower limit. This is due to the fact that the stress function must approximate to $\{P/(1+\lambda)t\}\frac{1}{2}x^2$ for large values of x and that a Fourier integral cannot represent such behaviour. The non-convergent part can be represented by

$$\int_0^{\infty} \frac{F(m,y)}{m^2}\sin mx\,dm,$$

where $F(0,y) \neq 0$. If this integral is replaced by

$$\int_0^{\infty} \left(\frac{F(m,y)}{m^3} - \frac{F(0,y)}{m^3}e^{-mt}\right)\sin mx\,dm + F(0,y)\int\int \tan^{-1}\frac{x}{t}\,dxdx,$$

where t is an arbitrary positive constant, then the modified form of Φ is such that $\nabla^4\Phi = 0$ and it is easily shown that the boundary conditions are satisfied. As the two expressions are identical after differentiating twice, both the original and modified forms of the stress function lead to identical values for the stresses.

Example

For the case where $\lambda = 1$ the shear stresses along the edge of the strip shown in Fig. 1 have been calculated. Only the terms involving D_1 and D_2 were used to reduce the end shear stresses but they were not found in the manner indicated above. These coefficients were determined by making the shear zero at the points $(0, 1)$ and $(0, \frac{1}{2})$ as a Fourier series would only converge slowly near the point $y = 1$. The expressions for the stresses were

checked to some extent by finding their limiting values at $x = 0$ and infinity. These were found by the use of the relations

$$\lim_{x\to\infty} \int_0^\infty F(m)\begin{Bmatrix}\sin\\ \cos\end{Bmatrix} mx\, dm = \tfrac{1}{2}\pi \lim_{m\to 0} m\, F(m)$$

and

$$\lim_{x\to 0} \int_0^\infty F(m)\sin mx\, dm = \tfrac{1}{2}\pi \lim_{m\to\infty} m\, F(m).$$

The first of these theorems is well known. The second can be proved if $m\,F(m)$ is continuous and also monotonic for large m. Both integrals must, of course, be convergent.

The infinite integrals were evaluated by means of the quadrature suggested by Filon (**3**) and also used by Howland (**1**). The result of these calculations is shown in Fig. 2 where a comparison is made with the shear stresses obtained from a photoelastic investigation carried out by the author. The residual shear stress left acting over the end is also shown. It is seen that the agreement obtained is good.

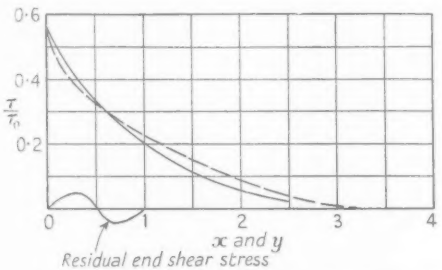

FIG. 2. Comparison of the theoretical and experimental shear stress distribution along $y = 1$.
—— theoretical, – – – experimental.

The author wishes to thank the Chief Scientist, Department of Supply, Australia, for permission to publish this paper.

REFERENCES

1. R. C. HOWLAND, *Proc. Roy. Soc.* A, **124** (1929), 89.
2. H. G. HOPKINS, *Proc. Cambridge Phil. Soc.* **46** (1950), 164.
3. L. N. G. FILON, *Proc. Roy. Soc. Edin.* **49** (1929), 38.

THE DIFFRACTION AND REFLECTION OF SHOCK WAVES

By W. CHESTER (*Dept. of Mathematics, The University, Bristol*)

[Received 17 July 1952; revised 4 December 1952]

SUMMARY

The pressure field produced behind a plane shock wave of arbitrary strength when it encounters an infinite yawed wedge at incidence is investigated. A linearized solution is obtained on the assumption that the shock meets the boundary at near glancing incidence. The solution is used to describe the pressure distribution on the wedge for different values of the pressure ratio across the shock front, and various angles of yaw up to a certain limiting value.

A more accurate investigation is made of the boundary of the perturbed region, and the strength of the non-uniform shock which occurs there is calculated.

1. Introduction

A THEORETICAL investigation of the flow field produced by the interaction of a plane shock wave and a rigid obstacle is difficult, not only because of the non-linear nature of the problem, but also because of the fact that the non-uniform shock waves which occur imply variations in the entropy of the fluid and a loss of the irrotational character of the motion. To simplify the problem sufficiently for a theoretical attack to be successful, two possible courses are open. The first is to linearize the basic equations of motion on the assumption that the incident shock is weak. Since the entropy change across a weak shock is of the third order in the shock strength, the entropy variations are also effectively eliminated and, in fact, the problem belongs to the theory of acoustics. This method was used by Sommerfeld (**1**) to solve the problem of diffraction by a semi-infinite plane, and by many later writers.

The second possibility is to consider an incident plane shock of arbitrary strength and linearize the basic equations on the assumption that the obstacle produces only small perturbations in the uniform flow behind the shock. Although entropy variations are no longer negligible, it appears that they can be suppressed from the theoretical investigation by basing the analysis on the pressure variations in the fluid. This method was first used successfully by Lighthill (**2**) to solve a two-dimensional problem in diffraction, and later by Ting and Ludloff (**3**), who solved a similar problem by a different technique.

The present investigation belongs to this second category. It is an extension of Lighthill's theory (**2**) and considers the interaction of a plane shock wave with an infinite thin wedge at small angles of incidence relative to the uniform flow behind the shock, and arbitrary angles of yaw up to

a certain limiting value depending on the shock strength. Suppose the velocity of the shock is U and the wedge is yawed through an angle β (see Fig. 1). Then the point of intersection of the shock front and the leading edge of the wedge travels along the leading edge with a velocity $U/\sin\beta$. Let an equal and opposite velocity be superimposed on the whole field. If a supersonic velocity of the fluid behind the now stationary shock results, we then have a problem of steady flow behind the shock which is in many respects similar to the well-known cone-field problem of Busemann (**4**).

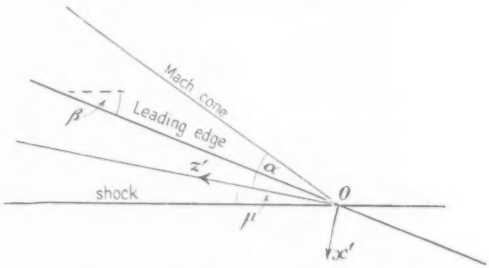

FIG. 1. Configuration in the (x', z') plane.

If the component velocity of the fluid normal to the leading edge is subsonic, the region of perturbed flow is bounded by the shock and the Mach cone with vertex at the junction of the shock and the leading edge. But if the fluid velocity normal to the leading edge is supersonic, the cone intersects the wedge and the boundary must be augmented by the tangent plane from the leading edge to the cone. This latter boundary will be a shock wave or Prandtl–Meyer expansion, and behind it the flow will be uniform and parallel to the wedge, at least until the Mach cone is reached.

The simplifying feature of the problem arises from the lack of a fundamental length in the data defining the problem, implying that the flow variables must be constant along straight lines from the vertex of the Mach cone. The novel feature is the extra boundary, in the form of the incident shock, on which certain boundary conditions must be satisfied. It will be shown that the governing equation for the pressure can be reduced to Laplace's equation, and the solution is then obtained by conformal transformation.

2. Notation and basic equations

Behind the shock there will be a region of uniform flow which is not affected by the presence of the wedge. In this region the fluid velocity, pressure, density, and sonic velocity are denoted by q_1, p_1, ρ_1, and a_1 respectively; ahead of the shock the corresponding quantities are θ_0, p_0, ρ_0,

and a_0. If U is the velocity of the shock, then, taking the adiabatic index $\gamma = 1{\cdot}4$, the shock transition relations give

$$q_1 = \tfrac{5}{6}U(1-a_0^2\,U^{-2}), \qquad p_1 = \tfrac{5}{6}\rho_0(U^2-\tfrac{1}{7}a_0^2), \qquad \rho_1 = 6\rho_0/(1+5a_0^2\,U^{-2}). \quad (1)$$

Let $M = U/a_0\,(>1)$ be the Mach number of the shock, and let $M_1 = q_1/a_1$ be the Mach number of the uniform flow behind the shock. Then, from equations (1),

$$M_1 = \frac{5(M^2-1)}{[(7M^2-1)(M^2+5)]^{\frac{1}{2}}}. \quad (2)$$

As suggested in the previous section, it is convenient to superimpose on the whole configuration a velocity $U/\sin\beta$ along the leading edge of the wedge so that the shock is reduced to rest. The velocity in the region of uniform flow behind the shock is then $\mathbf{V}_1$, say, where

$$V_1^2 = U^2/\sin^2\beta + q_1^2 - 2Uq_1. \quad (3)$$

This velocity is supersonic provided that

$$U^2/\sin^2\beta + q_1^2 - 2Uq_1 > a_1^2,$$

which is equivalent to

$$\tan^2\beta < \frac{6M^4}{(M^2-1)(M^2+5)}. \quad (4)$$

The right-hand side of this last inequality is singular for $M = 1$ ($\beta < \frac{1}{2}\pi$) and decreases rapidly to a minimum value of $\frac{10}{3}$ ($\beta < 61^\circ{\cdot}28$) for $M^2 = \frac{5}{2}$. Thereafter it increases monotonically to an asymptotic value of 6 ($\beta < 67^\circ{\cdot}80$) as $M \to \infty$.

Henceforth we assume that condition (4) is satisfied. The perturbations introduced by the presence of the wedge are then confined to the region bounded by the shock front and the Mach cone with vertex at the junction of the shock and the wedge leading edge (the point O of Fig. 1). The axis of the Mach cone is in the direction of $\mathbf{V}_1$, and subtends an angle μ with the shock, where

$$\tan\mu = (1-q_1U^{-1})\tan\beta = \frac{(M^2+5)\tan\beta}{6M^2}. \quad (5)$$

The semi-angle of the Mach cone is α, where

$$\sin\alpha = \frac{a_1}{V_1} = \frac{a_1\sin\mu}{U-q_1} = \left(\frac{7M^2-1}{M^2+5}\right)^{\frac{1}{2}}\sin\mu. \quad (6)$$

Let (x', y', z') be rectangular Cartesian coordinates in the field with origin at the point O and the z'-axis in the direction of $\mathbf{V}_1$. If the flow quantities in the region of perturbed flow behind the shock are designated by the

suffix 2, the equations of conservation of mass, momentum, and entropy are then

$$\left.\begin{aligned} \mathbf{V}_2.\nabla\rho_2 &= -\rho_2\nabla.\mathbf{V}_2 \\ (\mathbf{V}_2.\nabla)\mathbf{V}_2 &= -\frac{1}{\rho_2}\nabla p_2 \\ \mathbf{V}_2.\nabla s_2 &= 0 \end{aligned}\right\}, \tag{7}$$

where s_2 denotes the entropy.

The wedge is assumed to lie approximately in the plane $y' = 0$; equations (7) may then be linearized if the flow variables are assumed to differ by small quantities from their values in the region of uniform flow behind the shock. If $\mathbf{V}_2 = (u_2, v_2, V_1+w_2)$, we then have

$$\left.\begin{aligned} V_1\frac{\partial\rho_2}{\partial z'} &= -\rho_1\left(\frac{\partial u_2}{\partial x'}+\frac{\partial v_2}{\partial y'}+\frac{\partial w_2}{\partial z'}\right) \\ V_1\frac{\partial u_2}{\partial z'} = -\frac{1}{\rho_1}\frac{\partial p_2}{\partial x'};\quad V_1\frac{\partial v_2}{\partial z'} &= -\frac{1}{\rho_1}\frac{\partial p_2}{\partial y'};\quad V_1\frac{\partial w_2}{\partial z'} = -\frac{1}{\rho_1}\frac{\partial p_2}{\partial z'};\quad \frac{\partial s_2}{\partial z'} = 0 \end{aligned}\right\}. \tag{8}$$

The left-hand side of the first of these equations, by virtue of the last equation, may also be written $V_1\partial p_2/a_1^2\partial z'$, since the density is a function of the pressure and the entropy.

One further simplification is possible: since there is no fundamental length in the data defining the problem, the flow variables are expressible as functions of $x'/z', y'/z'$ only. We thus make the following transformations:

$$x = \frac{x'}{z'\tan\alpha}, \qquad y = \frac{y'}{z'\tan\alpha}; \tag{9}$$

$$p = \frac{p_2-p_1}{a_1\rho_1 q_1}, \quad \rho = \frac{a_1}{\rho_1 q_1}(\rho_2-\rho_1), \quad u = \frac{u_2}{q_1\cos\alpha}, \quad v = \frac{v_2}{q_1\cos\alpha}, \quad w = \frac{V-w_2}{q_1\sin\alpha}. \tag{10}$$

Equations (8) then yield

$$x\frac{\partial u}{\partial x}+y\frac{\partial u}{\partial y} = \frac{\partial p}{\partial x}, \qquad x\frac{\partial v}{\partial x}+y\frac{\partial v}{\partial y} = \frac{\partial p}{\partial y}, \qquad \left(x\frac{\partial}{\partial x}+y\frac{\partial}{\partial y}\right)p, \rho, w = \frac{\partial u}{\partial x}+\frac{\partial v}{\partial y}. \tag{11}$$

Apart from the equation for w, these are formally identical with the equations obtained by Lighthill in the two-dimensional problem of diffraction by an edge (L. 8).† Also, the independent variables defined by (9) are easily seen to reduce to (L. 7) if we take a fixed set of coordinates (X, Y, Z) for which

$$X = x'+\frac{U\sin(\beta-\mu)}{\sin\beta}t, \qquad Y = y, \qquad Z = z'-\frac{U\cos(\beta-\mu)t}{\sin\beta}, \tag{12}$$

† This denotes equation (8) of reference (2).

where, for the purpose of this transformation, the origin O is considered to be moving along the leading edge with velocity $U/\sin\beta$.

We now have

$$x = \frac{x'}{z' \tan\alpha} \to \frac{X - q_1 t}{a_1 t}, \qquad y = \frac{y'}{z' \tan\alpha} \to \frac{Y}{a_1 t} \tag{13}$$

as $\beta \to 0$.

We note that the last of equations (11) imply that the difference between

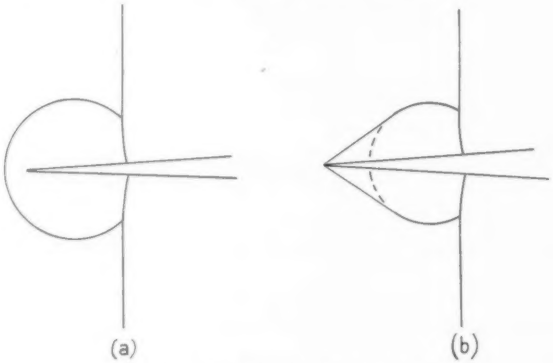

FIG. 2. Configuration in the (x, y) plane.
(a) Subsonic flow behind the shock.
(b) Supersonic flow behind the shock.

any two of p, ρ, or w is a function of y/x only. Since these quantities are zero on the Mach cone, it follows that they are all equal in the region bounded by the Mach cone and the two planes extending from the z'-axis to the lines of intersection of the Mach cone with the shock front. The entropy variations are also zero in this region, for to the present degree of accuracy s_2 is zero on the Mach cone and it is easily deduced from the last of equations (8) that s_2 is a function only of y/x. The motion is thus effectively irrotational, the reason being that the fluid in this region has not crossed the perturbed portion of the incident shock, so that only through crossing the Mach cone could entropy variations ensue. Since, as will appear later, this boundary can be a shock whose strength is at most of the second order, it is not surprising that the entropy variations are negligible on a linear theory.

It is in the remaining portion of the perturbed region, which has the incident shock as part of its boundary, that the rotational character of the flow becomes evident. The variation of ρ or w in this region is deducible from a knowledge of their values at the shock and a knowledge of the pressure field.

From the pressure one can also calculate the two remaining components

of velocity, u and v, from their values on the boundary. This is done by integrating along radii vectores in the (x, y)-plane, starting from the boundary of the perturbed region and using the first two of equations (11).

3. The boundary conditions on the shock

The undisturbed part of the shock front lies in the plane

$$x'/z' = \tan\mu$$

or

$$x = \frac{\tan\mu}{\tan\alpha} = k. \tag{14}$$

Consequently we take the equation of the perturbed shock front to be

$$x\tan\alpha = \tan\mu + f(y)\sec\mu$$

or

$$x'\cos\mu - z'\sin\mu - z' f\left(\frac{y'}{z'\tan\alpha}\right) = 0, \tag{15}$$

where f is assumed to be uniformly small.

The direction cosines of the normal to the shock front are then proportional to

$$\cos\mu, \quad -f'\cot\alpha, \quad -(\sin\mu + f - yf'), \tag{16}$$

and, if $\mathbf{n}$ is a unit vector normal to the shock, we have

$$\mathbf{n} = \{\cos\mu - \sin\mu\cos\mu(f - yf'),\ -f'\cot\alpha,\ -\sin\mu - \cos^2\mu(f - yf')\} \tag{17}$$

to the first order.

Now the shock transition relations will depend on the normal component of the velocity in front of the shock; in fact the relations for a stationary shock may be written

$$\mathbf{V}_2 - \mathbf{V}_0 = \tfrac{5}{6}\mathbf{V}_n\left(\frac{a_0^2}{V_n^2} - 1\right), \qquad p_2 = \tfrac{5}{6}\rho_0\{V_n^2 - \tfrac{1}{7}a_0^2\}, \tag{18}$$

where $\mathbf{V}_0$ is the velocity in front of the shock, in the present case $U/\sin\beta$ parallel to the wedge leading edge, and $\mathbf{V}_n$ is the component of this velocity normal to the shock.

Since $\mathbf{V}_0 = \{-U\sin(\beta-\mu)/\sin\beta,\ 0,\ U\cos(\beta-\mu)/\sin\beta\}$ and $\mathbf{V}_n = (\mathbf{V}_0.\mathbf{n})\mathbf{n}$ it follows, with the help of (17), that

$$\mathbf{V}_n = -U\{1 + \cot\beta\cos\mu(f - yf')\}\mathbf{n}. \tag{19}$$

Equations (17), (18), and (19) then yield the following relations:

$$\left.\begin{aligned} u &= \frac{5}{6}\frac{U\cos\mu}{q_1\sin\beta\cos\mu}\{\cos(\beta+\mu) + M^{-2}\cos(\beta-\mu)\}(f - yf') \\ v &= -f'/\sin\alpha \\ w &= \frac{5}{6}\frac{U\cos\mu}{q_1\sin\beta\sin\alpha}\{\sin(\beta+\mu) - M^{-2}\sin(\beta-\mu)\}(f - yf') \\ p &= \frac{5}{3}\frac{\rho_0 U^2}{a_1\rho_1 q_1}\cot\beta\cos\mu(f - yf'). \end{aligned}\right\} \tag{20}$$

Thus, on the shock, we must have

$$u = Ap, \qquad w = A'p, \qquad y\frac{\partial v}{\partial y} = B\frac{\partial p}{\partial y}, \tag{21}$$

where

$$A = \frac{a_1\rho_1}{2\rho_0 U}\frac{\cos(\beta+\mu)+M^{-2}\cos(\beta-\mu)}{\cos\alpha\cos\beta}$$

$$= \frac{1}{2}\left(\frac{7M^2-1}{M^2+5}\right)^{\frac{1}{2}}\frac{\cos(\beta+\mu)+M^{-2}\cos(\beta-\mu)}{\cos\alpha\cos\beta}, \tag{22}$$

$$A' = \frac{a_1\rho_1}{2\rho_0 U}\frac{\sin(\beta+\mu)-M^{-2}\sin(\beta-\mu)}{\sin\alpha\cos\beta}$$

$$= \frac{1}{2}\left(\frac{7M^2-1}{M^2+5}\right)^{\frac{1}{2}}\frac{\sin(\beta+\mu)-M^{-2}\sin(\beta-\mu)}{\sin\alpha\cos\beta}, \tag{23}$$

$$B = \frac{3}{5}\frac{a_1\rho_1 q_1\tan\beta}{\rho_0 U^2\sin\alpha\cos\mu} = \frac{3}{5}\frac{\rho_1 q_1}{\rho_0 U}\sec^2\mu$$

$$= 3\left(\frac{M^2-1}{M^2+5}\right)\sec^2\mu. \tag{24}$$

Equations (22) and (24) reduce to (L. 15) when $\beta = 0$.

In conjunction with the basic equations (11), the first and last of equations (21) yield the following condition on p, to be satisfied when $x = k$ (L. 19),

$$\frac{\partial p}{\partial x}\Big/\frac{\partial p}{\partial y} = \frac{(A+k)y - Bky^{-1}}{1-k^2}. \tag{25}$$

If the upper surface of the wedge is inclined at an angle δ to the plane $y = 0$ (δ is defined as a rotation about a line in the plane $y = 0$ parallel to the shock), then the boundary condition on the wedge is $v = \delta\sec\alpha$. In particular this is true at the shock, and so we must also have

$$\int \frac{\partial v}{\partial y}\,dy = \int \frac{B}{y}\,dp = -\delta\sec\alpha, \tag{26}$$

where the integral is taken along the shock from the wall to the Mach cone.

4. The boundary condition on $y = 0$

We assume first that the leading edge of the wedge lies outside the Mach cone, the condition for which is $\alpha < (\beta-\mu)$ or, by (6),

$$\left(\frac{7M^2-1}{M^2+5}\right)^{\frac{1}{2}}\sin\mu < \sin(\beta-\mu).$$

With the help of equation (5), this gives

$$\frac{5(M^2-1)\cos\beta}{\{(M^2+5)(7M^2-1)\}^{\frac{1}{2}}} > 1$$

or $M_1\cos\beta > 1$, as one would expect.

In this case the flow patterns above and below the wedge are independent, and for the upper half-plane the boundary condition on $y = 0$ is $v = \delta \sec \alpha$. Since $\partial p/\partial y = x\,\partial v/\partial x$ on $y = 0$, by (11), this also implies $\partial p/\partial y = 0$ on $y = 0$.

In the subsonic case ($M_1 \cos\beta < 1$) it is more convenient to separate the symmetrical and antisymmetrical contributions to the inclination, say δ_s and δ_a (again these are the contributions to the effective inclination of the upper surface relative to the flow behind the shock so that, for example, the semi-angle of the wedge would be $\delta_s \sec\beta$). We then have two contributions to the pressure; the first, p_s, is symmetrical about $y = 0$ and so $\partial p_s/\partial y = 0$ on $y = 0$ remains true. However, at the leading edge,

$$\lim_{y\to 0} \int_{-m-c}^{-m+c} \frac{\partial p_s}{\partial y}\,dx = -m \int_{-m-c}^{-m+c} \frac{\partial v_s}{\partial x}\,dx = -m\delta_s \sec\alpha, \tag{27}$$

where

$$m = \frac{\tan(\beta-\mu)}{\tan\alpha} \tag{28}$$

and $-m$ is the x-coordinate of the leading edge.

The second contribution, p_a, is antisymmetrical about $y = 0$, and continuous for $-1 < x < -m$. Hence $p_a = 0$ for $-1 < x < -m$, and $\partial p_a/\partial y = 0$ for $-m < x < k$. Furthermore,

$$\lim_{y\to 0+} \int_{-1}^{-m+c} \frac{1}{x}\frac{\partial p_a}{\partial y}\,dx = \lim_{y\to 0+} \int_{-1}^{-m+c} \frac{\partial v_a}{\partial x}\,dx = \delta_a \sec\alpha. \tag{29}$$

5. The boundary condition on the Mach cone

In the subsonic case the boundary condition on the Mach cone is $p = 0$, but in the supersonic case this is true only from the shock to the point of contact of the tangent plane from the wedge leading edge. The latter will represent a weak shock wave (or Prandtl–Meyer expansion if the inclination is negative). Between this weak shock and the Mach cone the flow is uniform and the pressure is, to a linear approximation,

$$p_2 = p_1 + \rho_1 q_1^2 \frac{\delta\cos\beta}{(M_1^2\cos^2\beta - 1)^{\frac{1}{2}}},$$

or

$$p = \frac{\delta M_1 \cos\beta}{(M_1^2\cos^2\beta - 1)^{\frac{1}{2}}} = \frac{m}{(m^2-1)^{\frac{1}{2}}}\,\delta\sec\alpha. \tag{30}$$

The last relation follows from the fact that

$$M_1\cos\beta = \frac{\sin(\beta-\mu)}{\sin\alpha},$$

deducible from equations (5) and (6).

Thus on the Mach cone p is zero only for $-m^{-1} < x < k$; in the interval $-m < x < -m^{-1}$ it is given by (30).

6. The solution in terms of the pressure

The boundary conditions required are now all expressed in terms of the pressure. Also it may be deduced from equations (11) that (L. 16)

$$\nabla^2 p = \left(x\frac{\partial}{\partial x}+y\frac{\partial}{\partial y}+1\right)\left(x\frac{\partial p}{\partial x}+y\frac{\partial p}{\partial y}\right). \tag{31}$$

With the transformation

$$x = \frac{2\rho}{1+\rho^2}\cos\theta, \qquad y = \frac{2\rho}{1+\rho^2}\sin\theta \tag{32}$$

equation (31) reduces to Laplace's equation (L. 22) with (ρ, θ) as polar coordinates. The Mach cone becomes that part of the circle $\rho = 1$ upstream of the incident shock, the latter being an arc of the circle $2\rho\cos\theta = k(1+\rho^2)$ cutting $\rho = 1$ orthogonally at $\cos\theta = k$ in the (ρ, θ)-plane.

The shock-boundary condition (28) becomes (L. 28)

$$\frac{\partial p}{\partial n}\Big/\frac{\partial p}{\partial s} = \frac{Ak\tan\theta - B\cot\theta}{(1-k^2\sec^2\theta)^{\frac{1}{2}}}, \tag{33}$$

where ds and dn are positive tangential and outward normal elements to the curve.

The leading edge of the wedge becomes the point

$$\theta = \pi, \qquad \rho = \{1-(1-m^2)^{\frac{1}{2}}\}/m$$

and conditions (27) and (29) become, respectively,

$$\lim_{\theta\to\pi}\int \frac{1-\rho^2}{1+\rho^2}\frac{\partial p_s}{\rho\,\partial\theta}d\rho = -m\delta_s\sec\alpha$$

or

$$\lim_{\theta\to\pi}\int \frac{\partial p_s}{\rho\,\partial\theta}\,d\rho = -\frac{m}{(1-m^2)^{\frac{1}{2}}}\,\delta_s\sec\alpha \tag{34}$$

and

$$\lim_{\theta\to\pi}\int \frac{1-\rho^2}{2\rho}\frac{\partial p_a}{\rho\,\partial\theta}\,d\rho = -\delta_a\sec\alpha. \tag{35}$$

In (34) the interval of integration should include the point representing the leading edge; in (33) the integration is taken along a path from $\rho = 1$ to a point on the upper surface of the wedge.

We now require a harmonic function which satisfies certain conditions on the closed boundary defined by an arc of the circle $\rho = 1$, an arc of the circle $2\rho\cos\theta = k(1+\rho^2)$, and the polar axis $\theta = 0, \pi$.

With $\zeta = \rho e^{i\theta}$ and $k' = (1-k^2)^{\frac{1}{2}}$, the region is transformed into the upper half of the z_1-plane by the successive transformations (L. 31, 35)

$$Z = (k+ik')\left\{i-\frac{2k'}{\zeta-(k+ik')}\right\}, \tag{36}$$

$$z_1 = (x_1+iy_1) = \tfrac{1}{2}(Z^2+Z^{-2}), \qquad Z^2 = z_1+(z_1^2-1)^{\frac{1}{2}}. \tag{37}$$

The boundaries in the (ρ, θ)-plane defined by the arcs of the curves $\rho = 1$, $2\rho\cos\theta = k(1+\rho^2)$ and $\theta = 0,\ \pi$ now become, respectively, the three portions of the real axis defined by $-\infty < x_1 < -1$, $-1 < x_1 < 1$, and $1 < x_1 < \infty$. The boundary condition (33), which holds for $x_1 > 1$, $y_1 = 0$ now becomes (L. 36)

$$\frac{\partial p}{\partial y_1}\Big/\frac{\partial p}{\partial x_1} = 2^{-\frac{1}{2}}(x_1-1)^{-\frac{1}{2}}\left[\frac{Bk}{1-k^2}(x_1+1)-A(x_1-1)\right]. \tag{38}$$

The condition to be satisfied on the real axis for $-\infty < x_1 < -1$, which now represents the Mach cone, is $\partial p/\partial x_1 = 0$.

For $-1 < x_1 < 1$, $y = 0$ the boundary condition, in the symmetrical and supersonic cases, is $\partial p/\partial y_1 = 0$, but in the antisymmetrical subsonic problem this is only true for $x_0 < x_1 < 1$, where x_0 is the point corresponding to the leading edge, i.e. to $\zeta = -\{1-(1-m^2)^{\frac{1}{2}}\}/m$. Thus

$$x_0 = 1-\frac{2(k+m)^2}{(1+km)^2} > -1. \tag{39}$$

For $-1 < x_1 < x_0$ the boundary condition is $\partial p/\partial x_1 = 0$.

In addition, relation (34) or (35) must be satisfied in the subsonic case. In the z_1-plane they become, respectively,

$$\lim_{y_1\to 0}\int_{x_0-c}^{x_0+c}\frac{\partial p_s}{\partial y_1}dx_1 = -\frac{m}{(1-m^2)^{\frac{1}{2}}}\delta_s\sec\alpha \tag{40}$$

and

$$\lim_{y_1\to 0}\int_{-1}^{x_0+c}\frac{k'(1+x_1)^{\frac{1}{2}}}{(1-x_1)^{\frac{1}{2}}-2^{\frac{1}{2}}k}\frac{\partial p_a}{\partial y_1}dx_1 = -\delta_a\sec\alpha. \tag{41}$$

The corresponding condition in the supersonic case arises from the fact that p changes discontinuously, by the amount given in (30), at a point on the Mach cone represented by $\zeta = -m+i(1-m^{-2})^{\frac{1}{2}}$. This point is represented in the z_1-plane by the same expression as the x_0 in (39), but now, of course, $x_0 < -1$. We thus have, by (30),

$$\lim_{y_1\to 0}\int_{x_0-c}^{x_0+c}\frac{\partial p}{\partial x_1}dx_1 = \frac{m}{(m^2-1)^{\frac{1}{2}}}\delta\sec\alpha. \tag{42}$$

The boundary conditions have now to be satisfied on the real axis, and impose certain conditions on $\partial p/\partial x_1$ and $\partial p/\partial y_1$.

We consider first the supersonic case. If we put

$$W(z_1) = \frac{\partial p}{\partial y_1}+i\frac{\partial p}{\partial x_1} \tag{43}$$

then, on $y_1 = 0$, W must be real for $-\infty < x_1 < -1$, and wholly imaginary for $-1 < x_1 < 1$.

On the real axis, for $x_1 > 1$,

$$\arg W(z_1) = \tan^{-1}\left\{\frac{2^{\frac{1}{2}}(x_1-1)^{\frac{1}{2}}}{Bk(1-k^2)^{-1}(x_1+1)-A(x_1-1)}\right\}$$

$$= \tan^{-1}\frac{(x_1-1)^{\frac{1}{2}}}{\gamma_1} + \tan^{-1}\frac{(x_1-1)^{\frac{1}{2}}}{\gamma_2}, \tag{44}$$

where
$$\frac{\gamma_1\gamma_2}{\gamma_1+\gamma_2} = \frac{2^{\frac{1}{2}}Bk}{1-k^2}, \qquad \frac{2^{\frac{1}{2}}}{\gamma_1+\gamma_2} = A - \frac{Bk}{1-k^2}. \tag{45}$$

Using equations (5), (6), (22), and (24), these give

$$\gamma_1, \gamma_2 = 2^{\frac{1}{2}}kM\left\{M \pm \frac{M^2-1}{(M^2+5)^{\frac{1}{2}}}\right\}. \tag{46}$$

In terms of W relation (42) indicates that, near $z_1 = x_0$,

$$W \sim -\frac{m\delta \sec\alpha}{\pi(m^2-1)^{\frac{1}{2}}(z_1-x_0)}. \tag{47}$$

A function which satisfies all these conditions and in addition is integrable at all points in the upper half-plane, except $z_1 = x_0$, is (L. 45 with the sign of δ changed)

$$W = \frac{-C\delta[D(z_1-x_0)-1]}{(z_1^2-1)^{\frac{1}{2}}(z_1-x_0)[\gamma_1-i(z_1-1)^{\frac{1}{2}}][\gamma_2-i(z_1-1)^{\frac{1}{2}}]}. \tag{48}$$

The constant C is determined by (47) and is given by

$$C = \frac{m}{\pi\cos\alpha}\left(\frac{x_0^2-1}{m^2-1}\right)^{\frac{1}{2}}[\gamma_1+(1-x_0)^{\frac{1}{2}}][\gamma_2+(1-x_0)^{\frac{1}{2}}]$$

$$= \frac{2m(m+k)k'(\gamma_1+\gamma_3)(\gamma_2+\gamma_3)}{\pi(1+mk)^2\cos\alpha}, \tag{49}$$

where
$$\gamma_3^2 = 1-x_0 = \frac{2(m+k)^2}{(1+mk)^2}. \tag{50}$$

The value of D is obtained from equation (24). Since, on the shock,

$$y = k'\left(\frac{x_1-1}{x_1+1}\right)^{\frac{1}{2}}, \tag{51}$$

we must have

$$\delta \sec\alpha = -\int_1^\infty \frac{B}{y}\frac{\partial p}{\partial x_1}\,dx_1$$

$$= \int_1^\infty \frac{B}{k'}\left(\frac{x_1+1}{x_1-1}\right)^{\frac{1}{2}} \frac{C\delta[D(x_1-x_0)-1](\gamma_1+\gamma_2)(x_1-1)^{\frac{1}{2}}\,dx_1}{(x_1^2-1)^{\frac{1}{2}}(x_1-x_0)(\gamma_1^2+x_1-1)(\gamma_2^2+x_1-1)}$$

$$= \frac{BC\delta(\gamma_1+\gamma_2)\pi}{k'}\,\frac{(D\gamma_3^2-1)(\gamma_1+\gamma_2+\gamma_3)/\gamma_1\gamma_2\gamma_3+D}{(\gamma_2+\gamma_3)(\gamma_3+\gamma_1)(\gamma_1+\gamma_2)}. \tag{52}$$

With the help of (49) this gives the following relation, which enables D to be calculated:

$$\frac{(mk+1)^2}{2Bm(m+k)} = \frac{D(\gamma_1+\gamma_3)(\gamma_2+\gamma_3)}{\gamma_1\gamma_2} - \frac{\gamma_1+\gamma_2+\gamma_3}{\gamma_1\gamma_2\gamma_3}. \tag{53}$$

In the subsonic symmetrical case W_s satisfies the same boundary conditions, but the asymptotic equality corresponding to (47) is now, by virtue of (40),

$$W_s \sim -\frac{im\delta_s \sec\alpha}{\pi(1-m^2)^{\frac{1}{2}}(z_1-x_0)} \tag{54}$$

near $z = x_0$. Thus

$$W_s = -\frac{C_s\delta_s[D_s(z_1-x_0)-1]}{(z_1^2-1)^{\frac{1}{2}}(z_1-x_0)[\gamma_1-i(z_1-1)^{\frac{1}{2}}][\gamma_2-i(z_1-1)^{\frac{1}{2}}]}, \tag{55}$$

where C_s and D_s are still given by (49) and (53).

The boundary conditions in the subsonic antisymmetrical problem are that, on the real axis, w_a is real for $x_1 < x_0$ and wholly imaginary for $x_0 < x_1 < 1$. When $x_1 > 1$ relation (44) is to be satisfied.

Now
$$W_a = -\frac{C_a\delta_a[D_a(z_1-x_0)-1]}{(z_1-1)^{\frac{1}{2}}(z_1-x_0)^{\frac{1}{2}}[\gamma_1-i(z_1-1)^{\frac{1}{2}}][\gamma_2-i(z_1-1)^{\frac{1}{2}}]} \tag{56}$$

satisfies all these conditions and is integrable at all points in the upper half-plane except $z_1 = x_0$. A singularity in the pressure at $z_1 = x_0$ (i.e. at the leading edge) seems inevitable: indeed it is expected in a linear theory for subsonic flow round a sharp edge. This being so, the boundary conditions do not define the function completely, and (56) is the solution with the weakest singularity at $z_1 = x_0$, subject to being integrable at all other points and to being sufficiently general for conditions (24) and (41) to be satisfied. Such a singularity in the pressure at a subsonic leading edge (an inverse square root) is well known in the linearized theory for steady flow (see, for example, reference **5**). The fact that W_s/δ_s and W_a/δ_a tend to equality as $M_1\cos\beta \to 1$ from below is also encouraging (that this is so follows from the fact that $x_0 \to -1$ and condition (41) becomes equivalent to (40), giving a value of C equal to (49)). Thus, comparing (48) with the

sum of (55) and (56), and remembering that $\delta = \delta_a + \delta_s$, we see that the solution is continuous at $M_1 \cos\beta = 1$.

In general, the relations which determine C_a and D_a, namely (24) and (41), give respectively

$$\begin{aligned} 1 &= -\delta_a^{-1} \int_1^\infty \frac{B}{y} \frac{\partial p_a}{\partial x_1}\, dx_1 \\ &= \int_1^\infty \frac{B}{k'}\left(\frac{x_1+1}{x_1-1}\right)^{\frac{1}{2}} \frac{C_a[\,D_a(x_1-x_0)-1](\gamma_1+\gamma_2)(x_1-1)^{\frac{1}{2}}\, dx_1}{(x_1-1)^{\frac{1}{2}}(x_1-x_0)^{\frac{3}{2}}[\gamma_1^2+(x_1-1)][\gamma_2^2+(x_1-1)]} \\ &= \frac{2BC_a(\gamma_1+\gamma_2)}{k'} \int_0^\infty \frac{(x^2+2)^{\frac{1}{2}}[\,D_a(x^2+\gamma_3^2)-1]\, dx}{(x^2+\gamma_3^2)^{\frac{3}{2}}(x^2+\gamma_1^2)(x^2+\gamma_2^2)} \end{aligned} \tag{57}$$

and

$$\begin{aligned} 1 &= {}^*\!\int_{-1}^{x_0} \frac{C_a k'(1+x_1)[\,D_a(x_1-x_0)-1]\, dx_1}{(1-x_1)^{\frac{1}{2}}(x_0-x_1)^{\frac{3}{2}}[(1-x_1)^{\frac{1}{2}}-2^{\frac{1}{2}}k][\gamma_1+(1-x_1)^{\frac{1}{2}}][\gamma_2+(1-x_1)^{\frac{1}{2}}]} \\ &= -2C_a k' \,{}^*\!\int_{\gamma_3}^{2^{\frac{1}{2}}} \frac{(2-x^2)^{\frac{1}{2}}[\,D_a(x^2-\gamma_3^2)+1]\, dx}{(x^2-\gamma_3^2)^{\frac{3}{2}}(x-2^{\frac{1}{2}}k)(x+\gamma_1)(x+\gamma_2)}, \end{aligned} \tag{58}$$

where the asterisk denotes that the finite part of the integral is to be taken (6).

7. The pressure distribution on the face of the wedge

In the z_1-plane the upper face of the wedge is represented by the real axis for $x_0 < x_1 < 1$ (corresponding to $-m < x < k$). At a point $(x_1, 0)$ on the wedge we thus have, in the supersonic case and the subsonic symmetrical case,

$$p(x_1) = C\delta \int_{-1}^{x_1} \frac{[D(x_1-x_0)-1]\, dx_1}{(1-x_1^2)^{\frac{1}{2}}(x_1-x_0)[\gamma_1+(1-x_1)^{\frac{1}{2}}][\gamma_2+(1-x_1)^{\frac{1}{2}}]}, \tag{59}$$

since p is zero at $x_1 = -1$. After some algebra this can be evaluated and gives

$$\begin{aligned} \frac{p}{2C\delta} = {} & \frac{\gamma_1\gamma_2+\gamma_3^2}{\gamma_3(\gamma_1^2-\gamma_3^2)(\gamma_2^2-\gamma_3^2)(2-\gamma_3^2)^{\frac{1}{2}}} \coth^{-1}\left\{\frac{\gamma_3\tan\phi}{(2-\gamma_3^2)^{\frac{1}{2}}}\right\} - \\ & - \frac{\gamma_1+\gamma_2}{(\gamma_1^2-\gamma_3^2)(\gamma_2^2-\gamma_3^2)(2-\gamma_3^2)^{\frac{1}{2}}} \coth^{-1}\left\{\frac{2^{\frac{1}{2}}\sin\phi}{(2-\gamma_3^2)^{\frac{1}{2}}}\right\} + \\ & + \left\{D+\frac{1}{\gamma_1^2-\gamma_3^2}\right\}\frac{1}{(\gamma_2-\gamma_1)(\gamma_1^2-2)^{\frac{1}{2}}}\left[\tan^{-1}\left\{\frac{\gamma_1\tan\phi}{(\gamma_1^2-2)^{\frac{1}{2}}}\right\} - \tan^{-1}\left\{\frac{2^{\frac{1}{2}}\sin\phi}{(\gamma_1^2-2)^{\frac{1}{2}}}\right\}\right] - \\ & - \left\{D+\frac{1}{\gamma_2^2-\gamma_3^2}\right\}\frac{1}{(\gamma_2-\gamma_1)(\gamma_2^2-2)^{\frac{1}{2}}}\left[\tan^{-1}\left\{\frac{\gamma_2\tan\phi}{(\gamma_2^2-2)^{\frac{1}{2}}}\right\} - \tan^{-1}\left\{\frac{2^{\frac{1}{2}}\sin\phi}{(\gamma_2^2-2)^{\frac{1}{2}}}\right\}\right], \end{aligned} \tag{60}$$

where
$$\cos\phi = \left(\frac{1-x_1}{2}\right)^{\frac{1}{2}} = \frac{k-x}{1-kx}, \tag{61}$$
since, for $-1 < x_1 < 1$,
$$x_1 = 1 - \frac{2(k-x)^2}{(1-kx)^2}. \tag{62}$$

The antisymmetrical contribution, on the upper surface of the wedge, is given by
$$p_a(x_1) = C_a \delta_a \overset{*}{\int_{x_0}^{x_1}} \frac{[D_a(x_1-x_0)-1]\,dx_1}{(1-x_1)^{\frac{1}{2}}(x_1-x_0)^{\frac{1}{2}}[\gamma_1+(1-x_1)^{\frac{1}{2}}][\gamma_2+(1-x_1)^{\frac{1}{2}}]} \tag{63}$$
or
$$\frac{p_a}{2C_a\delta_a} = \frac{\gamma_1\gamma_2+\gamma_3^2}{\gamma_3^2(\gamma_1^2-\gamma_3^2)(\gamma_2^2-\gamma_3^2)}\cot\psi - \frac{\gamma_1+\gamma_2}{\gamma_3(\gamma_1^2-\gamma_3^2)(\gamma_2^2-\gamma_3^2)}\operatorname{cosec}\psi +$$
$$+\left\{D_a+\frac{1}{\gamma_1^2-\gamma_3^2}\right\}\frac{1}{(\gamma_2-\gamma_1)(\gamma_1^2-\gamma_3^2)^{\frac{1}{2}}}\left[\tan^{-1}\left\{\frac{\gamma_1\tan\psi}{(\gamma_1^2-\gamma_3^2)^{\frac{1}{2}}}\right\}-\tan^{-1}\left\{\frac{\gamma_3\sin\psi}{(\gamma_1^2-\gamma_3^2)^{\frac{1}{2}}}\right\}\right]-$$
$$-\left\{D_a+\frac{1}{\gamma_2^2-\gamma_3^2}\right\}\frac{1}{(\gamma_2-\gamma_1)(\gamma_2^2-\gamma_3^2)}\left[\tan^{-1}\left\{\frac{\gamma_2\tan\psi}{(\gamma_2^2-\gamma_3^2)^{\frac{1}{2}}}\right\}-\tan^{-1}\left\{\frac{\gamma_3\sin\psi}{(\gamma_2^2-\gamma_3^2)^{\frac{1}{2}}}\right\}\right], \tag{64}$$
where
$$\cos\psi = \frac{(1-x_1)^{\frac{1}{2}}}{\gamma_3} = \frac{2^{\frac{1}{2}}(k-x)}{\gamma_3(1-kx)}. \tag{65}$$

8. The unyawed wedge

Equations (13) give the limiting form of the independent variables, and all the parameters occurring tend to finite limiting values as $\beta \to 0$.

The Mach cone now becomes part of a cylinder of radius $a_1 t$, and its axis, in the physical problem, travels downstream with the velocity of the fluid behind the shock. The supersonic case now arises when the fluid velocity behind the shock is itself supersonic, that is when $M_1 > 1$ or, by (2), when $M > 2{\cdot}068$. The present results for the unyawed supersonic case, and for the symmetrical wedge in the subsonic case, agree with those originally obtained by Lighthill (**2**).

The variation of the quantity
$$\frac{p_2-p_1}{\delta(p_1-p_0)} = \frac{p}{\delta}\left\{\frac{7M^2-1}{M^2+5}\right\}^{\frac{1}{2}} \tag{66}$$
on the face of the wedge is graphed in Fig. 3 for $\beta = 0$ and $p_1/p_0 = 1, 2, 3, 4{\cdot}823$. These values of the pressure ratio across the incident shock correspond respectively to $M = 1$, $1{\cdot}36277$, $1{\cdot}64751$, $2{\cdot}06809$ and to $M_1 = 0$, $0{\cdot}47245$, $0{\cdot}72739$, 1.

A typical distribution when supersonic flow prevails behind the shock is shown in Fig. 6. The scale is adjusted to make the distance between the leading edge and the shock the same in all cases.

The pressure distributions in the symmetrical and supersonic cases are based on calculations kindly made available by Professor Lighthill.

In the subsonic case the pressure is singular at the leading edge, decreases rapidly to a minimum, then rises steadily until the shock is reached. The

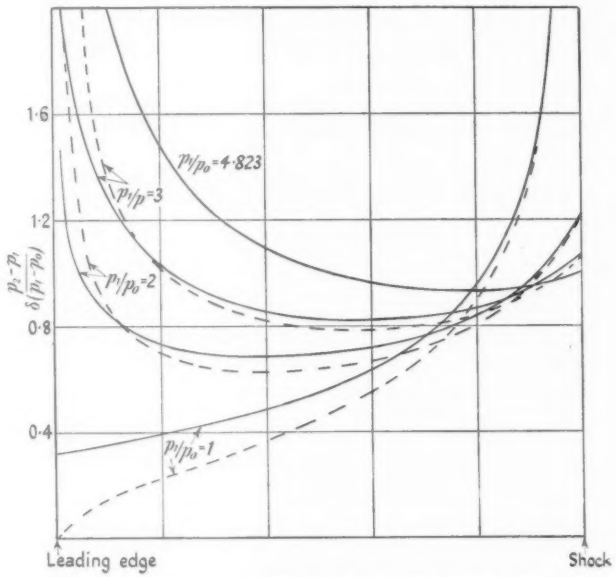

FIG. 3. Pressure distribution on the wedge for $\beta = 0$ and various values of the shock strength.
——— symmetrical case.
---------- antisymmetrical case.

symmetrical and antisymmetrical contributions are roughly comparable for given shock strengths, complete agreement being obtained for the case of sonic flow behind the shock. In so far as they differ the symmetrical contribution is consistently higher in absolute value except near the edge, where the logarithmic singularity is outstripped by the stronger inverse square root occurring in the antisymmetrical case. No singularity appears in the limiting case $p_1/p_0 = 1$, when the incident shock becomes an acoustic pulse. This is a result of the limiting process. If $M = 1+\epsilon$, then $k \sim 1-\epsilon$ and (62) gives

$$x_1+1 \sim 4\epsilon\frac{1+x}{1-x}. \tag{67}$$

Further, one can show that, in both the symmetrical and antisymmetrical cases,

$$CD \sim \frac{2^{\frac{3}{2}}\epsilon^{-\frac{1}{2}}}{\pi},$$

and that C is negligible compared with CD. Consequently the numerators of the integrands in (59) and (63) can be replaced by $D(x_1-x_0)$ (except near $x_1 = x_0$), and the term which produces the singularity disappears. Since γ_1, γ_2, γ_3 all tend to $2^{\frac{1}{2}}$ as $\epsilon \to 0$, (59) yields

$$p_s = \frac{2^{\frac{3}{2}}\epsilon^{-\frac{1}{2}}\delta_s}{\pi} \int_{-1}^{x} \frac{1}{8.2^{\frac{1}{2}}} \left\{\frac{4\epsilon(1+x)}{(1-x)}\right\}^{\frac{1}{2}} \frac{dx_1}{dx}\, dx$$

$$= \frac{\delta_s}{\pi} \int_{-1}^{x} \frac{dx}{(1+x)^{\frac{1}{2}}(1-x)^{\frac{3}{2}}} = \frac{\delta_s}{\pi}\left\{\frac{1+x}{1-x}\right\}^{\frac{1}{2}}. \tag{68}$$

The corresponding result in the antisymmetrical case, deducible from (63), is

$$p_a = \frac{\delta_a}{\pi}\left\{\frac{2x}{1-x}\right\}^{\frac{1}{2}}. \tag{69}$$

The pressure distributions for $p_1/p_0 = 1$ in Fig. 3 are based on (68) and (69).

In the case of an acoustic pulse, the pressure distributions are, in fact, known for arbitrary values of δ. The extension of (69), for example, when δ_a is not small would be, in the present notation,

$$\pi p_a = \pi - 2\tan^{-1}\left\{\frac{(1-x)^{\frac{1}{2}}}{(2x)^{\frac{1}{2}}\sin\frac{1}{2}\delta_a}\right\} \tag{70}$$

(see, for example, **7**, p. 535). When δ_a is small, (69) and (70) agree to the first order except at the shock front ($x = 1$), where (69) is singular but (70) predicts the well-known doubling of the pressure. Similar conclusions are obtained in the symmetrical case (L., p. 469). Thus the limiting distributions, as described by (68) and (69), are not reliable near the shock. This objection, however, should disappear once Mach reflection is well established, for then there is neither theoretical nor experimental reason to expect unduly large changes at this point.

9. The effect of yaw

In Fig. 4 is shown the pressure distributions on the face of the wedge for $p_1/p_0 = 2$, $\delta_a = 0$, and $\beta = 0°$, 40°, and 61°·9, the latter value of β being the maximum angle of yaw permissible for this particular shock strength. The pressure is plotted along a line perpendicular to the axis of the Mach cone, and the scale is again adjusted to make the distance between the leading edge and the shock the same for all angles of yaw. The computation involved in the production of the curves was considerably eased by the fact that, for a given shock strength, γ_1, γ_2, and γ_3 are all proportional to k, C_s is proportional to k^3, and D_3 inversely proportional to k^2. It is not difficult to verify the truth of these assertions from the relevant equations (it is also true of C and D in the supersonic case, but not of C_a or D_a).

Thus, if in (60) the parameter C is absorbed into the coefficients multiplying the inverse trigonometrical or hyperbolic functions, then these coefficients vary with yaw only through the terms $(2-\gamma_3^2)^{\frac{1}{2}}$, $(\gamma_1^2-2)^{\frac{1}{2}}$, or $(\gamma_2^2-2)^{\frac{1}{2}}$.

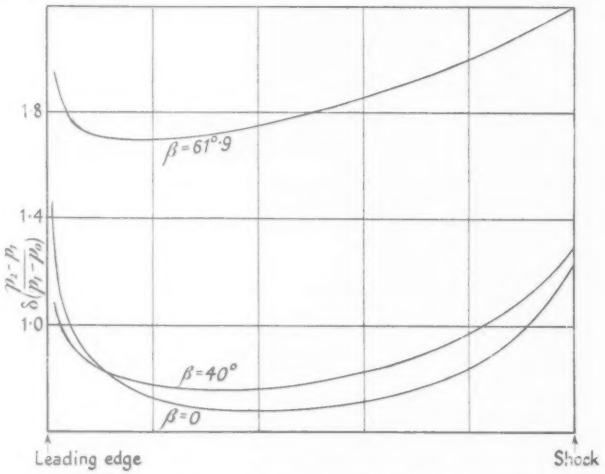

FIG. 4. Pressure distribution on symmetrical wedge for $p_1/p_0 = 2$ and various angles of yaw.

A minor modification is necessary in (60) when γ_1 or γ_2 is less than $2^{\frac{1}{2}}$. If, for example, $\gamma_1 < 2^{\frac{1}{2}}$ then

$$\frac{1}{(\gamma_1^2-2)^{\frac{1}{2}}}\tan^{-1}\frac{\gamma_1\tan\phi}{(\gamma_1^2-2)^{\frac{1}{2}}}$$

should read

$$-\frac{1}{(2-\gamma_1^2)^{\frac{1}{2}}}\coth^{-1}\frac{\gamma_1\tan\phi}{(2-\gamma_1^2)^{\frac{1}{2}}},$$

and similarly for the other terms.

As the extreme angle of yaw is approached it is the limiting behaviour of (60) that must be considered, for the Mach angle tends to $\frac{1}{2}\pi$. If $\cos\alpha = \epsilon$ then, from equations (14), (28), (50), and (61) we have

$$k \sim \epsilon\tan\mu,$$

$$m \sim \epsilon\tan(\beta-\mu),$$

$$\gamma_3 \sim 2^{\frac{1}{2}}\{\tan(\beta-\mu)+\tan\mu\}\epsilon = 2^{\frac{1}{2}}\bar{\gamma}_3\epsilon,$$

$$x \sim \frac{x'\epsilon}{z'},$$

$$\cos\phi \sim (\tan\mu - x'/z')\epsilon = \bar{x}\epsilon.$$

By virtue of the simple dependence of γ_1, γ_2, γ_3, C, and D on k, it follows

that the coefficients in (60) (when multiplied by C) have definite limiting values as $\epsilon \to 0$. Further

$$\coth^{-1}\left\{\frac{\gamma_3 \tan\phi}{(2-\gamma_3^2)^{\frac{1}{2}}}\right\} \to \coth^{-1}(\bar{\gamma}_3/\bar{x}) = \log\left(\frac{\bar{\gamma}_3+\bar{x}}{\bar{\gamma}_3-\bar{x}}\right)$$

and

$$\coth^{-1}\left\{\frac{2^{\frac{1}{2}}\sin\phi}{(2-\gamma_3^2)^{\frac{1}{2}}}\right\} \sim \coth^{-1}\{1+\tfrac{1}{2}(\bar{\gamma}_3^2-\bar{x}^2)\epsilon^2\}$$

$$\sim \log(4/\epsilon^2)-\log(\bar{\gamma}_3^2-\bar{x}^2).$$

The terms in the last two expressions of (60) behave similarly, and the singular terms cancel leaving a finite limiting value for the pressure.

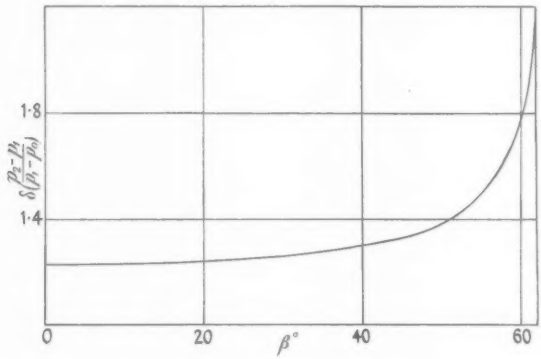

FIG. 5. Symmetrical wedge, $p_1/p_0 = 2$. Effect of yaw on pressure at wedge shock junction.

It will be observed from Fig. 4 that there is only a slight increase in pressure between $\beta = 0$ and $\beta = 40°$, but a marked increase at all points of the wedge for $\beta = 61°{\cdot}9$. This is shown more clearly in Fig. 5, where the pressure at the junction of the wedge and shock is plotted against the angle of yaw. There is a relatively small increase in pressure up to $\beta = 50°$, beyond which the pressure increases rapidly.

In Fig. 6 the pressure distribution on the wedge produced by a stronger incident shock ($p_1/p_0 = 10$, $M = 2{\cdot}95200$, $M_1 = 1{\cdot}34463$) is shown for the two limiting values of β. When $\beta = 0$ there is no singularity at the corner, for the flow behind the incident shock is now supersonic and is deflected discontinuously at the leading edge by a weak shock. In the region of uniform flow before the Mach cone is reached the pressure is constant, after which it decreases monotonically. However, at the extreme angle of yaw ($\beta = 64°{\cdot}3$) the leading edge lies inside the Mach cone and a singularity in the pressure again appears. The transition will occur when $M_1 \cos\beta = 1$, or $\beta = 42°$, for this particular shock strength.

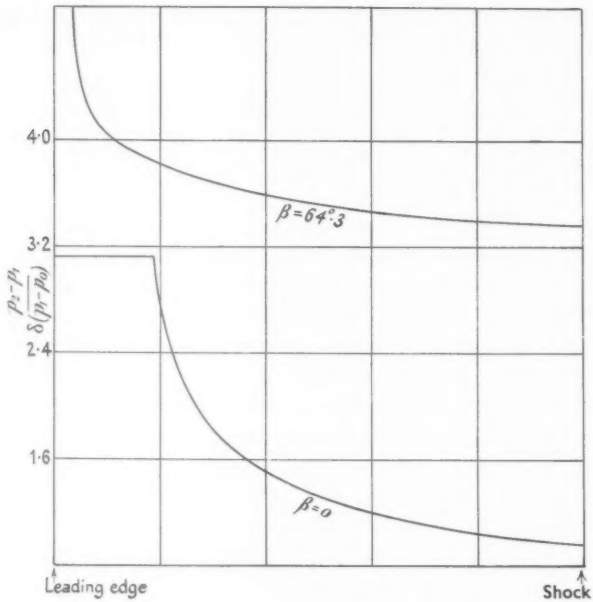

FIG. 6. Pressure distribution on symmetrical wedge for $p_1/p_0 = 10$.

10. Further investigation of the Mach cone

One of the boundary conditions imposed in deriving the present solution is that the pressure should be continuous at the Mach cone. A closer study of the pressure field near this boundary shows, however, that the normal derivative is singular. For, if $\partial p/\partial n$ denotes the pressure derivative along the inward normal to the circle $\rho = 1$ in the (ρ, θ) plane, and if (r, θ) are polar coordinates in the (x, y) plane, we must have

$$p-(p)_{r=1} \sim \frac{\partial p}{\partial n}(1-\rho) \sim \frac{\partial p}{\partial n}[2(1-r)]^{\frac{1}{2}} \tag{71}$$

near $r = 1$.

Since, as will appear, $\partial p/\partial n$ is in general finite and non-zero,

$$\partial p/\partial r \sim -(1-r)^{-\frac{1}{2}}\, \partial p/\partial n$$

near $r = 1$, which cannot describe the actual behaviour in the fluid. The same singularity occurs in Busemann's cone-field theory (see **5**), where there is experimental evidence of a shock. In an attempt to reconcile theory and experiment in the case of the Busemann cone field, Lighthill (**8**) has evolved an elaborate theory, based on the full non-linear equations of motion, by which a more accurate picture of the behaviour near $r = 1$ may be deduced simply from a knowledge of the linearized solution.

Now the essential difference between the present problem and the Busemann cone field is that in the latter the whole flow is effectively irrotational if terms of the third order of the strength of any shocks which may occur are neglected. But it has already been shown that entropy variations in the present problem are significant only in the fluid which is swept by the non-uniform part of the incident shock, and that the condition of irrotationality is effectively true of the fluid in the neighbourhood of the Mach boundary. Thus the governing equations of flow are the same for both problems in the region to be investigated. Since Lighthill's results depend only on the basic equations of motion and the nature of the singularity at $r = 1$, it follows that they may be applied directly in the present problem. A detailed description of the procedure will be found in the above-mentioned paper and only the final results will be quoted.

It appears that the actual behaviour of the flow near $r = 1$ depends on the sign of the normal derivative of the pressure there. If

$$p_2 - (p_2)_{r=1} \sim \rho_1 V_1^2 F(\theta)(1-r)^{\frac{1}{2}} \tag{72}$$

as $r \to 1$, then the Mach cone is the linear approximation to a shock wherever $F(\theta) > 0$. To a second approximation the discontinuity in pressure across this shock is

$$\Delta p_2 = \tfrac{3}{4}\gamma(\gamma+1)p_1 \frac{V_1^6}{a_1^4(V_1^2-a_1^2)} F^2(\theta), \tag{73}$$

where γ here denotes the adiabatic index (**8**, equations (26) and (39)). The strength of the shock is thus $O(\delta^2)$. But when $F(\theta) < 0$ the conclusion is that, although to a higher approximation there will still be a shock, its strength will be at most $O(\delta^3)$ and it will be followed immediately by an expansive flow which is relatively stronger (the expansion produces pressure changes of order δ^2).

From (71) it follows that

$$p_2 - (p_2)_{r=1} \sim a_1 \rho_1 q_1 \frac{\partial p}{\partial n}[2(1-r)^{\frac{1}{2}}], \tag{74}$$

and hence, by (72), that

$$F(\theta) = \frac{2^{\frac{1}{2}} a_1 q_1}{V_1^2}\left(\frac{\partial p}{\partial n}\right). \tag{75}$$

If (75) is substituted in (73) and γ is given the value 1·4, one finds that the strength of the shock compared with that of the incident shock is

$$\frac{\Delta p_2}{p_1 - p_0} = K^2(\theta) \tag{76}$$

if $K(\theta) > 0$, where

$$K(\theta) = \frac{3}{\cos\alpha}\left\{\frac{2(M^2-1)}{M^2+5}\right\}^{\frac{1}{2}}\left(\frac{\partial p}{\partial n}\right). \tag{77}$$

It only remains now to find $\partial p/\partial n$. This follows at once from (48), (55), and (56) with $x_1 < -1$ and $y = 0$. In the supersonic case we have

$$\frac{\partial p}{\partial n} = -\left|\frac{dz_1}{d\zeta}\right| \frac{C\delta[D(x_1-x_0)-1]}{(x_1^2-1)^{\frac{1}{2}}(x_0-x_1)[\gamma_1+(1-x_1)^{\frac{1}{2}}][\gamma_2+(1-x_1)^{\frac{1}{2}}]}. \tag{78}$$

The subsonic symmetrical contribution to $\partial p/\partial n$ will be a similar expression with C_s, D_s, δ_s replacing C, D, δ. The results for the unyawed wedge were first obtained by Tan (9).

The antisymmetrical contribution is

$$\frac{\partial p_a}{\partial n} = -\left|\frac{dz_1}{d\zeta}\right| \frac{C_a\delta_a[D_a(x_1-x_0)-1]}{(1-x_1)^{\frac{1}{2}}(x_0-x_1)^{\frac{1}{2}}[\gamma_1+(1-x_1)^{\frac{1}{2}}][\gamma_2+(1-x_1)^{\frac{1}{2}}]}. \tag{79}$$

The above results have been used to investigate the true behaviour at the Mach cone in the two limiting cases, namely at zero yaw and at the maximum permissible angle of yaw. Of course, in the latter case the Mach angle tends to $\frac{1}{2}\pi$ and the Mach cone degenerates into a plane perpendicular to the direction of uniform flow (in the steady problem). However, Δp_2 does tend to a definite value which provides at least a limiting picture at the boundary of the perturbed region.

It is convenient to consider the case of maximum yaw first. Since k tends to zero in this case we have, by virtue of the dependence of γ_1, γ_2, γ_3, C_s, and D_s on k,

$$\frac{\partial p_s}{\partial n} \sim \left|\frac{dz_1}{d\zeta}\right| \frac{C_s\delta_s D_s}{(x_1^2-1)^{\frac{1}{2}}(1-x_1)}. \tag{80}$$

Now, for $x_1 < -1$, $y_1 = 0$,

$$\left|\frac{dz_1}{d\zeta}\right| = \frac{2^{\frac{1}{2}}(x_1^2-1)^{\frac{1}{2}}}{k'}\{(1-x_1)^{\frac{1}{2}}-2^{\frac{1}{2}}k\} \sim 2^{\frac{1}{2}}(x_1^2-1)^{\frac{1}{2}}(1-x_1)^{\frac{1}{2}} \tag{81}$$

as $k \to 0$. Thus

$$\frac{\partial p_s}{\partial n} \sim C_s D_s \delta_s \left(\frac{2}{1-x_1}\right)^{\frac{1}{2}}. \tag{82}$$

Furthermore, on the Mach cone,

$$x_1 = -\frac{1}{2}\left[\frac{1-\cos(\theta+\chi)}{1-\cos(\theta-\chi)} + \frac{1-\cos(\theta-\chi)}{1-\cos(\theta+\chi)}\right], \tag{83}$$

where $\cos\chi = k$. Thus, when $k \to 0$,

$$x_1 \sim -\frac{1+\sin^2\theta}{1-\sin^2\theta}, \tag{84}$$

and so

$$\frac{\partial p_s}{\partial n} \sim -C_s D_s \delta_s \cos\theta \tag{85}$$

if the positive square root is taken appropriate to the interval $\frac{1}{2}\pi \leqslant \theta \leqslant \frac{3}{2}\pi$.

When (85) is substituted in (77) it gives, in the limit as $k \to 0$,

$$K_s(\theta) = -3^{\frac{1}{2}}\left(\frac{C_s D_s}{k}\right)\delta_s \cos\theta, \tag{86}$$

where use has been made of equations (4) and (5). The limiting value of $C_s D_s/k$ is implied, though this quantity is actually independent of k. The magnitude of K_s for various incident shock pressure ratios may be deduced from Table 1. It is singular in the limit $p_1/p_0 \to 1$ (though Δp_2 itself tends to a finite limit). As p_1/p_0 increases, K_s decreases rapidly to a minimum and thereafter increases steadily.

TABLE 1

The value of K_s at maximum permissible angle of yaw

p_1/p_0	1	2	3	4·823	10
$-\dfrac{K_s(\theta)}{\delta_s \cos\theta}$	∞	5·963	8·001	12·468	26·116

In the antisymmetrical case, although C_a and D_a are not strictly proportional to k^3 and k^{-2} respectively, as is the case for C_s and D_s, it may be deduced from (57) and (58) that the statement is true in an asymptotic sense as $k \to 0$. Hence, by (79),

$$\begin{aligned} \frac{\partial p_a}{\partial n} &\sim \left|\frac{dz_1}{d\zeta}\right| \frac{C_a D_a \delta_a}{(1-x_1)^2} \\ &\sim 2^{\frac{1}{2}} C_a D_a \delta_a \frac{(x_1^2-1)^{\frac{1}{2}}}{(1-x_1)^{\frac{3}{2}}} \\ &\sim -C_a D_a \delta_a \sin\theta \cos\theta. \end{aligned} \tag{87}$$

It follows that, in the limit,

$$K_a(\theta) = -\lim_{k\to 0}\left(\frac{C_a D_a}{k}\right)\frac{3^{\frac{1}{2}}\delta_a}{2}\sin 2\theta. \tag{88}$$

The range of θ runs from $\frac{1}{2}\pi$ at the incident shock, through π on the plane $y = 0$ to $\frac{3}{2}\pi$ at the shock in the lower half-plane. Thus for a symmetrical wedge with $\delta_a = 0$, the whole of the boundary is a shock, but for a semi-infinite flat plate inclined at an angle δ_a to the plane $y = 0$, only that part of the boundary in the upper half-plane is a shock if quantities as small as δ_a^3 are neglected. In the lower half-plane the boundary would be a much weaker shock followed immediately by a relatively stronger expansion.

It will be observed that not only is the strength of the shock zero where it meets the incident shock, but that Δp_2, being proportional to $K^2(\theta)$, increases only as the square of the arc distance from the triple point. The symmetrical contribution is monotonic in $\frac{1}{2}\pi \leqslant \theta \leqslant \pi$ and attains its maximum at the plane $y = 0$; the antisymmetrical contribution has a maximum at $\theta = \frac{3}{4}\pi$. This is by no means the case when $\beta = 0$, as is shown in Figs. 7 and 8,

where $K(\theta)$ is plotted against the fraction of arc distance along the circular boundary beginning at $\theta = \pi$ and finishing at the triple point $\theta = \cos^{-1}k$ ($K(\theta)$ is chosen, rather than its square, because the symmetrical and anti-symmetrical contributions are then additive). The strength of the reflected shock is still zero at the triple point, but even though the figures give the

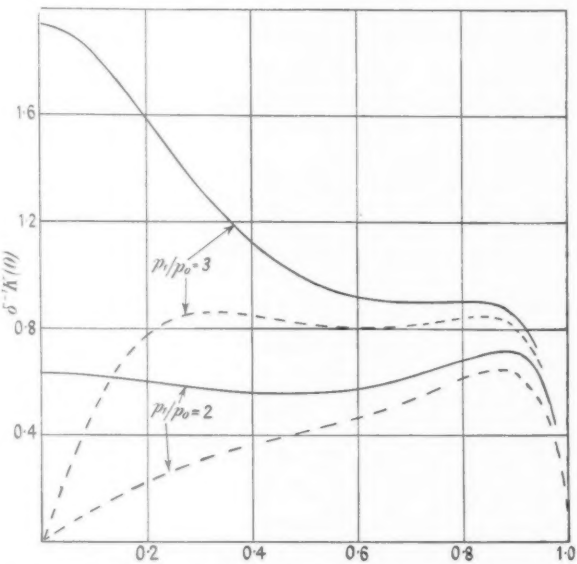

FIG. 7. Variation of $K(\theta)$ when $\beta = 0$ (the abscissa is the fraction of arc length along the Mach cone from the plane $y = 0$ to the incident shock).

square root of the pressure discontinuity, it is clear that there is a steep rise in strength within 10 per cent. of the arc distance from the triple point (corresponding to an angular distance of roughly 13°). Indeed, when $p_1/p_0 = 2$, the maximum strength is attained within 12 per cent. of the arc distance from the triple point. It is suggested that this fact reconciles theory and experiment to some extent, for it is known that, experimentally, a contact discontinuity appears in the perturbed region starting from the triple point, and such discontinuities are associated with three shock configurations. Interferometer photographs also indicate that the strength of the contact discontinuity decreases as the triple point is approached (see, for example, **10**, fig. 7), and this would be compatible with a local decrease in the strength of the reflected shock.

In the general subsonic case $\partial p/\partial n$, and hence the behaviour at the Mach cone, will be determined by two contributions which augment each other in the upper half-plane (assuming that both δ_s and δ_a are positive) but tend to cancel out in the lower half-plane. One may therefore consider the question of where the transition takes place from a shock, to what is

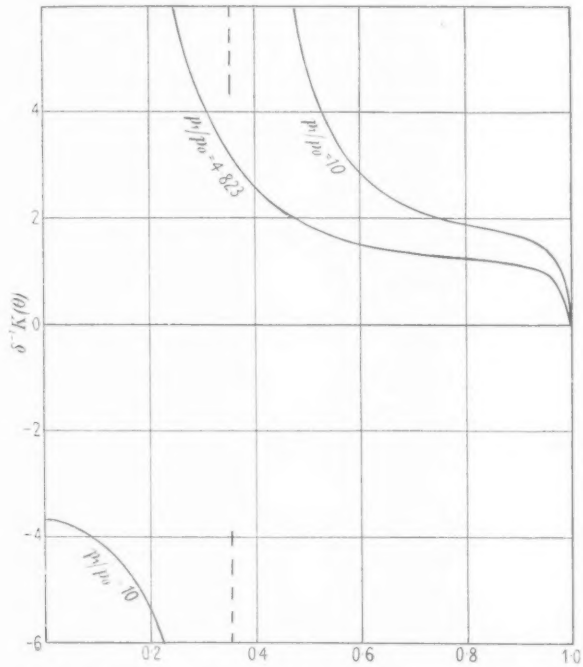

FIG. 8. Variation of $K(\theta)$ when $\beta = 0$ (the abscissa is the fraction of arc length along the Mach cone from the plane $y = 0$ to the incident shock).

effectively an expansion if terms of the third order are ignored. If transition is to take place at all $\partial p/\partial n$ should be negative near the triple point in the lower half-plane. As this point is approached $x_1 \to -\infty$ and so, from (78) and (79) (with the sign of $\partial p_a/\partial n$ changed), one gets the condition

$$\delta_a/\delta_s > C_s D_s/C_a D_a. \tag{89}$$

The value of the right-hand side of (89) is given in Table 2 for $\beta = 0$ and various values of the incident shock-pressure ratio p_1/p_0. It is apparent that transition will begin to occur almost immediately after the lower face of the wedge becomes positively inclined to the plane $y = 0$.

TABLE 2

The minimum values of δ_a/δ_s for which a transition point occurs on the circular boundary

p_1/p_0	1	2	3	4·823
$C_s D_s/C_a D_a$	1	1·068	1·049	1

Table 3 gives the angular distance (in absolute value) from the plane $y = 0$ at which transition occurs when $\beta = 0$ and $\delta_a = 3\delta_s$. This may be calculated from Fig. 7, or directly from (78) and (79). In the latter case it is the root of a cubic.

TABLE 3

Angular distance of point of transition from $y = 0$ ($\beta = 0, \delta_a = 3\delta_s$)

p_1/p_0	1	2	3	4·823
$\theta - 180°$	39°·0	24°·4	16°·5	0°

In the supersonic case, when the flow patterns in the upper and lower half-planes are independent, transition occurs where the tangent plane from the leading edge touches the Mach cone. Not only does Δp_2 change sign but, as shown in Fig. 8, it becomes infinite where the transition takes place. This apparent breakdown of the solution can be explained by the fact that the tangent plane is a linear approximation to the position of a shock or Prandtl–Meyer expansion, and the position would change slightly to a second approximation. When the modification is effected it appears that the shock (or Prandtl–Meyer expansion), which starts from the leading edge, interferes with the Mach cone and prevents θ from attaining the value at which $K(\theta)$ becomes infinite. The actual behaviour (which is here deduced from the analysis of an analogous problem in **8**) is as follows. With $\delta > 0$ that part of the Mach cone which lies between the incident and leading-edge shocks is itself a linear approximation to a shock. The strength of the latter is in general $O(\delta^2)$ and, except near the transition point, deducible from equation (77). The shock increases in strength with θ (see Fig. 8) and actually attains a strength of the same order as the leading-edge shock (namely $O(\delta)$) when the two meet. Between the leading-edge shock and the wedge there is effectively an expansion of strength $O(\delta^2)$ in general, which also increases in strength as the leading-edge shock is approached, but is quickly annihilated once it encounters the latter.

When $\delta < 0$ the tangent plane from the leading edge should be replaced by a Prandtl–Meyer expansion; between the latter and the wedge the

Mach cone becomes a shock to a higher approximation (for $K(\theta)$ is now positive). The strength of this shock increases rapidly and becomes $O(\delta)$ when the region of transition is reached. In passing through the Prandtl-Meyer expansion the shock is weakened and, when it emerges, becomes effectively an expansion whose strength decreases as the incident shock is approached. When $\beta = 0$ and $p_1/p_0 = 10$, for example, the strength of the shock which replaces part of the Mach cone will be deducible from the negative portion of the relevant curve in Fig. 8 (except the part near the singularity).

REFERENCES

1. Sommerfeld, A., *Z. Math. Phys.* **46** (1901), 11.
2. Lighthill, M. J., *Proc. Roy. Soc.* A, **198** (1949), 454.
3. Ting, L., and Ludloff, H. F., *J. Aero. Sci.* **19** (1952), 317.
4. Busemann, A., *Luftfahrstforsch.* **20** (1943), 105.
5. Goldstein, S., and Ward, G. N., *Aero. Quart.* **2** (1950), 39.
6. Hadamard, J., *Lectures on Cauchy's Problem* (Yale University Press, 1923).
7. Chester, W., *Phil. Trans. Roy. Soc.* A, **242** (1950), 527.
8. Lighthill, M. J., *Phil. Mag.* **40** (1949), 1202.
9. Tan, H. S., *J. Aero. Sci.* **18** (1951), 768.
10. Fletcher, C. H., Taub, A. H., and Bleakney, W., *Rev. Mod. Phys.* **23** (1951), 271.

THE EFFECT OF RAPID DISTORTION OF A FLUID IN TURBULENT MOTION

By G. K. BATCHELOR *and* IAN PROUDMAN
(*Trinity College, Cambridge*)

[Received 17 July 1952]

SUMMARY

This paper is concerned with the calculation of the changes produced in a homogeneous turbulent motion when the fluid is subjected to a superimposed uniform distortion. The distortion is assumed to occur so rapidly that the contribution to the change in relative position of fluid particles from the turbulence is negligible. On this basis G. I. Taylor found the effect of an arbitrary distortion on a purely sinusoidal velocity field, and in this paper the effect on homogeneous turbulence is obtained by integrating over all such Fourier components. In the case of turbulence which is initially isotropic, the relative changes in the energies of the three velocity components are found to be independent of the properties of the turbulence and are determined numerically.

Asymptotic results for the important practical case in which one of the three extension ratios is large compared with unity are presented. For the case of a large symmetrical contraction (the common wind-tunnel case), of area ratio c^{-1}, the effect on any one Fourier component depends on c in a manner which tends asymptotically to the laws given by Prandtl, but this is not so for the component energies of the whole turbulent motion since the energy after contraction is dominated by a decreasingly small range of wave-numbers. The same asymptotic dependence on c is found for all kinds of homogeneous turbulence, although the numerical constants vary. When one extension ratio of an otherwise arbitrary distortion becomes large compared with the other two, the asymptotic effect on isotropic turbulence is the same, in all important respects, as the effect of a large symmetrical contraction, the reason being that the vorticity ultimately is everywhere parallel to the line of greatest extension.

No comparison with experiment is possible, since it can be shown that in none of the cases in which measurements have been made is the distortion sufficiently rapid for the above linear theory to be valid. Some of the distortions occurring in aerodynamic practice are rapid enough for the theory to apply, but these will be uncommon, and a consideration of the non-linear effects is very desirable.

1. Introduction

It has been known empirically for many years that the properties of a turbulent motion carried along by a stream can be altered drastically by imposing large distortions on the stream. Wind tunnels are usually designed in such a way that the stream is subjected to a reduction in cross-sectional area immediately before entering the working section, for the reason that such a contraction is known to reduce the ratio of the energy of any turbulence that may be present to the energy of the stream. A large contraction ratio in a wind tunnel is in fact essential if the intensity of the turbulent

motion is to be reduced below the level at which it affects the characteristics of the boundary layers on models at the large Reynolds numbers commonly used. Other kinds of stream distortion occur in wind tunnels and ducts and pipes, although a contraction in the cross-sectional area of the stream is probably the case of greatest practical interest.

From a different point of view the process of superimposed distortion of fluid in turbulent motion may be regarded as occurring in a general turbulent flow. Large-scale variations of the turbulent velocity produce a coordinated strain over a large region of fluid, and so far as small-scale velocity variations are concerned this large-scale strain can be regarded as a superimposed distortion of the fluid.

Thus there is some interest in an attempt to determine quantitatively the effect of a specified distortion of a region of fluid on the turbulent motion of the fluid. The problem is a difficult one, even when very simple kinds of distortion and turbulent motion are considered, and it is only on a very limited basis that progress can be made. The first work on the problem seems to be due to Prandtl (**1**), who considered the effect of a symmetrical contraction (which reduces the area by a factor c^{-1}) on small steady disturbances (which vary with neither time nor distance downstream) carried along by a uniform wind-tunnel stream. The lateral velocity components are here determined uniquely by the component of vorticity parallel to the stream, and since this vorticity component is increased by the factor $c^{\frac{1}{2}}$ by passage through the contraction, the lateral velocity components are increased by the same factor. The energy of these components relative to that of the stream therefore decreases by the factor c^{-1}. For the longitudinal component Prandtl argued that the pressure drop accompanying passage through the contraction is approximately the same for all streamlines, so that, to the first order in the disturbance velocity, the longitudinal component must be reduced by the factor c^{-1} on passage through the contraction. These arguments are obviously valid, but their bearing on the effect of the contraction on disturbances which vary with distance downstream is uncertain, and no results about the effect on turbulence can be inferred with confidence—except perhaps that the longitudinal velocity component will be reduced by a contraction to a greater extent than the lateral component.

The first step towards a calculation of the effect of stream distortion on turbulence was taken by Taylor (**2**), who worked out the changes in a small disturbance which varies sinusoidally with respect to all three space coordinates, for a distortion which is sufficiently rapid. This likewise gives an inaccurate guide to the effect of the distortion on turbulence, but inasmuch as a sinusoidal disturbance can be regarded as a typical member

of the set of Fourier components into which the turbulence can be resolved, it is possible to 'integrate' Taylor's result to give the effect of a rapid distortion on a genuine turbulent motion. It is the purpose of this paper to show how the 'integration' may be carried out for the case of isotropic turbulence and an *arbitrary* distortion, and to present the whole problem systematically as a preliminary to attempts to treat the case of a distortion which is not rapid enough for the following analysis to apply.

After this paper had been prepared reference (**3**) came to our notice. It appears that Ribner and Tucker have recently worked out the effect of a symmetrical contraction on isotropic turbulence, with methods and results similar to those to be described below; these same results are also in the text of reference (**4**) and in the dissertation submitted in 1951 by one of us (I. P) for the degree of Ph.D. of the University of Cambridge. However, the present paper goes rather further than any of these references, inasmuch as it describes the effect of an arbitrary distortion on isotropic turbulence and the asymptotic effect of a large contraction on homogeneous turbulence, and we feel that it justifies independent publication.

2. Linearization of the problem for a sufficiently rapid distortion

The essential meaning of the assumption which will be adopted, following Taylor, in order to render the problem linear in the turbulent velocity, is that during the process of distortion the displacement history of each fluid particle is determined uniquely by the history of the distortion. For this assumption to be valid it is clearly necessary that the influence of the turbulence on the relative separation of any two fluid particles, whose initial separation is given, be negligibly small at all stages of the distortion. It is in this sense that we require the distortion to be sufficiently rapid.

The analysis is best carried out with the aid of Cauchy's equations for the vorticity associated with an element of an incompressible, inviscid fluid (**5**), viz.

$$\omega_i(\mathbf{a}) = \frac{\partial x_i}{\partial a_j}\omega_j'(\mathbf{a}) \tag{2.1}$$

(the repeated suffix being summed), where $\boldsymbol{\omega}'(\mathbf{a})$ is the vorticity of the fluid element at the beginning of the distortion (time t'), when its position is given by the vector coordinate $\mathbf{a}$, and $\boldsymbol{\omega}(\mathbf{a})$ is the vorticity of the same element at any stage of the distortion (time t), when its position is $\mathbf{x}$. Neglect of the effect of viscosity is not in general a justifiable approximation in a discussion of the mechanics of turbulent flow in the absence of superimposed stream distortion; nor would it be justifiable in the problem under discussion at times long after the distortion commences, for it is well known that the effects of inertia and viscous forces on vorticity quickly come into

statistical equilibrium. In the problem of distortion of the turbulence, the neglect of viscous effects is evidently justified if the process of distortion takes place in a time interval small compared with the interval required for appreciable viscous decay to occur. That is, if $\epsilon(t)$ is the rate of viscous dissipation at time t, during the distortion, when the energy of the turbulence† is $\frac{1}{2}\overline{\mathbf{u}^2}$, we shall require

$$\int_{t'}^{t} \epsilon(t)\, dt \ll \tfrac{1}{2}\overline{\mathbf{u}^2} \tag{2.2}$$

for all relevant values of t. An approximate version of (2.2) is obtained by using the initial values of the quantities ϵ and $\overline{\mathbf{u}^2}$, and by making use of the well-known empirical relation $\epsilon \propto (\overline{\mathbf{u}^2})^{\frac{3}{2}}/l$, where l is the length scale of the energy-containing eddies of the turbulence, viz.

$$t - t' \ll \left(\frac{l}{\sqrt{\overline{\mathbf{u}^2}}}\right)_{t=t'}. \tag{2.3}$$

If the effect of the distortion on a particular Fourier component of the turbulence is to be examined, a condition analogous to (2.2) for that Fourier component alone will need to be satisfied.

Returning to (2.1), contributions to the tensor $\partial x_i/\partial a_j$ will arise from the velocity field $\mathbf{U}(\mathbf{a}, t)$ which exists in the neighbourhood of the fluid element as a result of the superimposed distortion alone (i.e. $\mathbf{U}$ is the total velocity of the element in the absence of any turbulence) and from the additional velocity field $\mathbf{u}(\mathbf{a}, t)$ which is a consequence of the turbulence. We have

$$\frac{\partial x_i}{\partial a_j} = \delta_{ij} + \int_{t'}^{t} \left(\frac{\partial U_i}{\partial a_j} + \frac{\partial u_i}{\partial a_j}\right) dt, \tag{2.4}$$

where δ_{ij} is the unit diagonal tensor, and the assumption to be made is that the contribution from the second term in the integrand is unimportant for the purposes at hand. The quantity $\int_{t'}^{t} \frac{\partial u_i}{\partial a_j}\, dt$ is random, and an appropriate *necessary* condition for the assumption to be valid is that

$$\int_{t'}^{t}\int_{t'}^{t} \overline{\frac{\partial u_i(t_1)}{\partial a_j}\frac{\partial u_i(t_2)}{\partial a_j}}\, dt_1\, dt_2 \ll \int_{t'}^{t} \frac{\partial U_i}{\partial a_j}\, dt \int_{t'}^{t} \frac{\partial U_i}{\partial a_j}\, dt. \tag{2.5}$$

Since $\partial u_i/\partial a_j$ at any time other than t' depends on the effect which the distortion has on the turbulence, it is not easy to reduce the condition (2.5) to a form involving properties of the turbulence at the initial instant

† i.e. of the velocity fluctuations which are additional to the velocity field produced by the distortion in the absence of turbulence.

only. A criterion which probably expresses (2.5) correctly until the distortion alters the order of magnitude of $\partial u_i/\partial a_j$ is obtained by using only the initial value of the integrand, viz. $\overline{\frac{\partial u_i'}{\partial a_j}\frac{\partial u_i'}{\partial a_j}}$, where $\mathbf{u}' \equiv \mathbf{u}(t')$. When the turbulence is homogeneous (as will be approximately the case in general, so far as velocity derivatives are concerned) the condition thus becomes

$$\frac{\epsilon(t')}{\nu}(t-t')^2 \ll \int_{t'}^{t} \frac{\partial U_i}{\partial a_j}\,dt \int_{t'}^{t} \frac{\partial U_i}{\partial a_j}\,dt, \tag{2.6}$$

where ν is the kinematic viscosity of the fluid. In the simple case of an axially symmetrical distortion which multiplies the length of all lines parallel to the axis of symmetry by a factor c, the requirement is

$$t-t' \ll \left[\frac{l}{\sqrt{\overline{\mathbf{u}^2}}}\left(\frac{\nu}{l\sqrt{\overline{\mathbf{u}^2}}}\right)^{\frac{1}{2}}\right]_{t=t'} [(c-1)^2+2(c^{-\frac{1}{2}}-1)^2]^{\frac{1}{2}}, \tag{2.7}$$

which is a more stringent condition than (2.3) in the early stages of the distortion.

Thus there are two conditions to be satisfied. The first, expressed by (2.2), requires the duration of the distortion to be so small that viscous dissipation does not produce a significant change in the turbulent energy, and the second, expressed by (2.5), requires the contribution to the relative velocity of two neighbouring particles from the turbulence to be small compared with that from the superimposed distortion. When these conditions are satisfied at all times during the process of distortion, the changes in the vorticity of the turbulence are described by the linear equation

$$\omega_i(\mathbf{a}) = S_{ij}(t)\omega_j'(\mathbf{a}), \tag{2.8}$$

where the distortion tensor $S_{ij}(t)$ is

$$S_{ij}(t) = \delta_{ij} + \int_{t'}^{t} \frac{\partial U_i(t)}{\partial a_j}\,dt. \tag{2.9}$$

The remaining assumption on which the subsequent analysis will be based is that $\partial U_i(t)/\partial a_j$ and $S_{ij}(t)$ are independent of $\mathbf{a}$, i.e. that the superimposed distortion is *uniform*. Then if $\mathbf{x}$ and $\mathbf{a}$ are referred to the same origin, the position of a fluid particle at time t is given by

$$x_i(t) = a_j\frac{\partial x_i}{\partial a_j} = a_j S_{ij}(t), \tag{2.10}$$

that is, the vector $\mathbf{x}(t)$ is obtained from $\mathbf{a}$ by a linear transformation of the axes of reference. This assumption is exactly true if the fluid is confined within boundaries and the distortion is imposed by a motion of the boundaries such that points on the boundary at any time t are related to points

on the boundary at the initial instant t' by a linear transformation, for the fluid necessarily then moves in exactly the same way. However, practical interest in the effect of distortion on turbulence usually arises in connexion with problems in which the boundaries are stationary and the turbulence is carried past them, as in a wind-tunnel contraction, and for such problems the distortion tensor $S_{ij}(t)$ is not exactly uniform. The particles of fluid which lie on a lateral plane, far upstream of a contraction, will not lie on a plane after being carried downstream (as they should if S_{ij} is to be uniform), but will lie on a curved surface with the particles near the centre of the tunnel farther downstream than those near the walls. It is difficult to make general remarks about the degree of non-uniformity of S_{ij} in such cases, but at any rate it is clear that the radius of curvature of the above-mentioned curved surface will be of order of the tunnel width; hence, provided the scale of the turbulence is small compared with the tunnel width, the distortion tensor will be *approximately* uniform, although it may be necessary to use a different value of S_{ij} at different positions across the tunnel.

The distortion tensor S_{ij} can be written as the sum of a symmetrical and an anti-symmetrical second-order tensor, the first representing a *pure strain* and the second representing a *rotation*. A uniform rotation of the whole body of fluid has no effect on the turbulence, except to refer it to different axes of reference (since Coriolis forces arising from the presence of the turbulent velocities are to be neglected during the distortion), and we may therefore confine attention to symmetrical forms of $S_{ij}(t)$. Later we shall choose the principal axes of the pure strain at the time t under consideration as axes of reference, so that if e_1-1, e_2-1, e_3-1 are the principal extensions (with $e_1 e_2 e_3 = 1$ in order to satisfy the incompressibility condition), the components of the distortion tensor $S_{ij}(t)$ are

$$S_{11} = e_1, \qquad S_{22} = e_2, \qquad S_{33} = e_3, \qquad S_{ij} = 0 \quad \text{if } i \neq j.$$

If $T_{ij}(t)$ is the reciprocal distortion tensor defined by

$$T_{ij} S_{jk} = \delta_{ik},$$

the components of T_{ij} are

$$T_{11} = 1/e_1, \qquad T_{22} = 1/e_2, \qquad T_{33} = 1/e_3, \qquad T_{ij} = 0 \quad \text{if } i \neq j.$$

3. Effect of the distortion on the energy spectrum tensor

The linearization that has been discussed in the preceding section involves no assumptions about the nature of the turbulent motion, and we now turn to this part of the problem. Since the superimposed distortion has been assumed to be a uniform pure strain, it is obviously to our advantage to assume that the turbulence has a similar spatial uniformity; this is

in any case a valid approximation for the turbulence in wind-tunnel streams, although it will not be valid for fully developed turbulent flow in a pipe. We therefore assume the turbulence to be homogeneous.

Since the problem has been linearized, the standard resolution of the turbulent velocity distribution into its Fourier wave-number components (4) will be useful. We write the turbulent velocity distribution at time t' as

$$\mathbf{u}'(\mathbf{a}) = \int e^{\iota\boldsymbol{\kappa}\cdot\mathbf{a}}\, d\mathbf{Z}'(\boldsymbol{\kappa}), \tag{3.1}$$

where $\iota = \sqrt{(-1)}$, $\boldsymbol{\kappa}$ is a wave-number vector, and the integration is over all wave-number space. The increments $d\mathbf{Z}'(\boldsymbol{\kappa})$ are random (with rather 'pathological' properties), and statistically orthogonal, in view of the homogeneity of the turbulence, and the variance of $d\mathbf{Z}'(\boldsymbol{\kappa})$ is proportional to the energy spectrum tensor. Equally, the velocity distribution at any time t during the distortion can be written as a Fourier integral

$$\mathbf{u}(\mathbf{a}) = \int e^{\iota\boldsymbol{\kappa}\cdot\mathbf{a}}\, d\mathbf{Z}(\boldsymbol{\kappa}); \tag{3.2}$$

since both the superimposed strain and the initial turbulence are spatially uniform, it is clear that $\mathbf{u}(\mathbf{a})$ will also be a stationary random function of $\mathbf{a}$ at all values of t, and hence that $d\mathbf{Z}(\boldsymbol{\kappa})$ will have the same general properties as $d\mathbf{Z}'(\boldsymbol{\kappa})$.

Now the vector $\mathbf{x}$ specifies the position, at time t, of the particle which was initially (time t') at the position $\mathbf{a}$, and hence at any given value of t the vector $\mathbf{x}$ may be regarded as defining a new coordinate system. For coordinate systems obtained by a linear transformation of the Euclidean space $\mathbf{a}$, the formulae for vector differential operators remain the same. The relation (2.10) between $\mathbf{x}$ and $\mathbf{a}$ *is* linear, so that we have, with an appropriate change of notation describing functional dependence,

$$\omega_i(\mathbf{x}) = \epsilon_{ijk}\frac{\partial u_k(\mathbf{x})}{\partial x_j} = \epsilon_{ijk}\frac{\partial u_k(\mathbf{x})}{\partial a_l}T_{lj},$$

and, of course,

$$\omega_i'(\mathbf{a}) = \epsilon_{ijk}\frac{\partial u_k'(\mathbf{a})}{\partial a_j},$$

where ϵ_{ijk} is the unit alternating tensor. The basic relation (2.8) therefore becomes

$$\epsilon_{ijk}\frac{\partial u_k(\mathbf{x})}{\partial a_l}T_{lj} = \epsilon_{mnp}\frac{\partial u_p'(\mathbf{a})}{\partial a_n}S_{im}. \tag{3.3}$$

The corresponding relation between the Fourier coefficients of the velocity distributions at times t and t' is obtained by substituting (3.1) and (3.2) in (3.3):

$$\epsilon_{ijk}\kappa_l T_{lj}\, dZ_k(\boldsymbol{\kappa}) = \epsilon_{mnp}\kappa_n S_{im}\, dZ_p'(\boldsymbol{\kappa}). \tag{3.4}$$

The coordinate system defined by $\mathbf{x}$ provides a more natural framework

for Fourier analysis of the velocity distribution at time t, so that it is convenient to define a new wave-number $\boldsymbol{\chi}$ by the relation

$$\boldsymbol{\chi}.\mathbf{x} = \boldsymbol{\kappa}.\mathbf{a},$$

that is

$$\chi_i = \kappa_j T_{ji} \quad \text{and} \quad \kappa_i = \chi_j S_{ji}, \tag{3.5}$$

and to regard $d\mathbf{Z}$ as a function of $\boldsymbol{\chi}$. The relation (3.4) then becomes, after multiplying by $\epsilon_{iqr}\chi_q$ (and making use of $\chi_k\, dZ_k = 0$, which is a consequence of the incompressibility condition $\partial u_k(\mathbf{x})/\partial x_k = 0$),

$$dZ_r(\boldsymbol{\chi}) = \frac{\epsilon_{iqr}\epsilon_{mnp}\chi_q\kappa_n S_{im}}{\chi^2}\, dZ'_p(\boldsymbol{\kappa}), \tag{3.6}$$

where $\chi^2 = \boldsymbol{\chi}^2$.

From this relation between the Fourier coefficients of the turbulent velocity distribution before and during the distortion it is possible to deduce the effect of the distortion on *any* of the statistical parameters describing the turbulence. Practical interest will usually be concentrated on the change in the energy spectrum tensor, and this is the only quantity that we shall consider here. The energy spectrum tensor (at the initial instant) is defined as (4)

$$\Phi'_{ij}(\boldsymbol{\kappa}) = \lim_{d\boldsymbol{\kappa}\to 0} \overline{\frac{d\overset{*}{Z}'_i(\boldsymbol{\kappa})\, dZ'_j(\boldsymbol{\kappa})}{d\boldsymbol{\kappa}}}$$

(where $d\boldsymbol{\kappa}$ is the element of volume of wave-number space at position $\boldsymbol{\kappa}$ to which the increment $d\mathbf{Z}(\boldsymbol{\kappa})$ corresponds, and $d\overset{*}{\mathbf{Z}}$ is the complex conjugate of $d\mathbf{Z}$) and is related to the velocity correlation tensor by

$$\overline{u'_i(\mathbf{a})u'_j(\mathbf{a}+\mathbf{r})} = \int e^{\iota\boldsymbol{\kappa}.\mathbf{r}}\Phi'_{ij}(\boldsymbol{\kappa})\, d\boldsymbol{\kappa}.$$

For the spectrum tensor $\Phi_{ij}(\mathbf{x})$ at time t we have similar relations, with $\mathbf{x}$ and $\boldsymbol{\chi}$ replacing $\mathbf{a}$ and $\boldsymbol{\kappa}$, and the expression for $\Phi_{ij}(\boldsymbol{\chi})$ in terms of $\Phi'_{ij}(\boldsymbol{\kappa})$ is found immediately from (3.6) to be

$$\Phi_{ij}(\boldsymbol{\chi})\, d\boldsymbol{\chi} = \epsilon_{ikl}\epsilon_{mnp}\epsilon_{jab}\epsilon_{uvw}\chi_l\chi_b\chi^{-4}\kappa_n\kappa_v S_{km}S_{au}\Phi'_{pw}(\boldsymbol{\kappa})\, d\boldsymbol{\kappa}. \tag{3.7}$$

This, together with the auxiliary relation (3.5) between $\boldsymbol{\kappa}$ and $\boldsymbol{\chi}$, gives explicitly the effect of a known distortion on the turbulent energy spectrum.

The relations (3.6) and (3.7) become more useful when the principal axes of the pure strain are used as axes of reference. We then have

$$(\kappa_1, \kappa_2, \kappa_3) = (e_1\chi_1, e_2\chi_2, e_3\chi_3)$$

(so that $d\boldsymbol{\kappa} = d\boldsymbol{\chi}$) and (3.6) becomes

$$dZ_1(\boldsymbol{\chi}) = \frac{1}{e_1}\, dZ'_1(\boldsymbol{\kappa}) - \frac{\kappa_1}{e_1\chi^2}\left[\frac{\kappa_1}{e_1^2}\, dZ'_1(\boldsymbol{\kappa}) + \frac{\kappa_2}{e_2^2}\, dZ'_2(\boldsymbol{\kappa}) + \frac{\kappa_3}{e_3^2}\, dZ'_3(\boldsymbol{\kappa})\right], \tag{3.8}$$

with two similar equations, where

$$\chi^2 = \kappa_1^2/e_1^2 + \kappa_2^2/e_2^2 + \kappa_3^2/e_3^2.$$

In the case in which $i = j = 1$, (3.7) becomes

$$\Phi_{11}(\boldsymbol{\chi}) = \frac{1}{e_1^2}\Phi'_{11}(\boldsymbol{\varkappa}) + \frac{\kappa_1^2}{e_1^2\chi^4}\left[\left(\frac{\kappa_2^2}{e_2^2}+\frac{\kappa_3^2}{e_3^2}\right)\left(\frac{1}{e_2^2}+\frac{1}{e_3^2}-\frac{2}{e_1^2}\right)+\kappa_1^2\left(e_1^2-\frac{1}{e_1^4}\right)\right]\Phi'_{11}(\boldsymbol{\varkappa}) + \\ + \frac{\kappa_2^2}{e_2^2\chi^4}(e_3^2-e_2^2)\left(\kappa_1^2+\kappa_2^2+\frac{e_2^2}{e_3^2}\kappa_3^2\right)\Phi'_{22}(\boldsymbol{\varkappa}) + \\ + \frac{\kappa_3^2}{e_3^2\chi^4}(e_2^2-e_3^2)\left(\kappa_1^2+\frac{e_3^2}{e_2^2}\kappa_2^2+\kappa_3^2\right)\Phi'_{33}(\boldsymbol{\varkappa}) \quad (3.9)$$

with similar expressions for the two other diagonal components of $\Phi_{ij}(\boldsymbol{\chi})$. Since $\Phi_{ij}(\boldsymbol{\chi})$ is a tensor with Hermitian symmetry which satisfies the continuity equation $\chi_i\Phi_{ij}(\boldsymbol{\chi}) = 0$, it is uniquely determined by its diagonal components, and the relation (3.9) is therefore sufficient to determine the effect of the distortion on any component of the spectrum tensor.

It is at this stage that we can recover the results that have already been obtained by Prandtl (**1**) and Taylor (**2**). The steady disturbance considered by Prandtl does not vary in the direction of the wind-tunnel stream (i.e. in the x_1-direction, say) and corresponds to a Fourier component with wave-number $(0, \kappa_2, \kappa_3)$. Putting $e_2 = e_3$ to correspond to an axially symmetrical contraction in (3.8) and the two similar equations then gives

$$dZ_1(\boldsymbol{\chi}) = e_1^{-1}dZ'_1(\boldsymbol{\varkappa}), \qquad dZ_2(\boldsymbol{\chi}) = e_1^{\frac{1}{2}}dZ'_2(\boldsymbol{\varkappa}), \qquad dZ_3(\boldsymbol{\chi}) = e_1^{\frac{1}{2}}dZ'_3(\boldsymbol{\varkappa}),$$

with $\boldsymbol{\chi} = (0, e_1^{\frac{1}{2}}\kappa_2, e_1^{\frac{1}{2}}\kappa_3)$, in agreement with the results already quoted. The results obtained by Taylor for the effect of the distortion on a purely sinusoidal velocity disturbance are identical with (3.8). As Taylor points out, if we put $e_2 = e_3 = e_1^{-\frac{1}{2}}$, and $e_1 \to \infty$,

$$dZ_1(\boldsymbol{\chi}) \to e_1^{-1}\frac{\kappa^2 dZ'_1(\boldsymbol{\varkappa})}{\kappa_2^2+\kappa_3^2}, \quad (3.10)$$

$$dZ_2(\boldsymbol{\chi}) \to e_1^{\frac{1}{2}}\kappa_3\frac{\kappa_3 dZ'_2(\boldsymbol{\varkappa})-\kappa_2 dZ'_3(\boldsymbol{\varkappa})}{\kappa_2^2+\kappa_3^2}, \qquad dZ_3(\boldsymbol{\chi}) \to e_1^{\frac{1}{2}}\kappa_2\frac{\kappa_2 dZ'_3(\boldsymbol{\varkappa})-\kappa_3 dZ'_2(\boldsymbol{\varkappa})}{\kappa_2^2+\kappa_3^2}. \quad (3.11)$$

Thus for any one Fourier component the longitudinal and lateral velocity components vary as e_1^{-1} and $e_1^{\frac{1}{2}}$ for a sufficiently large symmetrical contraction, which is the same as Prandtl's result; however, the presence on the right-hand sides of (3.10) and (3.11) but not of (3.8), of functions of $\boldsymbol{\varkappa}$ which have singularities at $\kappa_2^2+\kappa_3^2 = 0$, shows that this same result may not (and, in one case, as will be seen in the next section, *does* not) hold for integrals of the spectrum tensor components over all wave-numbers.

Although the problem has been solved in principle, the results will be useful only if it is possible to integrate the spectrum tensor over all values of the wave-number to obtain the effect of the distortion on the energies

associated with the different velocity components. It is clear that the complexity of the right side of (3.9) will prohibit such integration unless $\Phi'_{ij}(\boldsymbol{\kappa})$ has a simple form. For this reason we now assume the turbulence to be *isotropic* initially, and it is again fortunate that this will usually be a good approximation in the important case of wind-tunnel turbulence immediately upstream of a contraction. When the turbulence is initially isotropic we have

$$\Phi'_{ij}(\boldsymbol{\kappa}) = \frac{E(\kappa)}{4\pi\kappa^4}(\kappa^2\delta_{ij} - \kappa_i\kappa_j), \tag{3.12}$$

where $E(\kappa)$ is (initially) the density of kinetic energy with respect to wave-number magnitude $\left(\text{so that } \int_0^\infty E(\kappa)\,d\kappa = \tfrac{1}{2}\overline{\mathbf{u}^2}\right)$. In this case (3.9) becomes, after some reduction,

$$\Phi_{11}(\boldsymbol{\chi}) = \frac{E(\kappa)}{4\pi e_1^2\kappa^2\chi^4}\left[\kappa_1^2\left(\frac{\kappa_2^2}{e_2^4}+\frac{\kappa_3^2}{e_3^4}\right)+\left(\frac{\kappa_2^2}{e_2^2}+\frac{\kappa_3^2}{e_3^2}\right)^2\right], \tag{3.13}$$

and we find for the density in wave-number space ofcontributions to $\overline{\mathbf{u}^2}$

$$\Phi_{ii}(\boldsymbol{\chi}) = \frac{E(\kappa)}{4\pi\kappa^2\chi^2}[\kappa_1^2(e_2^2+e_3^2)+\kappa_2^2(e_3^2+e_1^2)+\kappa_3^2(e_1^2+e_2^2)]. \tag{3.14}$$

The turbulence is rendered anisotropic by the distortion, so that it is no longer possible to express the spectrum tensor in the form (3.12).

The effect of the distortion on the energy associated with any velocity component can now be found by integration with respect to $\boldsymbol{\kappa}$, the results of which are described in the following sections.

4. The case of a symmetrical contraction

The effect of a general distortion on the energy of turbulence which is initially isotropic can be found, but we shall first consider the simple and important case in which

$$e_2 = e_3 = e_1^{-\frac{1}{2}} = c^{-\frac{1}{2}},$$

c being the 'contraction ratio', or the factor by which the length of a material line element in the direction of the axis of symmetry is multiplied. Equation (3.13), and the sum of its two partners, now reduce to

$$\Phi_{11}(\boldsymbol{\chi}) = \frac{\kappa^2}{\chi^4}\Phi'_{11}(\boldsymbol{\kappa}) = \frac{1}{4\pi}E(\kappa)\frac{\kappa_2^2+\kappa_3^2}{\chi^4}, \tag{4.1}$$

$$\Phi_{22}(\boldsymbol{\chi})+\Phi_{33}(\boldsymbol{\chi}) = \frac{1}{4\pi}E(\kappa)\frac{c\chi^4+c^{-3}\kappa_1^2\kappa^2}{\kappa^2\chi^4}, \tag{4.2}$$

where $\chi^2 = c^{-2}\kappa_1^2+c(\kappa_2^2+\kappa_3^2)$.

The ratio of the energy of the longitudinal velocity component (i.e. along the axis of symmetry) at time t to that before the distortion is

$$\mu_1 = \frac{\overline{u_1^2}}{\overline{u_1'^2}} = \frac{\int \Phi_{11}(\boldsymbol{\chi})\, d\boldsymbol{\chi}}{\int \Phi'_{11}(\boldsymbol{\kappa})\, d\boldsymbol{\kappa}} = \frac{\int E(\kappa)\frac{\kappa_2^2+\kappa_3^2}{\chi^4}\, d\boldsymbol{\kappa}}{\int E(\kappa)\frac{\kappa_2^2+\kappa_3^2}{\kappa^4}\, d\boldsymbol{\kappa}}.$$

With the use of polar coordinates κ, θ, where $\kappa_1 = \kappa\cos\theta$, $(\kappa_2^2+\kappa_3^2)^{\frac{1}{2}} = \kappa\sin\theta$, we find that the integrations with respect to κ cancel, giving

$$\begin{aligned}\mu_1 &= \int_0^\pi \frac{\sin^3\theta\, d\theta}{(c^{-2}\cos^2\theta + c\sin^2\theta)^2} \Big/ \int_0^\pi \sin^3\theta\, d\theta \\ &= \tfrac{3}{4}c^{-2}\left(\frac{1+\alpha^2}{2\alpha^3}\log\frac{1+\alpha}{1-\alpha} - \alpha^{-2}\right), \end{aligned} \tag{4.3}$$

where $\alpha^2 = 1-c^{-3}$. Likewise the ratio of the energy of the two lateral velocity components at time t to that before distortion is

$$\begin{aligned}\mu_2 = \mu_3 = \frac{\overline{u_2^2}+\overline{u_3^2}}{\overline{u_2'^2}+\overline{u_3'^2}} &= \frac{\int [\Phi_{22}(\boldsymbol{\chi})+\Phi_{33}(\boldsymbol{\chi})]\, d\boldsymbol{\chi}}{\int [\Phi'_{22}(\boldsymbol{\kappa})+\Phi'_{33}(\boldsymbol{\kappa})]\, d\boldsymbol{\kappa}} = \frac{\int E(\kappa)\frac{c\chi^4 + c^{-3}\kappa_1^2\kappa^2}{\kappa^2\chi^4}\, d\boldsymbol{\kappa}}{\int E(\kappa)\frac{\kappa^2+\kappa_1^2}{\kappa^4}\, d\boldsymbol{\kappa}} \\ &= \frac{c\int_0^\pi \left[1+\frac{\cos^2\theta}{c^6(\sin^2\theta+c^{-3}\cos^2\theta)^2}\right]\sin\theta\, d\theta}{\int_0^\pi (1+\cos^2\theta)\sin\theta\, d\theta} \\ &= \tfrac{3}{4}c+\tfrac{3}{4}c^{-2}\left(\tfrac{1}{2}\alpha^{-2} - \frac{1-\alpha^2}{4\alpha^3}\log\frac{1+\alpha}{1-\alpha}\right). \end{aligned} \tag{4.4}$$

The ratio of the total energy of the turbulence at time t to that before distortion is, from (4.3) and (4.4),

$$\frac{\overline{u_i u_i}}{\overline{u_i' u_i'}} = \tfrac{1}{3}(\mu_1+\mu_2+\mu_3) = \tfrac{1}{2}c + \frac{1}{4c^2\alpha}\log\frac{1+\alpha}{1-\alpha}. \tag{4.5}$$

Numerical values of μ_1 and μ_2 when $c > 1$, as given by (4.3) and (4.4), are exhibited in Fig. 1. μ_1 and μ_2 are found to be always less than and greater than 1 respectively, as might be expected from a rough use of Prandtl's arguments (although Taylor was led to conclude, from the results for a single Fourier component, that μ_2 would first decrease and later increase with increase of c). The increase in the lateral energy dominates the total energy of the turbulence, which is always increased by the contraction. However, the energy of the turbulence *relative* to that of the stream which

transports it through the contraction in a wind tunnel—and it is the relative energy which is significant so far as the effect of turbulence as an aerodynamic disturbance is concerned—is altered by the factors μ_1/c^2 and μ_2/c^2, both of which are always less than 1 (provided $c > 1$). In many

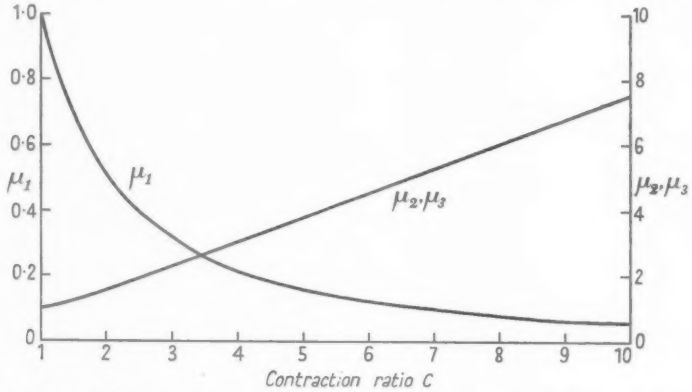

FIG. 1. Effect of a symmetrical contraction on the energies of the longitudinal and lateral components of velocity.

practical cases c will be large compared with 1, and expansions of μ_1 and μ_2 in powers of c^{-3} are useful. We find

$$\mu_1 = \tfrac{3}{4}c^{-2}[(1+c^{-3}+\tfrac{9}{8}c^{-6}+\ldots)\log 4c^3-(1+2c^{-3}+\tfrac{7}{4}c^{-6}+\ldots)],$$
$$\mu_2 = \tfrac{3}{4}c[(1+\tfrac{1}{2}c^{-3}+\tfrac{1}{2}c^{-6}+\ldots)-(\tfrac{1}{4}c^{-6}+\ldots)\log 4c^3],$$

and for c greater than about 2, the approximation

$$\mu_1 = \tfrac{3}{4}c^{-2}(\log 4c^3-1), \qquad \mu_2 = \tfrac{3}{4}c \tag{4.6}$$

will usually be quite good enough.

It appears that the distortion factor μ_1 does not vary with c, when c is large, in the manner suggested by Prandtl and Taylor (viz. $\mu_1 \propto c^{-2}$). The reason, as already hinted at in the preceding section, is that when c is large the expression for $\int \Phi_{11}(\boldsymbol{\chi})\, d\boldsymbol{\chi}$ is dominated by a region of wave-number space in the neighbourhood of $\chi_2^2+\chi_3^2 = 0$ (Fourier components with wave-number vectors in this region being much less suppressed by the distortion), and the extent of this region itself varies with c. Thus the asymptotic dependence on c of the effect of the distortion on the energy of any one Fourier component is not the same as the behaviour of the distortion factor for an integral over all wave-number space. A similar cause gives rise to a logarithmic term in the expression for μ_2, but this is not the leading term when c is large.

The asymptotic dependence on c of the factors μ_1 and μ_2 can be shown

to have the same form for *any* kind of homogeneous turbulence, whether isotropic or not. We refer back to (3.9) and find that when $e_2 = e_3 = e_1^{-\frac{1}{2}} = c^{-\frac{1}{2}}$,

$$\Phi_{11}(\boldsymbol{\chi}) = \frac{\kappa^4}{\chi^4}\Phi'_{11}(\boldsymbol{\kappa}), \tag{4.7}$$

with no assumption about the turbulence. Likewise the two other equations of which (3.9) is typical, give

$$\Phi_{22}(\boldsymbol{\chi})+\Phi_{33}(\boldsymbol{\chi}) = c[\Phi'_{22}(\boldsymbol{\kappa})+\Phi'_{33}(\boldsymbol{\kappa})]-c^3\frac{\kappa_1^2(\kappa_2^2+\kappa_3^2)}{\chi^4}\Phi'_{11}(\boldsymbol{\kappa}). \tag{4.8}$$

The distortion factors for the longitudinal and lateral energies are now obtained by integration over all values of $\boldsymbol{\chi}$ (or $\boldsymbol{\kappa}$). Taking spherical polar coordinates κ, θ, ϕ, where $\theta = 0$ is the κ_1-axis, we have for the longitudinal energy,

$$\mu_1 = \frac{\int_0^\infty\int_0^\pi\int_0^{2\pi}\kappa^2\Phi'_{11}(\boldsymbol{\kappa})\dfrac{\sin\theta}{(c^{-2}\cos^2\theta+c\sin^2\theta)^2}\,d\phi d\theta d\kappa}{\int_0^\infty\int_0^\pi\int_0^{2\pi}\kappa^2\Phi'_{11}(\boldsymbol{\kappa})\sin\phi\;d\phi d\theta d\kappa}$$

$$= \frac{\int_0^\pi \Psi(\theta)\dfrac{\sin^3\theta}{(c^{-2}\cos^2\theta+c\sin^2\theta)^2}\,d\theta}{\int_0^\pi\Psi(\theta)\sin^3\theta\,d\theta}, \tag{4.9}$$

where

$$\Psi(\theta) = \frac{1}{\sin^2\theta}\int_0^\infty\int_0^{2\pi}\Phi'_{11}(\boldsymbol{\kappa})\kappa^2\,d\phi d\kappa, \qquad \int_0^\pi\Psi(\theta)\sin^3\theta\,d\theta = \overline{u_1'^2}.$$

Since $\Phi'_{11}(\boldsymbol{\kappa})$ is necessarily an even function of $\boldsymbol{\kappa}$ (by definition), and vanishes with $(\kappa_2^2+\kappa_3^2)^{\frac{1}{2}}$ (from continuity), $\Psi(\theta)$ will be finite at $\theta = 0$ (for isotropic turbulence $\Psi(\theta) = \frac{3}{4}\overline{u_1'^2}$, the dependence on θ being trivial in this case). Hence, when c is very large, and the value of the integral in the numerator of (4.9) is dominated by small ranges of θ near $\theta = 0$ and $\theta = \pi$, we shall have

$$\mu_1 \sim \frac{\Psi(0)}{\overline{u_1'^2}}\int_0^\pi\frac{\sin^3\theta}{(c^{-2}\cos^2\theta+c\sin^2\theta)^2}\,d\theta$$

$$\sim \frac{\Psi(0)}{\overline{u_1'^2}}c^{-2}\log c^3. \tag{4.10}$$

Similarly the expression for the distortion factor for the lateral energy is, from (4.8),

$$\mu_2 = c-\frac{c}{\overline{u_2'^2}+\overline{u_3'^2}}\int_0^\pi\Psi(\theta)\frac{c^2\sin^5\theta\cos^2\theta}{(c^{-2}\cos^2\theta+c\sin^2\theta)^2}\,d\theta, \tag{4.11}$$

which is well behaved when c is large; as $c \to \infty$,

$$\mu_2 \to c\left[1 - \frac{1}{\overline{u_2'^2} + \overline{u_3'^2}} \int_0^\pi \Psi(\theta) \sin\theta \cos^2\theta \, d\theta\right]. \tag{4.12}$$

Thus the asymptotic dependence of μ_1 and μ_2 on c has the same form for all kinds of turbulence, although the constants of proportionality vary. Somewhat surprisingly, the constants depend only on the energy spectrum of the component of velocity parallel to the axis of symmetry.

There do not appear to be any records of systematic measurements with which the results of this section can usefully be compared, although a number of incidental measurements demonstrating the damping effect of a contraction in a wind tunnel are known. D. C. MacPhail has made a set of measurements† of the mean squares of the velocity components u_1 and u_2 at a number of positions on the axis of a symmetrical contraction in a small wind tunnel, but this is not a case in which the conditions (2.3) and (2.7) for validity of the linear theory are satisfied and quantitative agreement with the theory is not good. Approximate values of l and $(\overline{\mathbf{u}^2})^{\frac{1}{2}}$ before contraction in MacPhail's experiments were 0·04 ft. and 0·25 ft. sec.$^{-1}$ respectively, so that the condition (2.7) requires

$$t - t' \ll 0{\cdot}02[(c-1)^2 + 2(c^{-\frac{1}{2}}-1)^2]^{\frac{1}{2}} \text{ sec.}$$

The linear theory will therefore be applicable, in this case, to positions whose axial distance d from the beginning of the contraction is such that

$$\frac{d}{l} \ll \frac{0{\cdot}02U}{l}[(c-1)^2 + 2(c^{-\frac{1}{2}}-1)^2]^{\frac{1}{2}} = 1{\cdot}7[(c-1)^2 + 2(c^{-\frac{1}{2}}-1)^2]^{\frac{1}{2}},$$

where U (= 3·5 ft. sec.$^{-1}$) is the wind-speed upstream of the contraction. The contraction ratio c is thus required to become large compared with unity in a distance of a few multiples of the scale of the turbulence, and this was not the case with the contraction used. The value of $(\overline{\mathbf{u}^2})^{\frac{1}{2}}/U$ is here rather large, which makes the condition (2.7) difficult to satisfy, but even so a contraction in a wind tunnel will have to be unusually rapid before the linear theory applies accurately.

5. Effect of an arbitrary distortion on the energy of the turbulence

As was remarked at the beginning of the preceding section, if a field of isotropic turbulence is subjected to a rapid distortion, the energy associated with each component of velocity in the resulting turbulence may be calculated for the general case in which no relation (other than the incompressibility condition $e_1 e_2 e_3 = 1$) exists between the extension ratios. The

† Carried out in Cambridge in 1943 and described in reference (6).

typical quantity to be calculated, as a function of any two of the variables e_1, e_2, and e_3, is

$$\mu_1 = \frac{\overline{u_1^2}}{\overline{u_1'^2}} = \frac{\int \Phi_{11}(\boldsymbol{\chi})\, d\boldsymbol{\chi}}{\int \Phi'_{11}(\boldsymbol{\varkappa})\, d\boldsymbol{\varkappa}},$$

where $\Phi'_{11}(\boldsymbol{\varkappa})$ has the isotropic form (3.12) and $\Phi_{11}(\boldsymbol{\chi})$ is given by (3.13). As a result of the initial isotropy of the turbulence and the homogeneity of the distortion, the integrations with respect to the wave-number magnitude κ cancel, and μ_1 is given by the integral

$$\mu_1 = \frac{3}{8\pi e_1^2 \kappa^2} \int\int \left\{ \kappa_1^2 \left(\frac{\kappa_2^2}{e_2^4} + \frac{\kappa_3^2}{e_3^4} \right) + \left(\frac{\kappa_2^2}{e_2^2} + \frac{\kappa_3^2}{e_3^2} \right)^2 \right\} \left(\frac{\kappa_1^2}{e_1^2} + \frac{\kappa_2^2}{e_2^2} + \frac{\kappa_3^2}{e_3^2} \right)^{-2} dS(\kappa) \qquad (5.1)$$

over the surface of a sphere of radius κ in $\boldsymbol{\varkappa}$-space.

After evaluating the line integral round the circle

$$\kappa = \text{const.}, \qquad \kappa_1 = \text{const.}$$

by changing the variable of integration to κ_3/κ_2, (5.1) becomes, after some algebra,

$$\mu_1 = \frac{3}{4} \left[\frac{2}{e_1^2} - \frac{1}{e_1^2 \kappa} \int_0^\kappa \frac{A_2 B_3 + A_3 B_2}{(B_2 B_3)^{\frac{1}{2}}}\, d\kappa_1 \right], \qquad (5.2)$$

where

$$\left. \begin{aligned} A_n &= \kappa_1^2 \left[\frac{1}{e_n^2} \left(\frac{2}{e_1^2} - \frac{1}{e_n^2} \right) \kappa^2 + \left(\frac{1}{e_1^2} - \frac{1}{e_n^2} \right) \kappa_1^2 \right] \\ B_n &= \frac{\kappa^2}{e_n^2} + \left(\frac{1}{e_1^2} - \frac{1}{e_n^2} \right) \kappa_1^2 \end{aligned} \right\}. \qquad (5.3)$$

Since (5.3) shows the integrand in (5.2) to be a rational function of κ_1 and

$$(B_2 B_3)^{\frac{1}{2}} = (\text{quartic in } \kappa_1)^{\frac{1}{2}},$$

it follows that μ_1 may be expressed in terms of elementary functions and standard elliptic integrals. Thus, with the formal transformation

$$t = \alpha \frac{\kappa_1}{\kappa}, \qquad (5.4)$$

and the notation $$\alpha^2 = 1 - \frac{e_3^2}{e_1^2}, \qquad k^2 = \frac{e_1^2 - e_2^2}{e_1^2 - e_3^2}, \qquad (5.5)$$

and leaving aside for the moment the question of the relative magnitudes of e_1, e_2, and e_3, and the consequent reality of α and k, (5.2) becomes

$$\mu_1 = \frac{3}{4} \left[\frac{1}{e_1^2} - \frac{e_1^{-2} - e_2^{-2} - e_3^{-2}}{(e_1^2 - e_2^2)(e_1^2 - e_3^2)^{\frac{1}{2}}} (X - Y) \right], \qquad (5.6)$$

where X and Y are the incomplete elliptic integrals

$$X = \int_0^\alpha \frac{dt}{(1-t^2)^{\frac{1}{2}}(1-k^2t^2)^{\frac{1}{2}}}, \qquad Y = \int_0^\alpha \left(\frac{1-k^2t^2}{1-t^2}\right)^{\frac{1}{2}} dt. \tag{5.7}$$

Moreover, since the formulae for μ_2 and μ_3 follow from a simple interchange of suffixes, and since numerical tables of X and Y are available, (5.6) represents the complete formal solution to the problem.

However, although the expressions for μ_1, μ_2, and μ_3 must obviously be real whatever the relative magnitudes of the extension ratios, it is important for practical purposes that the individual factors in these expressions should be real. This is particularly true of the elliptic integrals which are only tabulated under the conditions

$$0 < \alpha < 1, \qquad 0 < k^2 < 1. \tag{5.8}$$

For any prescribed set of extension ratios, only one of the expressions for the μ's, as given by (5.6), satisfies the condition (5.8) (or its equivalent after an interchange of suffixes). Hence alternative formulae must be found for two of the μ's.

Now, to fix ideas, we may choose

$$e_1 \geqslant e_2 \geqslant e_3 \tag{5.9}$$

without loss of generality. Thus, α and k are real quantities satisfying (5.8), and for analytical purposes it is convenient to regard these two quantities as the two parameters describing the distortion (in a symmetrical contraction $k = 1$ and α reduces to its meaning in (4.3)); (5.6) then represents the required form of the solution for the energy associated with the velocity component in the direction of greatest extension, and it remains to express μ_2 and μ_3 in terms of elliptic integrals with argument α and modulus k.

A cyclic interchange of suffixes in (5.4), (5.5), and (5.6) shows that μ_2 involves elliptic integrals X' and Y', corresponding to X and Y, with argument

$$\alpha' = \left(1 - \frac{e_1^2}{e_2^2}\right)^{\frac{1}{2}},$$

and modulus

$$k'^2 = \frac{e_2^2 - e_3^2}{e_2^2 - e_1^2}.$$

Thus

$$\alpha'^2 = -\frac{k^2\alpha^2}{1-k^2\alpha^2},$$

and

$$k'^2 = 1 - \frac{1}{k^2};$$

when arguments and moduli are related in this way, it may be shown that

$$X'-Y' = \frac{i}{k}\{(1-k^2)X-Y\}^{\frac{1}{2}}+ie_3^2(e_1^2-e_2^2)^{\frac{1}{2}},$$

where $i = \sqrt{(-1)}$. Hence the required result is, from (5.6),

$$\mu_2 = \frac{3}{4}\left[-\frac{1}{e_1^2}\frac{e_3^2}{e_2^2-e_3^2}+\frac{e_2^{-2}-e_3^{-2}-e_1^{-2}}{(e_1^2-e_2^2)(e_1^2-e_3^2)^{\frac{1}{2}}}\left\{X-\frac{e_1^2-e_3^2}{e_2^2-e_3^2}Y\right\}\right]. \tag{5.10}$$

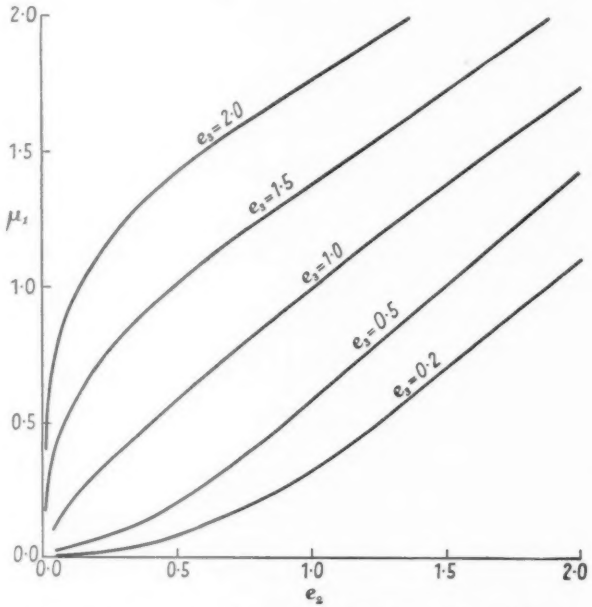

FIG. 2. Intensity changes in an arbitrary distortion.

A similar procedure yields the result

$$\mu_3 = \frac{3}{4}\left[\frac{1}{e_1^2}\frac{e_2^2}{e_2^2-e_3^2}+\frac{e_3^{-2}-e_1^{-2}-e_2^{-2}}{(e_2^2-e_3^2)(e_1^2-e_3^2)^{\frac{1}{2}}}Y\right]. \tag{5.11}$$

In Fig. 2 the information given by the solutions (5.6), (5.10), and (5.11) is shown graphically. In order to present all the information on one figure, μ_1 is considered as a function of e_2 and e_3 without restriction on the relative magnitudes of the extension ratios. In this way the above-mentioned three forms of the solution always refer to μ_1 for different ranges of values of e_2 and e_3. The figure shows the variation of μ_1 with e_2 for constant values of e_3.

Apart from being in a form suitable for computation, the results (5.6),

(5.10), and (5.11) provide a convenient expression for the calculation of the change in the total energy of the turbulence due to distortion. Thus,

$$\mu = \frac{\overline{u_1^2}+\overline{u_2^2}+\overline{u_3^2}}{\overline{u_1'^2}+\overline{u_2'^2}+\overline{u_3'^2}} = \tfrac{1}{3}(\mu_1+\mu_2+\mu_3)$$

$$= \frac{1}{2}\left[\frac{1}{e_1^2}+\frac{e_3^2}{(e_1^2-e_3^2)^{\frac{1}{2}}}X+(e_1^2-e_3^2)^{\frac{1}{2}}Y\right]. \tag{5.12}$$

This equation, together with (5.6), may be used to recover the results of the preceding section. For a symmetrical contraction $k^2 = 1$, so that

$$X = \tfrac{1}{2}\log\frac{1+\alpha}{1-\alpha}, \qquad Y = \alpha$$

and the relevant expressions for the μ's follow immediately.

We may also note the expressions for μ_1, μ_2, μ_3 for a distortion in which one of the extension ratios remain unity. This case, which corresponds to the flow of a turbulent stream through a passage whose cross-sectional area remains constant, has been studied experimentally by Townsend and the results are described in the accompanying paper in this journal (**7**). Putting

$$e_2 = 1, \qquad e_1 = e_3^{-1} = c > 1,$$

the results (5.6), (5.10), (5.11), and (5.12) become

$$\mu_1 = \frac{3}{4c^2}\left[1+\frac{c(c^4+c^2-1)}{(c^2-1)(c^4-1)^{\frac{1}{2}}}(x-y)\right], \tag{5.13}$$

$$\mu_2 = \frac{3}{4c^2(c^2-1)}\left[\frac{c(c^4-c^2+1)}{(c^4-1)^{\frac{1}{2}}}\{(c^2+1)y-x\}-1\right], \tag{5.14}$$

$$\mu_3 = \frac{3}{4(c^2-1)}\left[1+\frac{c(c^4-c^2-1)}{(c^4-1)^{\frac{1}{2}}}y\right], \tag{5.15}$$

and

$$\mu = \tfrac{1}{5}[c^{-2}+c^{-1}(c^4-1)^{-\frac{1}{2}}x+c^{-1}(c^4-1)^{\frac{1}{2}}y], \tag{5.16}$$

respectively, where

$$x = \int_0^{(1-c^{-4})^{\frac{1}{2}}} \{1-c^2t^2/(1+c^2)\}^{-\frac{1}{2}}(1-t^2)^{-\frac{1}{2}}\,dt, \tag{5.17}$$

$$y = \int_0^{(1-c^{-4})^{\frac{1}{2}}} \{1-c^2t^2/(1+c^2)\}^{\frac{1}{2}}(1-t^2)^{-\frac{1}{2}}\,dt. \tag{5.18}$$

Numerical values of μ_1, μ_2, and μ_3, as given by the above formulae, are shown in Fig. 3.

When c is large compared with 1,

$$\left.\begin{aligned}\mu_1 &= \tfrac{3}{4}c^{-1}(\log 4c-1)+O(c^{-3}\log c)\\ \mu_2 &= \tfrac{3}{4}c-\tfrac{3}{8}c^{-1}(\log 4c-\tfrac{3}{2})+O(c^{-3}\log c)\\ \mu_3 &= \tfrac{3}{4}c+\tfrac{3}{8}c^{-1}(\log 4c-\tfrac{1}{2})+O(c^{-3}\log c)\end{aligned}\right\}, \tag{5.19}$$

and when c is greater than about 2 the terms written out explicitly will usually provide a sufficiently good approximation to the solution. It may be noted that, when c is sufficiently large, the values of μ_2 and μ_3 become approximately equal to each other and to the value appropriate to a symmetrical contraction about the x_1-axis (cf. (4.6)). The explanation is that, when e_1 is much larger than e_2 and e_3, the vortex lines lie nearly

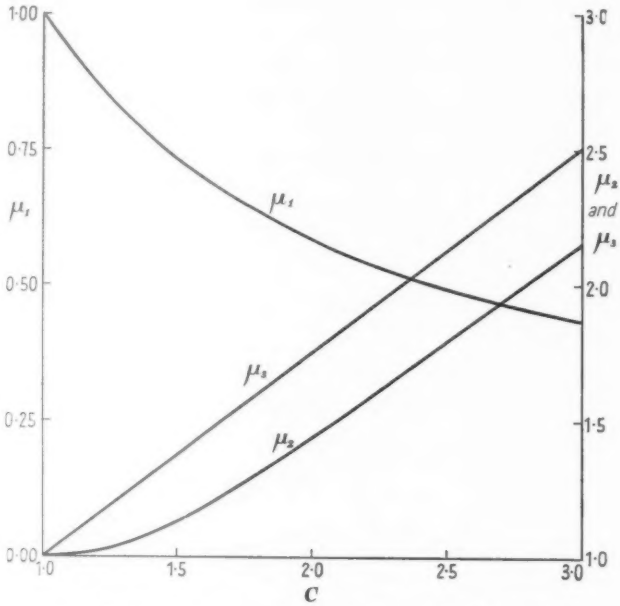

FIG. 3. Intensity changes in a constant-area distortion.

parallel to the x_1-axis and the dominant contribution to the change in the velocity components in the x_2- and x_3-directions arises from further stretching of these vortex lines.

Some approximate forms of the general solution are also of interest. Thus, for small distortions, as e_1, e_2, and e_3 all tend to unity subject to the condition (5.9), α tends to zero and k^2 tends to a real limit between 0 and 1. Hence, expressing (5.12) in terms of α and k only, we obtain

$$\mu = \tfrac{1}{2}(1-k^2\alpha^2)^{-\frac{1}{2}}(1-\alpha^2)^{-\frac{1}{2}}\left[(1-k^2\alpha^2)^{\frac{1}{2}}(1-\alpha^2)^{\frac{1}{2}}+\frac{1}{\alpha}\{(1-\alpha^2)(X-Y)+Y\}\right],$$

which, after a little algebra, may be expanded in the form

$$\mu = 1+\tfrac{2}{45}(1-k^2+k^4)\alpha^4+O(\alpha^6),$$

for small values of α. In terms of the extension ratios, the above expansion takes the more symmetrical form

$$\mu = 1+\tfrac{1}{45}[(e_1^2-e_2^2)^2+(e_2^2-e_3^2)^2+(e_3^2-e_1^2)^2]+\dots. \tag{5.20}$$

The change in total energy is thus of the second order in e_1-1, e_2-1, e_3-1, and to this order is always an increase.

On the other hand, expansions for large distortions will usually be of more practical value. In this case e_1 is large and e_3 is small, so that α tends to unity. The modulus k may tend to any limit, though this will also be unity unless e_2 is of the order of e_1. Considering the latter case first, the elliptic integrals X and Y tend to their complete forms

$$X_0(k) = \int_0^1 (1-k^2t^2)^{-\frac{1}{2}}(1-t^2)^{-\frac{1}{2}}\,dt, \qquad Y_0(k) = \int_0^1 (1-k^2t^2)^{\frac{1}{2}}(1-t^2)^{-\frac{1}{2}}\,dt, \tag{5.21}$$

and no particular simplification occurs in the expressions for the μ's. However, it may be noted from (5.6), (5.10), and (5.11) that

$$\mu_3 \to \mu_+ + \mu_2 \to \tfrac{3}{4}e_1 Y_0(k), \tag{5.22}$$

where, from (5.21), $\qquad 1 \leqslant Y_0(k) \leqslant \tfrac{1}{2}\pi,$

so that the increase in total energy is very largely determined by e_1. As $e_2 \to e_1$ (i.e. as the distortion becomes an expansion approximately symmetrical about the x_3-axis), (5.22) becomes

$$\mu_1 \to \mu_2 \to \tfrac{1}{2}\mu_3 \to \frac{3\pi}{16}e_1. \tag{5.23}$$

When $e_1 \gg e_2$, k tends to unity and, on putting $\alpha^2 = 1-\epsilon^2$, $k^2 = 1-k'^2$, where ϵ and k' are small, we find, after some algebra, that

$$X \to \log\{4/(\epsilon+(k'^2+\epsilon^2)^{\frac{1}{2}})\} \to \log\{4e_1/(e_2+e_3)\},$$
$$Y \to 1.$$

Thus, the relevant expressions for the μ's are

$$\left.\begin{aligned} \mu_1 &\to \tfrac{3}{4}\{(e_2^2+e_3^2)/e_1\}\{\log(4e_1/(e_2+e_3))-1\} \\ \mu_2 \to \mu_3 &\to \tfrac{3}{4}e_1 \end{aligned}\right\}. \tag{5.24}$$

As a check on the algebra, we may note that (5.24) reduces to (5.19) when $e_2 = 1$, and to (4.6) when $e_2 = e_3$. The results (5.22) and (5.24) show that the total energy always increases linearly with e_1 when e_1 is large and that the constant of proportionality can only vary between quite narrow limits. Moreover, half the total energy always resides in the x_3-component of velocity, and unless e_2 is of the same order of largeness as e_1 the other half resides in the x_2-component of velocity. Thus the distribution of energy usually tends to become symmetrical about the x_1-axis, and the symmetrical

contraction is more typical of the general case than might at first be supposed.

Analogous asymptotic results for the effect of large distortions on general homogeneous turbulence could probably be deduced in the way that (4.10) and (4.12) were obtained for a large symmetrical contraction.

While this paper was being prepared, one of us (I. P.) was the holder of a Senior Research Award from the Department of Scientific and Industrial Research.

REFERENCES

1. L. PRANDTL, *Handbuch der Experimentalphysik* (Leipzig, 1932), **4**, Part 2, p. 73.
2. G. I. TAYLOR, *Zeit. f. angew. Math. u. Mech.* **15** (1935), 91.
3. H. S. RIBNER and M. TUCKER, *Spectrum of Turbulence in a Contracting Stream*, N.A.C.A. Tech. Note 2606, 1952.
4. G. K. BATCHELOR, *The Theory of Homogeneous Turbulence* (Cambridge, 1953).
5. H. LAMB, *Hydrodynamics* (Cambridge, 1932), chap. 7.
6. D. C. MACPHAIL, *Turbulence Changes in Contracting and Distorting Passages*, R.A.E. Report, No. Aero 1928, 1944.
7. A. A. TOWNSEND, *Quart. J. Mech. and Applied Math.* **7** (1954), 104 (below).

THE UNIFORM DISTORTION OF HOMOGENEOUS TURBULENCE

By A. A. TOWNSEND (*Emmanuel College, Cambridge*)

[Received 29 July 1952]

SUMMARY

By passing the turbulence found downstream of a uniform grid through a constant-area distorting duct, the effect on isotropic turbulence of a suddenly imposed uniform mean rate of strain has been studied. A complete theory exists for the limiting case of an infinitely rapid strain, and the relevance of this theory to the experimental conditions is discussed. It is concluded that the rate of strain is too small to justify application of the theory, but that, for small strains, the structure of the energy-containing eddies is similar to that produced by an instantaneous strain. For larger total strains the turbulence develops an equilibrium structure in which the intensities are still changing, and the similarity of this structure to the structure of ordinary shear flows is considered. Finally it is found that, during the distortion, the dissipating eddies are not in a state of local isotropy, although the return to isotropy is rapid when the distortion ceases. This is interpreted as meaning that the direct influence of the mean rate of strain is appreciable at these Reynolds numbers, but that even highly anisotropic turbulence dissipates its energy through nearly isotropic eddies.

Introduction

THE persistence of the hypothesis that eddy transport of momentum may be described conveniently by assigning to the flow a coefficient of eddy viscosity is to be attributed to the general similarity of the irregular molecular motion which is responsible for the phenomenon of viscosity in gases and the irregular velocity pattern characteristic of a turbulent flow. In general, such a coefficient, defined as the quotient of the turbulent shear stress divided by the rate of shear, varies with position in any particular flow and depends on the Reynolds number of the flow, and clearly lacks the uniqueness of the coefficient of molecular viscosity. The principal reason for this behaviour is that the local turbulent velocities depend on transfer of energy from the mean flow acting through the turbulent stresses, and naturally this energy transfer varies greatly. The mixing length theories attempt to predict the variation by assuming that the turbulent intensity, and so the eddy viscosity, are determined by local conditions only, but recent work (Townsend (**1**)) has shown that the turbulent intensity at any point is strongly influenced by diffusion of energy from other parts of the flow, and this particular hypothesis seems to be without foundation. The relevance of the eddy viscosity hypothesis as distinct from methods for its determination has been stressed by the observation of Reichardt (**2**)

that the mean flow profiles of free turbulent flows, i.e. wakes, jets, and free mixing zones, may be described by assigning to any section a constant coefficient of eddy viscosity, and the author (**3**) has shown that, for a cylinder wake, the remaining discrepancies are completely removed by taking account of the observed intermittency in the outer parts of the wake. The known presence of large-scale mixing motions in these flows suggests that the fully turbulent fluid is almost homogeneous in intensity and capable of developing a shear stress proportional to its instantaneous rate of shear, the constant of proportionality, i.e. the eddy viscosity, then being a physically significant property of the turbulent fluid. Such rapidity of adjustment of turbulent shear stresses to changing conditions is difficult to reconcile with the growing number of observations of turbulent motion which tend to show turbulence as a relatively slow-moving and stable motion, at least in so far as the energy-containing eddies are concerned.

It is difficult to resolve these doubts by measurements in ordinary shear flows, and so an investigation of an extremely simple shear flow was undertaken. This flow is the uniform distortion of initially isotropic turbulence, carried out by changing the shape but not the cross-sectional area of the wind-tunnel duct, and is very nearly a homogeneous flow without the complicating factors present in ordinary flows. Somewhat similar experiments have been reported by MacPhail (**4**), but his results are difficult to interpret, and a repetition using more modern equipment and better experimental conditions appeared necessary.

Notation

The notation used is conventional for the description of homogeneous turbulent flows, using a Cartesian coordinate system and the following symbols:

U, V, W	components along the axes Ox, Oy, Oz of the mean velocity at a point,
u, v, w	components of the instantaneous turbulent velocity fluctuation at a point,
ξ, η, ζ	components of the instantaneous vorticity fluctuation,
P	the mean pressure,
p	the instantaneous pressure fluctuation,
ρ	the fluid density,
ν	the kinematic viscosity,
α, β, γ	strain ratios along the principal axes of strain,
l, m, n	components of the vector wave-number $\mathbf{k}$,

$$k^2 = l^2 + m^2 + n^2,$$

$F(\mathbf{k})$, $G(\mathbf{k})$, $H(\mathbf{k})$ the turbulent intensity spectrum functions for u, v, w respectively,

$\psi_u(l)$ the one-dimensional spectrum function for u with respect to x,

ϵ the rate of conversion of turbulent energy into heat,

$\lambda_e^2 = \dfrac{15\nu\overline{u^2}}{\epsilon}$,

$\lambda_u^2 = \overline{u^2}\Big/\overline{\left(\dfrac{\partial u}{\partial x}\right)^2}$,

L_u the longitudinal integral scale for u, defined by

$$\overline{u^2}L_u = \frac{2}{\pi}\int_{-\infty}^{\infty}\int F(0, m, n)\, dmdn,$$

L_v, L_w the corresponding scales for v and w.

For the experimental flow the origin is taken to be in the plane of the turbulence-producing grid and on the axis of the duct. Ox lies along this axis, and Oy is parallel to the direction of compression of the duct section.

Effect of an instantaneous distortion

It is interesting to inspect the consequences of assuming that the distortion of a homogeneous turbulent field is done so rapidly that movement of the fluid particles during the distortion is entirely due to the distortion and not at all to the turbulent motion. When this is true, viscous and inertial transfer terms in the equations of motion are negligible compared with the pressure terms, and the problem can be solved. If the distortion is a finite strain of principal strain ratios α, β, γ along the axes of reference ($\alpha\beta\gamma = 1$ if the fluid is incompressible), a particle originally at the point x_0, y_0, z_0 moves to $\alpha x_0, \beta y_0, \gamma z_0$, and the vorticity at the particle changes from ξ_0, η_0, ζ_0 to $\alpha\xi_0, \beta\eta_0, \gamma\zeta_0$. Given the original vorticity distribution, the final vorticity distribution can be written down, and, from this, the final velocity distribution. Taylor (**5**) did this for a single periodic motion in three dimensions, and applied his results to the change in intensity of turbulence passing through the contraction of a wind-tunnel. Batchelor and Proudman (**6**) have extended this work to give a complete solution for the instantaneous distortion of initially isotropic turbulence. For a uniform plane shear, defined by

$$\alpha = 1, \qquad \beta = \beta, \qquad \gamma = \beta^{-1},$$

the spectral density functions for u, v, w are given by

$$\left.\begin{aligned} k^4F &= k_0^4\phi(k_0)\left[m_0^2+n_0^2+(\beta^{-4}-1)\frac{m_0^2(l_0^2+m_0^2)}{k_0^2}+(\beta^4-1)\frac{n_0^2(l_0^2+n_0^2)}{k_0^2}\right] \\ k^4G &= k_0^4\phi(k_0)\left[n_0^2+l_0^2+(\beta^2-1)\frac{n_0^2(m_0^2+n_0^2)}{k_0^2}+(\beta^{-2}-1)\frac{l_0^2(m_0^2+l_0^2)}{k_0^2}\right] \\ k^4H &= k_0^4\phi(k_0)\left[l_0^2+m_0^2+(\beta^2-1)\frac{l_0^2(n_0^2+l_0^2)}{k_0^2}+(\beta^{-2}-1)\frac{m_0^2(n_0^2+m_0^2)}{k_0^2}\right] \end{aligned}\right\} \quad (1)$$

where $$k^2 = k_0^2+(\beta^{-2}-1)m_0^2+(\beta^2-1)n_0^2.$$

As a consequence of isotropy, the initial spectrum functions are

$$F_0 = (m_0^2+n_0^2)\phi(k_0),$$
$$G_0 = (n_0^2+l_0^2)\phi(k_0),$$
$$H_0 = (l_0^2+m_0^2)\phi(k_0).$$

It is clear from these equations that the turbulent intensities, defined by

$$\overline{u^2} = \int\int\int_{-\infty}^{\infty} F(l,m,n)\,dldmdn, \text{ etc.},$$

depend only on the original intensity and the strain ratio, β. For this particular type of strain the integration is not simple, but the results for small total strains are likely to be the most interesting for considering a uniform rate of strain. Provided $\beta^2+\beta^{-2}-2$ is small, the intensities are given by

$$\overline{u^2} = \overline{u_0^2}[1+\tfrac{8}{35}(\beta^2+\beta^{-2}-2)], \quad (2)$$

$$\overline{v^2}+\overline{w^2} = (\overline{v_0^2}+\overline{w_0^2})[1+\tfrac{3}{35}(\beta^2+\beta^{-2}-2)], \quad (3)$$

$$\overline{v^2}-\overline{w^2} = -\tfrac{4}{5}(\overline{v_0^2}+\overline{w_0^2})\frac{\beta^2-1}{\beta^2+1}[1+\tfrac{33}{112}(\beta^2+\beta^{-2}-2)]. \quad (4)$$

In this flow the directions of principal strain are the coordinate axes, unlike ordinary shear flows for which they are at 45° to the conventional axes, and the shear correlation coefficient of ordinary shear flows is in the present notation replaced by

$$K_0 = \frac{\overline{v^2}-\overline{w^2}}{\overline{v^2}+\overline{w^2}} = -\frac{4}{5}\frac{\beta^2-1}{\beta^2+1} \quad (5)$$

to the same degree of approximation.

The integral scales for the three components with respect to the Ox direction are determined by the intensities at zero wave-number of the appropriate one-dimensional spectrum functions, which turn out to be unchanged by the distortion. For any uniform distortion with no strain in the Ox direction, these scales are given by

$$\tfrac{1}{2}\pi\psi_u(0) = \overline{u^2}L_u = 2\overline{v^2}L_v = 2\overline{w^2}L_w = \overline{u_0^2}\,L_{u_0}. \quad (6)$$

Since the intensities undergo considerable changes, the one-dimensional spectra must change in shape, and it is found that, for not too small strains, $\psi_u(l)$ develops a maximum at a non-zero wave-number.

Effects of a finite rate of distortion

The experimental flow differs from that considered above in several respects. The most important difference is that the distortion of any particular fluid volume is carried out at a finite rate, and processes neglected in the instantaneous theory are now of considerable importance. Further, the flow is not completely homogeneous since intensity gradients exist in the direction of flow, and the initiation of even a finite rate of strain cannot be done instantaneously. Some information may be gained from the equations of motion.

The mean velocity distribution not too near the entrance or exit of a distorting duct whose linear dimensions in the Ox and Oy directions are given by

$$A = A_0 e^{-ax},$$

$$B = B_0 e^{ax}$$

is

$$\left.\begin{aligned} U &= \text{constant} \\ V &= -aUy \\ W &= aUz \end{aligned}\right\}. \tag{7}$$

The equations of mean flow are, in full,

$$\left.\begin{aligned} \frac{\partial \overline{u^2}}{\partial x}+\frac{\partial \overline{uv}}{\partial y}+\frac{\partial \overline{uw}}{\partial z} &= -\frac{1}{\rho}\frac{\partial P}{\partial x} \\ a^2U^2y+\frac{\partial \overline{uv}}{\partial x}+\frac{\partial \overline{v^2}}{\partial y}+\frac{\partial \overline{vw}}{\partial z} &= -\frac{1}{\rho}\frac{\partial P}{\partial y} \\ a^2U^2z+\frac{\partial \overline{uw}}{\partial x}+\frac{\partial \overline{vw}}{\partial y}+\frac{\partial \overline{w^2}}{\partial z} &= -\frac{1}{\rho}\frac{\partial P}{\partial z} \end{aligned}\right\}. \tag{8}$$

Along the Ox-axis, symmetry reduces these to

$$\left.\begin{aligned} \frac{\partial \overline{u^2}}{\partial x}+\frac{\partial \overline{uv}}{\partial y}+\frac{\partial \overline{uw}}{\partial z} &= -\frac{1}{\rho}\frac{\partial P}{\partial x} \\ 0 &= -\frac{1}{\rho}\frac{\partial P}{\partial y} \\ 0 &= -\frac{1}{\rho}\frac{\partial P}{\partial z} \end{aligned}\right\}. \tag{9}$$

Similarly, the equations for the turbulent intensities along the axis are

$$\left.\begin{aligned}
\tfrac{1}{2}U\frac{\partial\overline{u^2}}{\partial x}+\frac{1}{2}\frac{\partial\overline{u^3}}{\partial x}+\frac{1}{2}\frac{\partial\overline{u^2v}}{\partial y}+\frac{1}{2}\frac{\partial\overline{u^2w}}{\partial z} &= -\frac{1}{\rho}\overline{u\frac{\partial p}{\partial x}}+\nu\overline{u\nabla^2u}\\
\tfrac{1}{2}U\frac{\partial\overline{v^2}}{\partial x}-aU\overline{v^2}+\frac{1}{2}\frac{\partial\overline{uv^2}}{\partial x}+\frac{1}{2}\frac{\partial\overline{v^3}}{\partial y}+\frac{1}{2}\frac{\partial\overline{v^2w}}{\partial z} &= -\frac{1}{\rho}\overline{v\frac{\partial p}{\partial y}}+\nu\overline{v\nabla^2v}\\
\tfrac{1}{2}U\frac{\partial\overline{w^2}}{\partial x}+aU\overline{w^2}+\frac{1}{2}\frac{\partial\overline{uw^2}}{\partial x}+\frac{1}{2}\frac{\partial\overline{vw^2}}{\partial y}+\frac{1}{2}\frac{\partial\overline{w^3}}{\partial z} &= -\frac{1}{\rho}\overline{w\frac{\partial p}{\partial z}}+\nu\overline{w\nabla^2w}
\end{aligned}\right\}. \quad (10)$$

It is possible to neglect the diffusion terms involving gradients in the Ox direction since the turbulence level is low. The reasoning is that $\partial\overline{uv^2}/\partial x$ is of order $\partial(\overline{u^2})^{\frac{3}{2}}/\partial x$, which is small compared with $U(\partial\overline{u^2}/\partial x)$. Similar reasoning shows that, provided the intensities remain reasonably constant over the cross-section of the duct, which is actually the case, diffusion terms involving gradients in the Oy and Oz directions are also negligible. The equations now become

$$\left.\begin{aligned}
\tfrac{1}{2}U\frac{\partial\overline{u^2}}{\partial x} &= -\frac{1}{\rho}\overline{u\frac{\partial p}{\partial x}}+\nu\overline{u\nabla^2u}\\
\tfrac{1}{2}U\frac{\partial\overline{v^2}}{\partial x}-aU\overline{v^2} &= -\frac{1}{\rho}\overline{v\frac{\partial p}{\partial y}}+\nu\overline{v\nabla^2v}\\
\tfrac{1}{2}U\frac{\partial\overline{w^2}}{\partial x}+aU\overline{w^2} &= -\frac{1}{\rho}\overline{w\frac{\partial p}{\partial z}}+\nu\overline{w\nabla^2w}
\end{aligned}\right\}. \quad (11)$$

and the equation for the total intensity, $\overline{q^2}=\overline{u^2}+\overline{v^2}+\overline{w^2}$, is

$$\tfrac{1}{2}U\frac{\partial\overline{q^2}}{\partial x}-aU(\overline{v^2}-\overline{w^2})=\nu[\overline{u\nabla^2u}+\overline{v\nabla^2v}+\overline{w\nabla^2w}], \quad (12)$$

since the sum of the pressure terms may be shown to be small by reasoning similar to that used above in connexion with the diffusion terms.

These equations confirm that the experimental flow is nearly homogeneous and that it reproduces the theoretical box-type distortion at a finite uniform rate well enough for ordinary purposes.

Finally, the equation for $\overline{v^2}-\overline{w^2}$, which is a measure of the turbulent shear stress, is

$$\tfrac{1}{2}U\frac{\partial}{\partial x}(\overline{v^2}-\overline{w^2})-aU(\overline{v^2}+\overline{w^2})=-\frac{1}{\rho}\left(\overline{v\frac{\partial p}{\partial y}}-\overline{w\frac{\partial p}{\partial z}}\right)+\nu(\overline{v\nabla^2v}-\overline{w\nabla^2w}). \quad (13)$$

To compare this with the results obtained by assuming an instantaneous distortion, the total strain ratio β is equated to $e^{-a(x-x_1)}$, where $x=x_1$ is the section at which the distortion begins, and then equation (4) becomes, for small values of $a(x-x_1)$,

$$\overline{v^2}-\overline{w^2}=\tfrac{4}{5}a(x-x_1)(\overline{v^2}+\overline{w^2})$$

or
$$\frac{1}{2}\frac{\partial}{\partial x}(\overline{v^2}-\overline{w^2}) = \tfrac{2}{5}a(\overline{v^2}+\overline{w^2}). \tag{14}$$

Comparing with equation (13), and remembering that, for instantaneous distortion, viscosity effects are negligible, we have

$$\frac{1}{\rho}\left(v\overline{\frac{\partial p}{\partial y}}-w\overline{\frac{\partial p}{\partial z}}\right) = \tfrac{3}{5}aU(\overline{v^2}+\overline{w^2}) \tag{15}$$

valid for small values of $a(x-x_1)$ and high rates of strain. This shows that redistribution of energy among the velocity components is an integral part of the distorting process, and not a secondary effect, as is sometimes implied.

Experimental arrangements

A duct with the velocity distribution of equations (7) is approximately one of constant area and rectangular section, such that the horizontal width

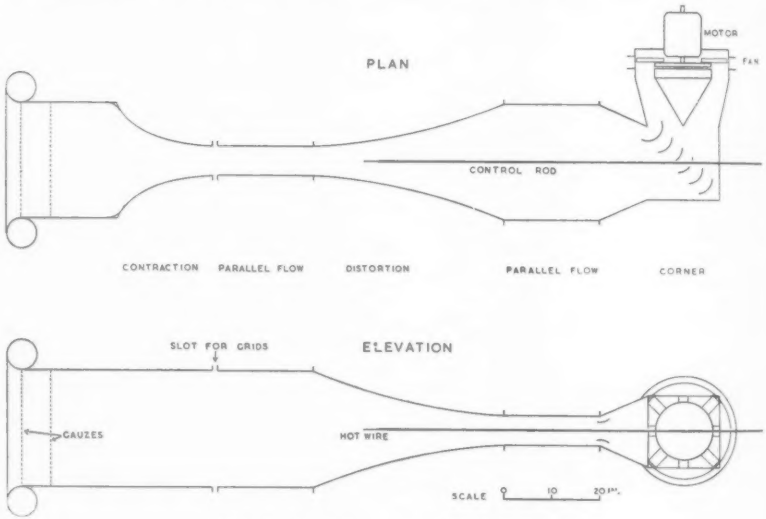

FIG. 1. Arrangement of wind-tunnel.

varies as $e^{a(x-x_1)}$, while the vertical depth varies as $e^{-a(x-x_1)}$. This would be exact but for the growth of boundary layers on the walls, so, to prevent an acceleration of the flow through the duct, the sectional area increases from 6 in. × 24 in. at the entrance to 24·25 in. × 6·25 in. at the exit. The distorting duct measures 40 in. along the axis and is constructed of tin-plate with perspex sides. It is installed in an open return wind-tunnel, arranged as shown in Fig. 1. The air enters through a bell-mouth and passes through two 16-mesh wire gauzes and a short settling length before the 4:1 ratio.

two-dimensional contraction. The working section consists of a 20 in. long parallel flow section, the distorting duct, and a final 20 in. long parallel flow recovery section. The air-stream is then turned through a right angle by corner vanes and exhausted to the atmosphere by an eight-bladed, axial flow fan driven by an electric motor of $\frac{1}{8}$ h.p.

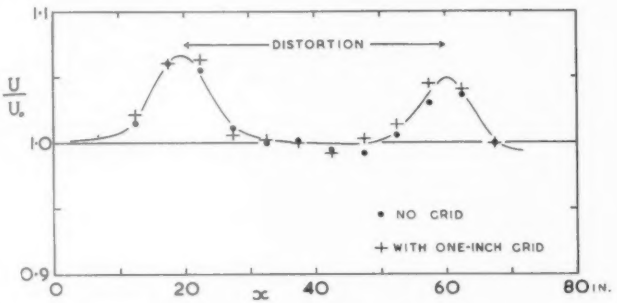

FIG. 2. Variations of mean speed along axis.

The mean velocity distribution along the axis is not completely uniform, owing to the sudden transitions between the parallel and distorting sections of the tunnel. Fig. 2 shows that, except in these regions, the axial velocity is reasonably constant. No appreciable change occurs when a turbulence-producing grid is inserted at the beginning of the working section.

Measurements of the turbulence were made using ordinary hot-wire anemometer equipment and techniques. The hot wires were supported at the end of a long rod running along the tunnel axis, which could be rotated through a right angle to compare the intensities of the two transverse components of the turbulent velocity or slid along to measure the variations of intensity along the axis.

In the absence of a grid the flow is steady, and the turbulent intensities at the entrance to the distorting section are

$$(\overline{u^2})^{\frac{1}{2}}/U = 0{\cdot}20\times10^{-2}, \qquad (\overline{v^2})^{\frac{1}{2}}/U = 0{\cdot}53\times10^{-2}, \qquad (\overline{w^2})^{\frac{1}{2}}/U = 0{\cdot}52\times10^{-2}.$$

The turbulence is composed of extremely intermittent bursts, probably originating in the boundary layers on the walls, which are only 3 in. from the centre line. These turbulence levels increase with distance from the entrance, and, at the extreme limit of observation, 70·5 in. from the entrance, they are

$$(\overline{u^2})^{\frac{1}{2}}/U = 0{\cdot}37\times10^{-2}, \qquad (\overline{v^2})^{\frac{1}{2}}/U = 0{\cdot}69\times10^{-2}, \qquad (\overline{w^2})^{\frac{1}{2}}/U = 0{\cdot}71\times10^{-2}.$$

The increase is again probably due to growth in thickness of the boundary layers on the walls. These levels are rather high, but no attempt has been

made to correct the final readings for background turbulence. There are two good reasons for this. In the first place, it is known that the insertion of a grid modifies the wall-boundary layers, and, in the second place, the theoretical analysis is equally applicable to the total flow.

The turbulence-producing grids are of the ordinary biplane type with a mesh diameter ratio of 5·33. Two were used, one of periodic spacing 0·5 in. and the other 1 in. At the mean air-speed used in the experiments (690 cm. sec.$^{-1}$), the corresponding mesh Reynolds numbers were 5850 and 11700.

Experimental results

The variations in intensity of the components of the turbulent velocity are shown in Figs. 3 and 4 for both of the grids, all measurements being

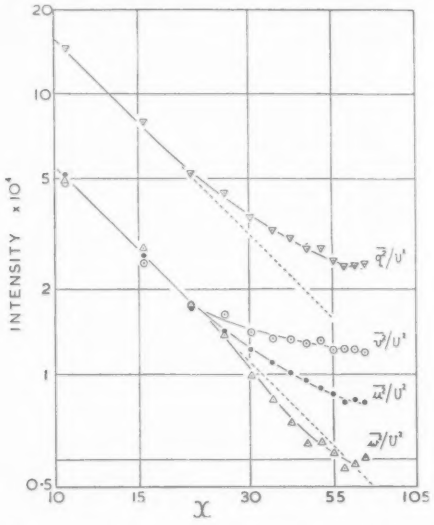

FIG. 3. Variations of intensity (half-inch grid).

made on the axis of the tunnel. For comparison, the intensities to be expected if the distorted duct were replaced by a parallel flow section are shown, calculated on the basis of the linear law of energy decay (Batchelor and Townsend (**7**)). It is clear that

(*a*) the total turbulent intensity decreases more slowly than it would in the absence of the distortion,

(*b*) while $\overline{v^2}$ decreases less rapidly than in parallel flow, $\overline{w^2}$ decreases more rapidly,

(*c*) the rate of decrease of $\overline{u^2}$ is intermediate between that of $\overline{v^2}$ and $\overline{w^2}$, and is less than it would be in the absence of a distortion.

The relations between the intensities are conveniently studied by the variation of the non-dimensional quantities

$$K_1 = \frac{\overline{v^2}-\overline{w^2}}{\overline{v^2}+\overline{w^2}} \quad \text{and} \quad K_2 = (3\overline{u^2}/\overline{q^2})-1.$$

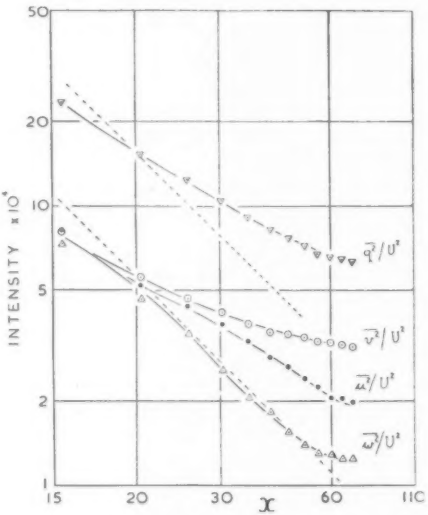

FIG. 4. Variations of intensity (one-inch grid).

The variation of these quantities is shown in Fig. 5, and it appears that K_2 is not significantly different from zero. On the other hand, K_1 increases throughout the distortion and appears to attain an asymptotic value near 0·42.

The rate of energy dissipation by viscosity depends on the intensities of the components of the rate of strain tensor, and three of these were measured, viz.

$$\overline{\left(\frac{\partial u}{\partial x}\right)^2}, \qquad \overline{\left(\frac{\partial v}{\partial x}\right)^2}, \qquad \overline{\left(\frac{\partial w}{\partial x}\right)^2}.$$

In Fig. 6 the variation of $\lambda_u^2 = \overline{u^2}/\overline{(\partial u/\partial x)^2}$ along the duct is shown. As indicated in the figure, in parallel flow $d\lambda_u^2/dx = 10\nu/U$, a rate of increase which is significantly greater than that observed here.

If the dissipating eddies are in a condition of local isotropy,

$$\overline{\left(\frac{\partial u}{\partial x}\right)^2} = \frac{1}{2}\overline{\left(\frac{\partial v}{\partial x}\right)^2} = \frac{1}{2}\overline{\left(\frac{\partial w}{\partial x}\right)^2}.$$

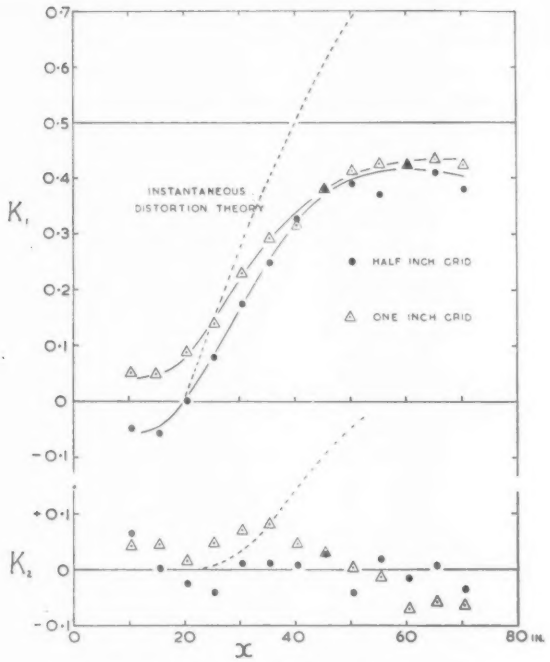

FIG. 5. Anisotropy of velocity components.

Non-dimensional parameters similar to those used for the turbulent intensities, i.e. which are zero in isotropic turbulence,

$$K_1' = \frac{\overline{\left(\frac{\partial v}{\partial x}\right)^2} - \overline{\left(\frac{\partial w}{\partial x}\right)^2}}{\overline{\left(\frac{\partial v}{\partial x}\right)^2} + \overline{\left(\frac{\partial w}{\partial x}\right)^2}},$$

$$K_2' = \frac{\overline{\left(\frac{\partial v}{\partial x}\right)^2} + \overline{\left(\frac{\partial w}{\partial x}\right)^2}}{4\overline{\left(\frac{\partial u}{\partial x}\right)^2}} - 1,$$

are given in Figs. 7 and 8. It is obvious that these eddies are not in a condition of local isotropy.

Finally, a series of measurements of spectra of the longitudinal velocity component were made at various positions in the distortion. It is noticeable that the shape of the spectrum changes considerably, and that the longitudinal scale (measured as the spectral intensity at small wave numbers

divided by the intensity) at first increases as is usual in developing isotropic turbulence but later decreases.

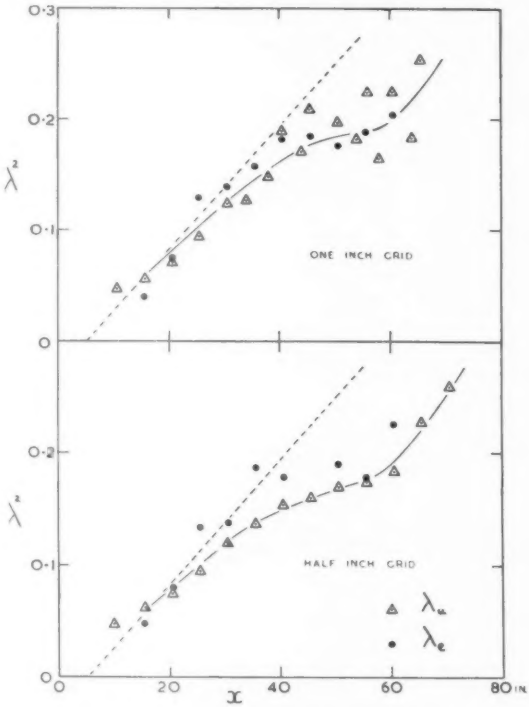

FIG. 6. Turbulent dissipation parameters.

These observations may be considered in their relation to several problems. The first problem is the most direct, the relevance of the instantaneous distortion theory to the initial behaviour of isotropic turbulence suddenly subjected to a uniform mean rate of strain, and the nature of the departures from this theory. The second is the relation of the behaviour of this flow to the behaviour of more complicated flows of greater practical importance. Finally, since laboratory studies of turbulence have been limited to flow Reynolds numbers insufficiently high for the satisfaction of the conditions for local similarity, it is interesting to inquire whether the observed departures from local isotropy of the dissipating eddies invalidate the useful approximation for the local energy dissipation rate

$$\epsilon = 15\nu\overline{\left(\frac{\partial u}{\partial x}\right)^2}.$$

Work on free turbulence indicates that the total energy dissipation can be obtained by integrating $15\nu\overline{(\partial u/\partial x)^2}$ over the flow, but no complete evidence is obtainable on its local validity.

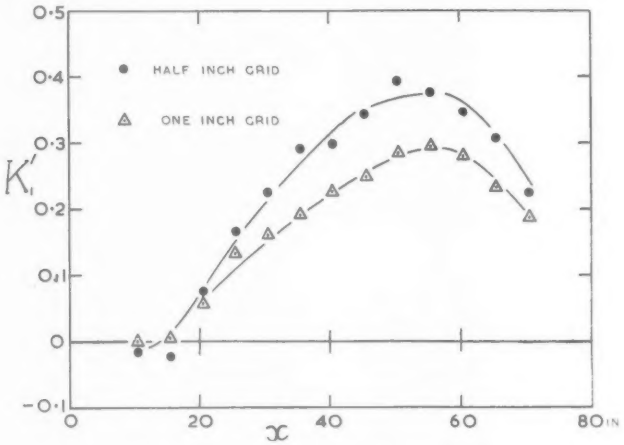

FIG. 7. Anisotropy of velocity gradients.

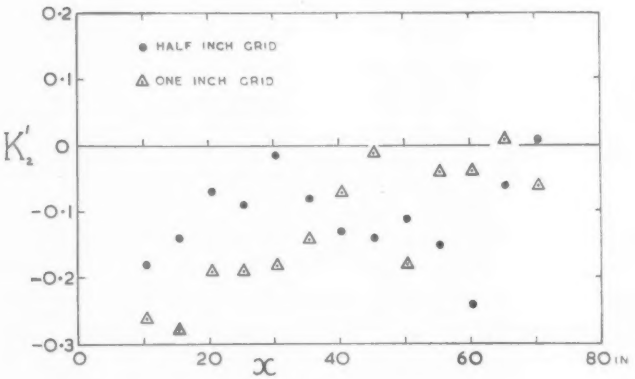

FIG. 8. Anisotropy of velocity gradients.

Discussion: instantaneous distortion theory

From measurements of the intensities alone it might be concluded that the relevance of the instantaneous theory to the actual behaviour of the experimental flow is not great, even in the early stages of the distortion. This conclusion would be based on the continued decrease in intensity of all three velocity components, in contrast to the predicted increase of $\overline{u^2}$

and $\overline{v^2}$, but it is easily shown that allowances for the direct effect of turbulent energy dissipation are sufficient to reconcile very nearly the initial behaviour with theory. If a uniform rate of strain is suddenly imposed on

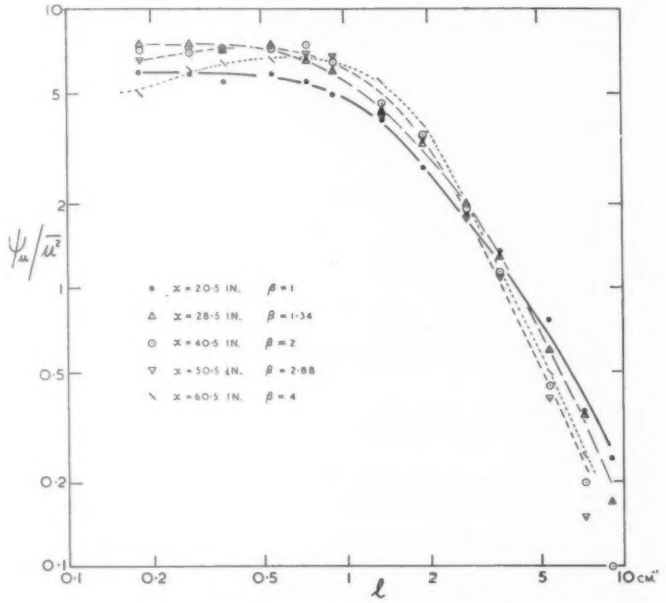

FIG. 9. Longitudinal spectra (half-inch grid).

a decaying field of isotropic turbulence, then, to the first order, the changes in the turbulence due to the uniform distortion and the normal processes of turbulent energy transfer and dissipation combine linearly. The reason is that changes in rate of any of these processes only arise from changes in the turbulent structure, which to the first order are small. Provided the change in the turbulence is small, for $t > t_1$,

$$\left.\begin{aligned} \overline{u^2} &= \overline{u_0^2} + \frac{d\overline{u^2}}{dt}(t-t_1) \\ \overline{v^2}+\overline{w^2} &= \overline{v_0^2}+\overline{w_0^2} + \frac{d(\overline{v^2}+\overline{w^2})}{dt}(t-t_1) \\ \overline{v^2}-\overline{w^2} &= \tfrac{4}{5}aU(\overline{v_0^2}+\overline{w_0^2})(t-t_1) \end{aligned}\right\} \qquad (16)$$

where the derivatives are taken just before the initiation of the distortion. The first two relations express the fact that $\overline{u^2}$ and $\overline{v^2}+\overline{w^2}$ show no sudden

change in rate of decay, which is confirmed in Figs. 3 and 4. The last relation may be written

$$K_1 = \frac{\overline{v^2}-\overline{w^2}}{\overline{v^2}+\overline{w^2}} = \tfrac{4}{5}a(x-x_1) \tag{17}$$

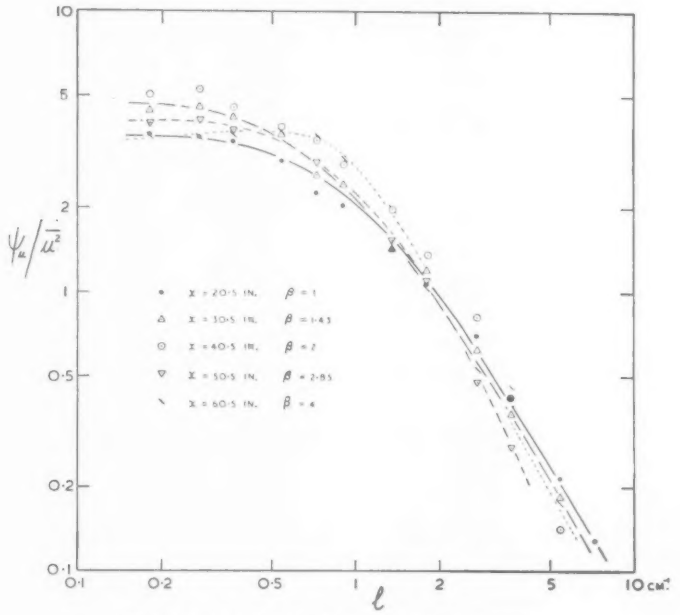

FIG. 10. Longitudinal spectra (one-inch grid).

while K_1 is small. In Fig. 5 the variation of K_1 predicted by the instantaneous distortion theory is shown, computed from the results given by Batchelor and Proudman (**6**). The initial slope of this curve is given by equation (17), and this slope is seen to be perhaps 30–40 per cent. greater than the maximum slope of the experimental curves. This discrepancy is probably due to the impossibility of commencing the distortion instantaneously, and the comparatively large values of K_1 which consequently are attained before the rate of strain becomes steady and the total strain known.

Further confirmation of the relevance of the instantaneous distortion theory is found in the shapes of spectra of the down-stream component. A computation using equations (1) and a defining function

$$\phi(k) = \frac{2\overline{u_0^2}p}{\pi^2(k^2+p^2)^3}$$

(which corresponds to an exponential correlation function) shows that, for values of the total strain ratio greater than 1·93, the one-dimensional spectrum function develops a maximum at a non-zero wave-number (Fig. 11).

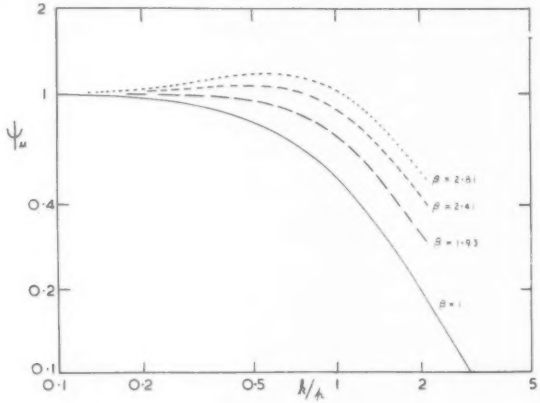

FIG. 11. Theoretical spectra.

Although the actual spectral intensities do not correspond at all closely, the similarity of general shape of the spectra at corresponding values of the total distortion is good. Not really distinct from this is the reversal of trend of the longitudinal scale, L_u, for large distortions, but a decrease in scale is very unusual in developing turbulence and deserves comment. It is concluded that, although turbulent energy transfer and dissipation lead to considerable differences between the observed intensities and the intensities predicted by the instantaneous distortion theory, in the early stages of a uniform distortion the structure of the turbulence is substantially that to be expected from an instantaneous distortion.

The significance of the approximate correspondence between the instantaneous distortion theory and the initial stages of the uniform distortion of isotropic turbulence lies in the conclusion that the structure of turbulence under shear is substantially independent of eddy interaction and transport and the corollary that the energy-containing eddies of turbulence are relatively stable in structure and slow moving. Their stability is directly confirmed by the comparatively slow approach to isotropy of the turbulence after the distortion ceases (Fig. 5) and by previous observations of the slow return to isotropy of the axi-symmetric turbulence obtained by passing initially isotropic turbulence through a fine wire gauze (Townsend (**8**)).

The only previous detailed study of the effect of distortion on isotropic turbulence is that of MacPhail (**4**), but his results show several

peculiar features and do not agree with those presented here. The relevant measurements were obtained by passing grid turbulence through a distorted passage resembling the one described above. It changed section slightly more rapidly (a 2:1 distortion in 15 in.), but had only half the total distortion and was of smaller cross-sectional area. The turbulence was produced by a biplane grid of periodic spacing 2 in., placed 26 in. upstream of the distorting section. Over the first half of the distorting section the behaviour of the turbulence was qualitatively similar to that observed here, but, farther downstream, the anisotropy diminished and at the end of the distortion it was nearly zero. In the parallel recovery section the anisotropy increased once more. MacPhail accounted for these results by supposing the eddies to precess under the action of couples due to the distortion, but the meaning of such an effect in fluid motion is doubtful. It is more probable that the results are due to the large scale of the turbulence relative to the duct dimensions, the influence of the boundary layers on the walls, and perhaps the closeness of the turbulence-producing grid to the distorting duct.

Discussion: turbulence in equilibrium under constant rate of shear

For total strain ratios greater than 2 the shear coefficient K_1 varies comparatively little, and it is possible that it approaches an asymptotic value near 0·42. While the individual intensities may also approach asymptotic values for large strain ratios, it is clear that they do so more slowly, and the interesting point is that the turbulence appears to develop an equilibrium structure after a strain insufficient to establish a time invariant equilibrium state. This result is consistent with previous analyses of the energy balance in turbulent shear flows, which show that energy-production processes are usually too slow to account for the development of Reynolds stresses, and that equilibrium, if it exists, must be structural. By this is implied that the final configuration of the turbulence is substantially independent of energy supply from the mean flow and is determined by realignment of vorticity under the strain imposed by the mean flow.

This establishment of an equilibrium structure for which the shear coefficient is constant may be described formally as an equilibrium between the orienting effect of the distortion and the tendency to isotropy of the turbulence. This description fails to account for the very slow return to isotropy after the distortion ceases and the rather more reliable observations of a similarly slow return to isotropy of axi-symmetric turbulence. Taken all together, it seems certain that, once set up, Reynolds stresses disappear very slowly in a uniform mean flow, and it follows that the competing process must also be part of the distortion. It is likely that the opposition to complete alignment is due to rapidly increasing energy transfer from

eddies whose vorticity is in the direction of positive rate of strain, probably a transfer to eddies one size smaller and containing less energy. The cause of this accelerated transfer could be the continued crowding together of the favoured eddies with consequent increases in the velocity gradients, while eddies whose directions are not such as to gain energy will in general move apart. This description is consistent with the slower rate of increase of λ_u^2 during distortion implying maintenance of a high rate of energy dissipation.

Complete equilibrium in which the turbulent energy remains constant is not attained in these experiments, and very little can be said about it. It must satisfy the energy equation

$$(\overline{v^2}-\overline{w^2})aU = \epsilon \tag{18}$$

and consequently

$$\lambda_e^2 = \frac{\overline{u^2}}{\overline{v^2}-\overline{w^2}}\frac{15\nu}{aU}. \tag{19}$$

Under the conditions of these experiments, λ_e^2 would be 0·28 cm.^{2} Since λ_u^2 is in the range 0·1–0·2 cm.^{2}, final equilibrium is clearly impossible. If, before entering the distortion, the turbulence were allowed to decay more, final equilibrium might be observed, but this is not practicable with the existing apparatus.

Discussion: equilibrium structure in ordinary shear flows

The comparatively rapid establishment of an equilibrium structure in turbulence acted on by a simple shear immediately suggests that the structure may be similar in all fully developed turbulent shear flows, as is postulated in the mixing-length theories. The simplest structure parameter is the shear coefficient, K_1, where the components are along the principal directions of the Reynolds stress, but a survey of published measurements shows that, while in any particular flow this parameter varies little over the regions of maximum shear, from one flow to another it varies between 0·40 and 0·65 (Corrsin (**9**); Liepmann and Laufer (**10**); Townsend (**3**); Dryden (**11**); Townsend (**12**); Laufer (**13**)). An examination of the values shows that, generally speaking, the higher values are found in flows for which the mean flow vorticity is everywhere of the same sign (boundary layers and free mixing layers) and the lower values in flows of zero total vorticity (jets and wakes). It might be thought that, in the latter class of flows, the equilibrium structure may never become fully developed owing to large-scale mixing between regions of positive and negative vorticity, but this is unlikely for two reasons. In the first place, the value for the uniform rate of strain flow is much closer to the jet and wake values than to the other values, although mixing could hardly affect the issue, and, secondly, there is experimental

evidence that the large-scale mixing in a wake is small between the two 'halves' though fairly vigorous inside them (Townsend (3)).

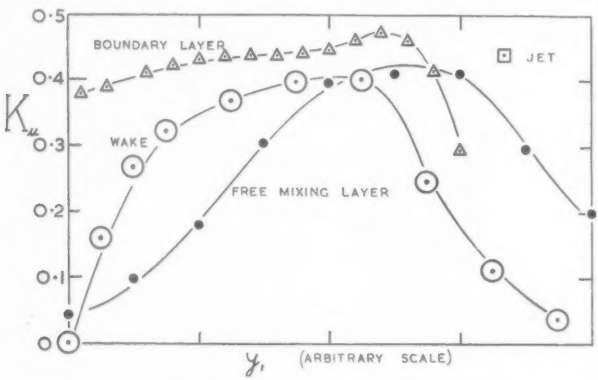

FIG. 12. Variations of K_u.

Although the notion of general similarity must be discarded, it is interesting that a less absolute structure parameter shows a very regular behaviour. When describing ordinary shear flows it is usual to use a coordinate system with Ox in the direction of mean flow and Oy in the direction of the mean velocity gradient. Denoting velocities in this system by the subscript 1, a convenient shear coefficient is

$$K_u = \overline{u_1 v_1}/\overline{u_1^2}.$$

This coefficient is found to be reasonably constant in magnitude over the greater part of the flow, and variation between one flow and another is comparatively small (Fig. 12). In addition, the mean value is close to the value of K_1 found for uniform rate of strain. Reasons for the constancy of K_u are difficult to discover, but, if this result is generally valid, it is clearly of considerable practical value.

The applicability of the eddy viscosity hypothesis to fully developed free turbulence must now be regarded as accidental, and the result of two factors, each of which tends to give a distribution of Reynolds stress of the type expected on the hypothesis. In jets and wakes there is sufficient transport of turbulent fluid in the central core that fully developed volumes of both signs of shear stress (arising from both halves of the flow) may alternate, more of one sign predominating farther from the centre of the flow. In the outer regions the effective shear stress is reduced, partly by the intermittency of the turbulence, and partly because the newly entrained fluid has not been distorted sufficiently to develop its equilibrium structure.

Discussion: structure of the dissipating eddies

Fig. 8 shows that, during the distortion, there is considerable and growing anisotropy of that part of the motion that contributes to the intensities of the velocity derivatives, a result apparently in conflict with previous evidence that the energy-dissipating eddies of free turbulence are isotropic in structure (Liepmann and Laufer (**10**); Townsend (**8**), (**14**)). The departures from isotropy observed here are large, especially at the lower of the two grid Reynolds numbers, and are probably caused by the direct influence of the mean rate of strain on the dissipating eddies. If it is supposed that transfer of energy from larger eddies to smaller eddies is through the rate of strain in the larger ones (as in Heisenberg's formulation of the transfer function (**15**)), then isotropy of the dissipating eddies demands that the mean rate of strain should be at least one order of magnitude less than the rate of strain imposed on the dissipating eddies by the rest of the turbulence. Since these larger eddies do not contribute appreciably to the dissipation, their rate of strain is at least one order of magnitude less than that of the dissipating eddies. It follows that the root mean square rate of strain in the dissipating eddies must be two orders of magnitude greater than the mean rate of strain if local isotropy of the dissipating eddies is to be possible. In the present experiments the mean rate of strain is 9·4 sec.$^{-1}$, while the values of $[\overline{(\partial u/\partial x)^2}]^{\frac{1}{2}}$ in the distorting section are roughly 20 sec.$^{-1}$ and 50 sec.$^{-1}$, neither of which are even one order of magnitude greater.

After the distortion ceases there is, by the standards of the energy-containing eddies, a rapid approach to isotropy of the dissipating eddies. This behaviour is consistent with the notion that it is the direct influence of the mean rate of strain that leads to the anisotropy and not the anisotropy of the energy-containing eddies. The conclusion that, even at comparatively low Reynolds numbers, the energy-containing eddies of turbulence, though themselves highly anisotropic, dissipate their energy through nearly isotropic eddies one size smaller, means that the turbulent transfer process transfers energy from the larger scale motion to all components of the smaller scale motion simultaneously. A distinction between the pressure-velocity and triple velocity correlations in the equations of motion as the agents of energy interchange between the velocity components and between different eddy sizes respectively is not physically sound.

That the dissipating eddies are anisotropic in uniform shear makes it very probable that they are also anisotropic in other shear flows of comparable Reynolds numbers. The evidence for isotropy in other shear flows rests on measurements of the intensities of the velocity derivatives where the axes of reference are the practical axes and not in the directions of principal rate

of strain. Since any anisotropy may be concealed unless the derivatives refer to the principal axes, this type of evidence cannot be considered conclusive or even very relevant.

Assumption of isotropy of the dissipating eddies has often been used to calculate the local turbulent energy dissipation from measurements of the intensity of a single velocity derivative. If the assumption is untrue, the question arises whether it is still possible to write the turbulent energy dissipation in the form

$$\epsilon = 15\nu\overline{\left(\frac{\partial u_1}{\partial x_1}\right)^2} \tag{20}$$

instead of the accurate expression

$$\epsilon = \nu\left[\overline{\left(\frac{\partial u_1}{\partial x_1}\right)^2}+\overline{\left(\frac{\partial u_1}{\partial y_1}\right)^2}+\overline{\left(\frac{\partial u_1}{\partial z_1}\right)^2}+\overline{\left(\frac{\partial v_1}{\partial x_1}\right)^2}+\overline{\left(\frac{\partial v_1}{\partial y_1}\right)^2}+\overline{\left(\frac{\partial v_1}{\partial z_1}\right)^2}+\right.$$
$$\left.+\overline{\left(\frac{\partial w_1}{\partial x_1}\right)^2}+\overline{\left(\frac{\partial w_1}{\partial y_1}\right)^2}+\overline{\left(\frac{\partial w_1}{\partial z_1}\right)^2}\right].$$

There is a certain amount of evidence that, in free turbulence,

$$\overline{\left(\frac{\partial u_1}{\partial x_1}\right)^2} = \frac{1}{2}\overline{\left(\frac{\partial v_1}{\partial x_1}\right)^2} = \frac{1}{2}\overline{\left(\frac{\partial w_1}{\partial x_1}\right)^2} = \frac{1}{2}\overline{\left(\frac{\partial u_1}{\partial y_1}\right)^2} = \frac{1}{2}\overline{\left(\frac{\partial u_1}{\partial z_1}\right)^2},$$

but there is no reliable information about the remaining four terms (Liepmann and Laufer (**10**); Townsend (**14**)). The validity of the short expression is suggested by the internal consistency of energy balances drawn up by using it, but a more exact test would be useful. One may be obtained from the energy balance of this flow. Since there is negligible energy transport, the energy equation becomes

$$\tfrac{1}{2}U\frac{\partial\overline{q^2}}{\partial x} - aU(\overline{v^2}-\overline{w^2})+\epsilon = 0. \tag{21}$$

To compare ϵ, computed from this equation, with the values computed from equation (20), λ_ϵ^2 defined by

$$\lambda_\epsilon^2 = \frac{15\nu\overline{u^2}}{\epsilon}$$

is compared with λ_u^2 in Fig. 6. The correspondence is reasonably close, and suggests that the approximation is valid while Ox_1 is in a direction of zero rate of strain, although local isotropy cannot be assumed.

REFERENCES

1. A. A. Townsend, *Phil. Mag.* **41** (1950), 890–906.
2. H. Reichardt, *J. Roy. Aero. Soc.* **47** (1943), 167.
3. A. A. Townsend, *Australian Journ. Sci. Res.* **2** (1949), 451.
4. D. C. MacPhail, Royal Aircraft Estab. Aero Rep. No. 1928 (1944).

5. G. I. Taylor, *Z.A.M.M.* **15** (1935), 91–96.
6. G. K. Batchelor and I. Proudman, *Quart. J. Mech. and Applied Math.* **7** (1954), 83–103 (above).
7. —— and A. A. Townsend, *Proc. Roy. Soc.* A, **193** (1948), 539.
8. A. A. Townsend, *Quart. J. Mech. and Applied Math.* **4** (1951), 308–20.
9. S. Corrsin, N.A.C.A. (U.S.A.) ACR No. 3L23 (1943).
10. H. W. Liepmann and J. Laufer, N.A.C.A. (U.S.A.) Tech. Note 1257 (1947).
11. H. L. Dryden, N.A.C.A. (U.S.A.) Tech. Note 1168 (1947).
12. A. A. Townsend, *Proc. Camb. Phil. Soc.* **47** (1951), 375.
13. J. Laufer, N.A.C.A. (U.S.A.) Tech. Note 2123 (1950).
14. A. A. Townsend, *Australian J. Sci. Res.* **1** (1948), 161.
15. W. Heisenberg, *Proc. Roy. Soc.* A, **195** (1949), 402.

APPENDIX

The spectrum functions of the turbulent velocity components after distortion, which are given by equations (1), can be integrated to give the ratio of the initial and final turbulent intensities. Batchelor and Proudman (**6**) have done this, expressing the final result in terms of elliptic functions, but the results quoted above may be derived directly. With the change of variables,

$$l_0 = kx, \qquad m_0 = k(1-x^2)^{\frac{1}{2}}\cos\theta, \qquad n_0 = k(1-x^2)^{\frac{1}{2}}\sin\theta$$

and some rearrangement of the integrand,

$$\overline{u^2} = \int_0^\infty k^4\phi(k)\,dk \int_{-1}^{1}\int_0^{2\pi}\left[1+\frac{Bx^2}{a-b\cos 2\theta}-\frac{x^2(1+Bx^2)}{(a-b\cos 2\theta)^2}\right]dx d\theta,$$

where

$$B = \beta^2+\beta^{-2}-2,$$
$$a = 1+\tfrac{1}{2}(1-x^2)B,$$
$$b = \tfrac{1}{2}(1-x^2)(\beta^2-\beta^{-2}).$$

Integrating with respect to θ,

$$\overline{u^2} = 4\pi I\left[1+\int_0^1\left[\frac{Bx^2}{\{1+Bx^2(1-x^2)\}^{\frac{1}{2}}}-\frac{ax^2(1+Bx^2)}{\{1+Bx^2(1-x^2)\}^{\frac{3}{2}}}\right]dx\right]$$

$$= 4\pi I\left[1+\int_0^1\frac{(\frac{1}{2}B-1)x^2+\frac{1}{2}B(B-1)x^4-\frac{1}{2}B^2x^6}{\{1+Bx^2(1-x^2)\}^{\frac{3}{2}}}\,dx\right],$$

where $I = \int_0^\infty k^4\phi(k)\,dk$.

For $B < 4$ the integrand may be represented by a power series, and integration of the series leads to

$$\overline{u^2} = \frac{8\pi I}{3}(1+\tfrac{8}{35}B+\ldots).$$

Similarly, using the same change of variables,

$$\overline{v^2}+\overline{w^2} = \int_0^\infty k^4\phi(k)\,dk \int_{-1}^{1}\int_0^{2\pi}\left[\frac{1}{a-b\cos 2\theta}+\frac{x^2(1+Bx^2)}{(a-b\cos 2\theta)^2}\right]dx d\theta$$

$$= 4\pi I\int_0^1\left[\frac{1}{\{1+Bx^2(1-x^2)\}^{\frac{1}{2}}}+\frac{ax^2(1+Bx^2)}{\{1+Bx^2(1-x^2)\}^{\frac{3}{2}}}\right]dx.$$

Expansion as a power series and integration gives

$$\overline{v^2}+\overline{w^2} = \frac{16\pi I}{3}(1+\tfrac{3}{35}B+\ldots).$$

In the same way

$$\overline{v^2}-\overline{w^2} = \int_0^\infty k^4\phi(k)\,dk\,\frac{2}{\beta^2-\beta^{-2}}\int_{-1}^{1}\int_0^{2\pi}\left[\frac{1-x^2+\frac{1}{2}B}{a-b\cos 2\theta}-\frac{(1+Bx^2)(1+\frac{1}{2}Bx^2)}{(a-b\cos 2\theta)^2}\right]dx d\theta$$

$$= \frac{8\pi I}{\beta^2-\beta^{-2}}\int_0^1\left[\frac{1-x^2+\frac{1}{2}B}{\{1+Bx^2(1-x^2)\}^{\frac{1}{2}}}-\frac{a(1+Bx^2)(1+\frac{1}{2}Bx^2)}{\{1+Bx^2(1-x^2)\}^{\frac{3}{2}}}\right]dx.$$

The leading terms of the series are then

$$\overline{v^2}-\overline{w^2} = \tfrac{64}{105}\pi I\frac{\beta^2-1}{\beta^2+1}(1+\tfrac{33}{112}B+\ldots).$$

The longitudinal scale, L_u, is defined by

$$\psi_u(0) = \int_{-\infty}^{\infty}\int_{-\infty}^{\infty} F(0,m,n)\,dmdn = \frac{2}{\pi}\overline{u^2}L_u,$$

and $\psi_u(0)$ is easily shown to be invariant during instantaneous distortion. With the change of variables

$$m_0 = k\cos\theta, \qquad n_0 = k\sin\theta$$

$$\psi_u(0) = \int_0^\infty\int_0^{2\pi}\phi(k)k^3\frac{1+(\beta^{-4}-1)\cos^4\theta+(\beta^4-1)\sin^4\theta}{(\beta^{-2}\cos^2\theta+\beta^2\sin^2\theta)^2}\,dkd\theta$$

$$= 2\pi\int_0^\infty\phi(k)k^3\,dk,$$

which is independent of β.

The longitudinal scale of the transverse component, v, is similarly defined by

$$\psi_v(0) = \int_{-\infty}^{\infty}\int_{-\infty}^{\infty} G(0,m,n)\,dmdn = \frac{2}{\pi}\overline{v^2}L_v.$$

Using the same change of variables, and after some rearrangement of the integrand,

$$\psi_v(0) = \int_0^\infty\int_0^{2\pi}\phi(k)k^3\frac{4\beta^2\sin^2\theta}{[\beta^2+\beta^{-2}-(\beta^2-\beta^{-2})\cos 2\theta]^2}\,dkd\theta$$

$$= \pi\int_0^\infty\phi(k)k^3\,dk,$$

which is also independent of β. The proof that $\psi_w(0)$ is independent of β is exactly similar.

The one-dimensional spectrum function for u is defined by

$$\psi_u(l) = \int_{-\infty}^{\infty}\int_{-\infty}^{\infty} F(l,m,n)\,dmdn.$$

Changing the variables to k, θ defined by

$$m_0 = (k^2-l^2)^{\frac{1}{2}}\cos\theta, \qquad n_0 = (k^2-l^2)^{\frac{1}{2}}\sin\theta,$$

$$\psi_u(l) = \int_l^\infty \int_0^{2\pi} k^3\phi(k)\left[1+\frac{Bl^2}{a'-b'\cos 2\theta}-\frac{l^2(k^2+Bl^2)}{(a'-b'\cos 2\theta)^2}\right] dkd\theta,$$

where

$$a' = k^2+\tfrac{1}{2}B(k^2-l^2),$$
$$b' = \tfrac{1}{2}(\beta^2-\beta^{-2})(k^2-l^2),$$

after some rearrangement. Integrating with respect to θ,

$$\psi_u(l) = 2\pi\int_l^\infty k^3\phi(k)\left[1+\frac{Bl^2}{(k^4+Bl^2k^2-Bl^4)^{\frac{1}{2}}}-\frac{l^2(k^2+Bl^2)\{k^2+\frac{1}{2}B(k^2-l^2)\}}{(k^4+Bl^2k^2-Bl^4)^{\frac{3}{2}}}\right] dk.$$

Assuming that the defining function is

$$\phi(k) = \frac{2\overline{u_0^2}\,p}{\pi(k^2+p^2)^3}$$

(corresponding to an exponential correlation function), and substituting

$$x = l^2/k^2$$

it is found that

$$\psi_u(l) = \frac{2\overline{u_0^2}\,p}{\pi}\left[\frac{1+2l^2/p^2}{(1+l^2/p^2)^2}+2\frac{l^4}{p^4}\int_0^1 x\,\frac{-1+\frac{1}{2}B(1-x)+\frac{1}{2}B^2x(1-x)}{\{1+Bx(1-x)\}^{\frac{3}{2}}}\,\frac{dx}{(x+l^2/p^2)^3}\right].$$

This integral has been computed for several values of B with the results shown in Fig. 11.

CORRIGENDUM

THE STABILITY OF A COMPRESSED ELASTIC RING AND OF A FLEXIBLE HEAVY STRUCTURE SPREAD BY A SYSTEM OF ELASTIC RINGS†

By G. W. H. STEVENS (*Royal Aircraft Establishment, Farnborough*)

[Received 17 April 1953]

In a private communication to the author, Arthur Boresi, University of Illinois, has shown that the criterion for the stability when the loads act towards the centre is incorrect in the above paper due to an error of algebraic manipulation. Equation (20.2) should read

$$q_0 = \frac{(k^2-1)^2}{k^2-2}\frac{EI}{r_0^3} + \frac{r_0 q_0'}{k^2-2}.$$

The statement preceding this equation, referring to equation (12), is correct and the sign convention of the paper remains consistent.

This slip has little bearing on the discussion of the hooped skirt because the assumption was made that the loads act normally. The comment following the table in section 5.2 of the paper is, however, incorrect because the value of $q_1 r_1^3/EI$ at each transition point is unaffected by the direction of loading. The revised criterion shows that if tangential forces were significant in the example of the hooped skirt then the transition ratios r_2/r_1 would all be lower.

† G. W. H. Stevens, *Quart. J. Mech. and Applied Math.* **5** (1952), 221–36.

THE PRINTING OF MATHEMATICS

AIDS FOR AUTHORS AND EDITORS AND RULES FOR COMPOSITORS AND READERS AT THE UNIVERSITY PRESS, OXFORD

By T. W. CHAUNDY (Reader in Mathematics, Oxford University), P. R. BARRETT (Mathematical Reader at the University Press, Oxford), and CHARLES BATEY (Printer to the University of Oxford). Royal 8vo, 106 pp., with 5 half-tone plates, 4 text-figures, and Index. 15s. net

As its sub-title states, this book does for mathematics what Hart did for general printing in his *Rules for Compositors and Readers*. It is designed not only to help the printer, but also to assist authors to understand the technical problems which are peculiar to the composition of mathematics. Detailed methods are recommended to authors by which they might ease the printer's task and their own. Publication of these Rules should help to standardize the technique of both writer and printer.

OXFORD UNIVERSITY PRESS

THE QUARTERLY JOURNAL OF MECHANICS AND APPLIED MATHEMATICS

VOLUME VII PART 1 MARCH 1954

CONTENTS

M. ROTHMAN: The Problem of an Infinite Plate under an Inclined Loading, with Tables of the Integrals of Ai ($\pm x$) and Bi ($\pm x$) 1

C. R. ILLINGWORTH: The Effect of Heat Transfer on the Separation of a Compressible Laminar Boundary Layer . . 8

J. W. CRAGGS: Characteristic Surfaces in Ideal Plasticity in Three Dimensions 35

A. R. MANWELL: The Variation of Compressible Flows . . 40

L. H. MITCHELL: A Fourier Integral Solution for the Stresses in a Semi-infinite Strip 51

W. CHESTER: The Diffraction and Reflection of Shock Waves . 57

G. K. BATCHELOR and I. PROUDMAN: The Effect of Rapid Distortion of a Fluid in Turbulent Motion 83

A. A. TOWNSEND: The Uniform Distortion of Homogeneous Turbulence 104

G. W. H. STEVENS (Corrigendum): The Stability of a Compressed Elastic Ring and of a Flexible Heavy Structure spread by a System of Elastic Rings 128

The Editorial Board gratefully acknowledge the support given by: Boulton Paul Aircraft Ltd., Courtaulds Scientific and Educational Trust Fund; English Electric Co., Ltd.; Imperial Chemical Industries Ltd.; Institution of Mechanical Engineers; C. A. Parsons & Co., Ltd.; Unilever Ltd.

The publishers are signatories to the Fair Copying Declaration in respect of this journal. Details of the Declaration may be obtained from the offices of the Royal Society upon application.